AD NUMBER

ADB222453

NEW LIMITATION CHANGE

TO

Approved for public release, distribution unlimited

FROM

Distribution authorized to U.S. Gov't. agencies only; Proprietary Info.; Sep 96. Other requests shall be referred to Commander, U.S. Army Medical Research and materiel Command, Attn: MCMR-RMI-S, Fort Detrick, Frederick, MD 21702-5012.

AUTHORITY

US Army Med Research and Mat Cmd, MCMR-RMI-S [70-1y], ltr 6 Jul 2000, Ft Detrick, MD

AD_____

GRANT NUMBER DAMD17-94-J-4310

TITLE: Lewis Y Antigen as a Target for Breast Cancer Therapy

PRINCIPAL INVESTIGATOR: Thomas Kieber-Emmons, Ph.D.

CONTRACTING ORGANIZATION: The Wistar Institute
Philadelphia, PA 19104

REPORT DATE: September 1996

TYPE OF REPORT: Annual

PREPARED FOR: Commander
U.S. Army Medical Research and Materiel Command
Fort Detrick, Frederick, Maryland 21702-5012

DISCLAIMER NOTICE

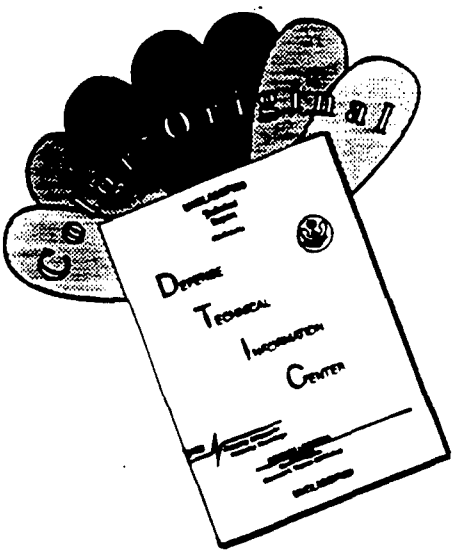

THIS DOCUMENT IS BEST QUALITY AVAILABLE. THE COPY FURNISHED TO DTIC CONTAINED A SIGNIFICANT NUMBER OF COLOR PAGES WHICH DO NOT REPRODUCE LEGIBLY ON BLACK AND WHITE MICROFICHE.

REPORT DOCUMENTATION PAGE

Form Approved
OMB No. 0704-0188

1. AGENCY USE ONLY *(Leave blank)*	2. REPORT DATE	3. REPORT TYPE AND DATES COVERED
	September 1996	Annual (1 Sep 95 - 31 Aug 96)

4. TITLE AND SUBTITLE Lewis Y Antigen as a Target for Breast Cancer Therapy

5. FUNDING NUMBERS
DAMD17-96-J-4310

6. AUTHOR(S)
Thomas Kieber-Emmons, Ph.D.

7. PERFORMING ORGANIZATION NAME(S) AND ADDRESS(ES)
The Wistar Institute
Philadelphia, PA 19104

8. PERFORMING ORGANIZATION REPORT NUMBER

9. SPONSORING/MONITORING AGENCY NAME(S) AND ADDRESS(ES)
U.S. Army Medical Research and Materiel Command
Fort Detrick
Frederick, Maryland 21702-5012

10. SPONSORING/MONITORING AGENCY REPORT NUMBER

11. SUPPLEMENTARY NOTES

12a. DISTRIBUTION / AVAILABILITY STATEMENT
Distribution authorized to U.S. Government agencies only; Proprietary Information, Sep 96. Other requests for this document shall be referred to Comander, U.S. Army Medical Research and Materiel Command, ATTN: MCMR-RMI-S, Fort Detrick, Frederick, MD 21702-5012

12b. DISTRIBUTION CODE

13. ABSTRACT *(Maximum 200*

The Lewis Y antigen is a breast cancer associated carbohydrate antigen The basis of the current program is to utilize structural information for Lewis Y-antibody interactions to develop novel immunotherapeutics for Breast Cancer treatment. To develop such immunotherapeutics, we have constructed smaller forms of anti-Lewis Y antibodies, established that bispecific antibodies that include anti-Lewis Y antibodies can enhance the targeting of breast tumors, and have developed peptides that mimic breast associated carbohydrate antigens capable of inducing immune responses to breast tumors, mediating their killing in vitro.

14. SUBJECT TERMS Breast Cancer, Single Chain Antibodies, Carbohydrate Mimics, Lewis Y

15. NUMBER OF PAGES
82

16. PRICE CODE

17. SECURITY CLASSIFICATION OF REPORT	18. SECURITY CLASSIFICATION OF THIS PAGE	19. SECURITY CLASSIFICATION OF ABSTRACT	20. LIMITATION OF ABSTRACT
Unclassified	Unclassified	Unclassified	Limited

FOREWORD

Opinions, interpretations, conclusions and recommendations are those of the author and are not necessarily endorsed by the US Army.

____ Where copyrighted material is quoted, permission has been obtained to use such material.

____ Where material from documents designated for limited distribution is quoted, permission has been obtained to use the material.

__N/A__ Citations of commercial organizations and trade names in this report do not constitute an official Department of Army endorsement or approval of the products or services of these organizations.

__N/A__ In conducting research using animals, the investigator(s) adhered to the "Guide for the Care and Use of Laboratory Animals," prepared by the Committee on Care and Use of Laboratory Animals of the Institute of Laboratory Resources, National Research Council (NIH Publication No. 86-23, Revised 1985).

____ For the protection of human subjects, the investigator(s) adhered to policies of applicable Federal Law 45 CFR 46.

__N/A__ In conducting research utilizing recombinant DNA technology, the investigator(s) adhered to current guidelines promulgated by the National Institutes of Health.

__N/A__ In the conduct of research utilizing recombinant DNA, the investigator(s) adhered to the NIH Guidelines for Research Involving Recombinant DNA Molecules.

____ In the conduct of research involving hazardous organisms, the investigator(s) adhered to the CDC-NIH Guide for Biosafety in Microbiological and Biomedical Laboratories.

Norman H. Sisman

PI - Signature Date

Table of Contents

Introduction

Lewis antigens are blood group carbohydrate antigens implicated as potential target antigens in a number of cancers (1). The expression of α1→ 2 fucosylated structures such as Lewis Y (LeY), H-2 and Lewis b (Leb) is inversely correlated with the survival of patients with primary lung adenocarcinoma, suggesting that these determinants promote invasiveness (2). The difucosylated neolactoseries structure Lewis Y, Fucα1→2Galβ1→4(Fucα1→3)GlcNAcβ1→R, associated with several human tumors such as breast, lung and gastrointestinal carcinomas is specifically detected by MAbs. Two antibodies called BR55-2 and BR15-6A have been previously described by Dr. Steplewski and colleagues, that bind to the LeY antigen on breast carcinoma cells that can be compared with others described in the literature (1, 3, 4). The monoclonal BR55-2 (IgG3) in particular, and its isotype switch variants directed against the LeY oligosaccharide are found to mediate ADCC (antibody-dependent cell mediated cytotoxicity) with human and murine effector cells, its IgG3 and IgG2a isotypes are highly active in CDC (complement-dependent cytotoxicity) and both efficiently inhibit tumor growth in xenografted nude mice (3-5).

The basis of the current program is to utilize structural information for Lewis Y-antibody interactions, particularly for BR55-2, to develop novel immunotherapeutics for breast cancer treatment. It is postulated that the LeY determinant on human breast adenocarcinoma cells is of key importance since it mediates internalization and lethal function of LeY specific MAb. Molecular probes based on structural information and newly developed MAbs or fragments can be applied for future diagnosis in tumor progression and micrometastasis as well as immunotherapy. In addition, it appears that anti-idiotypic antibodies that mimic the Lewis Y carbohydrate antigen represent potential surrogate immunogens for specific immunization for the treatment of breast cancer. During the current funding period, we have examined the molecular basis of recognition of anti-LeY antibodies for the LeY antigen using molecular modeling, have developed and screened a human single chain (scFv) library reactive with the Lewis Y antigen which is comparable with a humanized version of BR55-2, we are beginning to examine the synergistic effects of creating bispecific antibodies involving BR55-2 and antibodies that target other breast associated target molecules, we have examined the extent peptides that mimic carbohydrate subunits can induce humoral responses in mice that can target breast tumor cells and have examined how a Lewis Y mimicking peptide can bind to an anti-Lewis Y antibody that displays homology with BR55-2 to further define a vaccine or adjuvant approach targeting the LeY antigen.

Body

Antibody recognition of the Lewis Y antigen.

We have recently examined the recognition properties of BR55-2 conferring LeY specificity ((6) see manuscript #1 in appendix). The murine monoclonal antibody BR55-2 is directed against the tumor-associated antigen Lewis Y oligosaccharide. The Lewis Y core antigen is a difucosylated structure, displaying the tetrasaccharide core structure Fucα1→2Galβ1→4(Fucα1→3)GlcNAc. Analysis of binding profiles of lactoseries isomeric structures by BR55-2, suggest that the binding epitope includes the OH-4, and OH-3 groups of the β-D-Galactose unit, the 6-CH3 groups of the two fucose units, and the N-acetyl group of the subterminal β-D-N-acetyl-glucosamine (βDGlcNAc) (6). To elucidate the molecular recognition properties of BR55-2 for the LeY antigen, cDNA of BR55-2 was cloned, sequenced and the antibodies three-dimensional structure was examined by molecular modeling (6). The crystal structure of BR96, another anti-LeY antibody, solved in complex with a nonoate methyl ester Lewis Y tetrasaccharide, and the lectin IV protein in complex with a Lewis b tetrasaccharide core were used as a guide to probe the molecular basis for BR55-2 antigen recognition and specificity. Our modeling study (6) shows that BR55-2 shares similar recognition features for the difucosylated type 2 lactoseries Lewis Y structure observed in the BR96-sugar complex. We observe that a major source of specificity for the Lewis Y structure by anti-LeY antibodies emanates from interaction with the β-D-N-acetyl-glucosamine residue and the nature of the structures extended at the reducing site of the fucosylated lactosoamine.

Current procedures for predicting ligand-antibody interactions is limited, mainly due to the conformational flexibility of ligands and the role of solvent in mediating ligand recognition and binding.

However, modeling does provide an avenue for hypothesis testing when relevant alternative structural or binding information is available. In the present case, structures from lactoseries reactive antibodies and the crystal structure of GS4 have defined potential sites on Lewis structures that dictate their specificity. The model of BR55-2 emphasizes the role played by the fucose methyl groups facing the floor of the antibody combining site. These methyl groups might be mimicked by methyl group containing amino acid residues in a designed peptide that compete with LeY for anti-LeY antibodies. A peptide that mimics the LeY antigen has been described that contains such methyl groups and we have also identified such peptides upon BR55-2 screening of peptide phage displayed libraries (see later sections). These and related studies provide an understanding of the 3-dimensional basis for the molecular recognition of LeY by antibodies that can be applied to the development of more efficacious LeY reactive antibody forms for use in future diagnosis in tumor progression and micrometastases as well as in active immunotherapy.

Development of Human scFv library.

The construction and use of recombinant chimeric and later fully humanized (CDR-grafted) antibodies to tumor-associated antigens has reduced the immune response generated to these antibodies in clinical studies. However, their long circulating half-life is a disadvantage for tumor imaging and therapy. Fragments such as F(ab')2, Fab', Fv and single chain Fv (scFv) offer increasing penetrance of solid tumors and decreasing circulating half-life, as well as reducing immunogenicity, but also lower overall tumor doses. Generally, the increased pharmacokinetic properties of smaller antibody fragments over whole antibodies have led to interest in their use for in vivo imaging of neoplastic and other diseases. In addition, their production as fusion proteins with toxins and other molecules has allowed the development of antibody-like molecules with novel effector functions. Multivalent and multispecific antibodies with defined stoichiometry could provide valuable tools for biological and medical research and for the diagnosis and therapy of cancer. Several approaches are being considered to effectively influence clearance and tumor dosage. In one approach, the tumor targeting of several novel fragments produced by chemical cross-linking of Fab' or scFv to dimeric and trimeric species has been examined.

The smallest domain of an antibody necessary for antigen binding is thought to be the Fv domain. Recent advances have demonstrated that single chain antigen binding proteins (scFv) consisting of the variable domains of the heavy chain (VH) and light chain (VL) joined by short peptide linkers retain the original antigen binding properties of the Fv fragment. While LeY is considered non-immunogenic in humans in that there appears to be no evidence of circulating anti-LeY antibodies in humans, we decided to develop human antibodies reactive with LeY using a different strategy than isolating EBV transformed human monoclonal antibodies from breast cancer patients. In addition within the scope of the grant we wanted to make humanized single chain Fv fragments based upon BR55-2. To sped up the design process we decided we use a single chain library developed from an autoimmune patient. It was reasoned that autoimmune patients certainly generate antibodies to carbohydrates. Subsequently we might fish out reactive single chain human antibodies reactive with LeY that we can further manipulate.

In earlier studies we have utilized a bacterial vector for cloning and expressing isolated human antibody heavy chain variable regions (7). Lymphocytes from patients with clinically active SLE with anti-DNA and/or anti-phospholipid antibodies were utilized to develop a single domain recombinant antibody library, and DNA binding heavy chain variable region fragments were isolated. RNA was extracted from the peripheral blood mononuclear cells (PBMC), cDNA synthesized, and heavy chain V regions amplified with human VH specific oligonucleotide primers. The VH fragments were cloned into a bacterial expression plasmid including the PelB leader peptide to direct appropriate expression. Recombinant antibodies were screened for binding to 32P-labeled double-stranded plasmid DNA, and later also characterized for binding to single stranded DNA. Binding was confirmed by standard ELISA methodology. Following our line of reasoning, we have made a single chain recombinant phage library (scFv), in which PBMCs were obtained from an SLE patient with active disease (manifested by low complement levels and clinical disease activity). RNA was extracted and complementary DNA (cDNA) synthesized. Immunoglobulin (Ig)-V region sequences were amplified via the polymerase chain reaction

(PCR). The PCR products were combined into an Fv region by recombinant PCR with a previously described linker peptide utilized to physically link the light chain to the heavy chain V region. This was then restriction digested and cloned into Bluescript that included a PelB leader and gene VIII. This system utilizes a plasmid encoding the antibody variable regions as a fusion protein with the capsid protein(s) of filamentous bacteriophage. The antibodies are expressed as fusion proteins either with the bacteriophage gene III product (which is present in a few copies per phage particle) or the gene VIII product (which is present in multiple copies in the phage coat). Vectors based on both gene III and gene VIII have been developed and are currently in use by our group. The vectors (with inserts) and model recombinant phage are shown in figure 1 below.

These vectors are used in combination with helper phage to produce phage-display antibodies. Following several rounds of panning and rescue of the phage, free Fv regions are made utilizing an internal stop codon in the 3' V_H primer sequence. This stop codon (amber) was deliberately included in the primer so that the plasmid can be expressed either as a fusion protein in conjunction with the gene VIII protein when grown in strains of *E. coli* that contain amber suppresser tRNA molecules, or as a secreted protein by simply growing the plasmid in bacteria lacking the amber suppresser tRNA.

Figure 1. Schematic of scFV construction

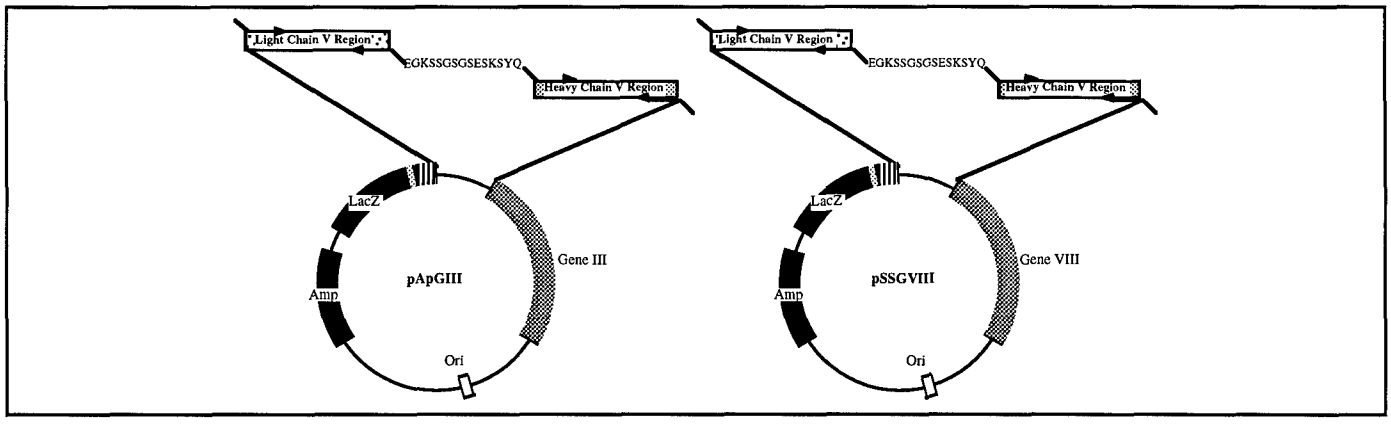

Isolation of LeY reactive human scFv

We have examined the human scFv library to isolate scFv fragments that bind to LeY and to an anti-idiotypic antibody to BR55-2, called E4. Ab displayed phage that bind to LeY and E4 were affinity selected by panning on antigen-coated wells. In these studies, Lewis Y antigen coupled to BSA or E4 was used to coat microtiter wells for panning. After three rounds of panning against synthetic antigen, we performed a final round of panning against E4. We then selected several clones for sequencing. In Figure 2 we compare the light and heavy chain sequences of the humanized BR55-2 (8) and two selected clones from the library. We are in the process of analyzing the structural relationships between the two species. However it is clear that the VH and VL genes are similar. This scFv in conjunction with the humanized construct will provide us with the ability to develop recombinant bispecific antibodies. In addition, based upon our modeling studies and available sequences for other anti-LeY antibodies that are correlated with binding studies, we plan on using site directed mutagenesis to enhance LeY recognition (6). We have also entered into a collaboration with Protein Design Labs who have humanized BR55-2 (8) to further foster its development as an immunotherapeutic for breast cancer .

Figure 2 Sequence of the light and heavy chain of isolated human scFv reactive with LeY.

LIGHT CHAIN

```
Hu-BR55-2 DIVNTQSPLSLPVTPGEPASISCRSSQSIVHSNGNTYLEWYLQKPGQSPQLLISKVSNRFS
HU-amhk13 DIVMTQSPSSLSASVGDRVTITCRAS     HNIIDYLSWYQQKPGKGPNLLIYAASRLQS
E419A     DIVMTQSPSSLSASVGDRVTITCRSS     QTIRNYLNWYQQKPGKAPKLLIYDASSLQS

HU-BR55-2       GVPDRFSGSGSGTDFTLKISRVEAEDLGVYYCFQGSHVPFTFGQGTKLEIK
HU-amhk13       GVPSRFSGSGSGTDFTLTISSLQPEDFATYYCQQSHFSPYTFGQGTKLEIK
E419A           GVPSRFSGSGSGTDFTLTISSLQPEDFATYYCQQSYSSPLTFGPGTKVDIK
```

HEAVY CHAIN

```
HU-BR55-2       EVQLLESGGGLVQPGGSLRLSCAASGFTFSDYYMYWVRQAPEKRLEWVA
HU-amhk13       EVALVDLGGNVVQPGGSLRLSCAASGFTFHDYTMHWVRQAPGKGLEWVS
E419A           EVALLVEWGAVVRPGGSLRLSCAASGFTFSSYAMSWVRQAPGKGLEWVS

HU-BR55-2       YISNGGGSSHYVDSVKGRFTISRDNSKNTLYLQMNSLRAEDTALYH
HU-amhk13       LISWHGHSTFYADSVKGRFTVSRDNSKYSLYLEMNSLTTDDTALYY
E419A           TISFSGSSTYHADSVKGRFTISRDNSKNTLYLQMNSLRAEDTAVYY

HU-BR55-2       CARGMDYGA          WFAYWGQGTLVTVSS
HU-amhk13       CAKEVSPSDTAMVTFRYHDAFDSWGQGTMVIVSSASTK
E419A           CAKAPLGDY     LWGSYPLDYWGQGTLVTVSSASTK
```

Generation of Bispecific antibodies

MAbs selected for binding to human tumors recognize surface antigens that are abundant on the tumor cells, but nevertheless are found at lower levels on normal tissues. To enhance tumor specificity, we are investigating the use of heterobispecific antibodies (BAbs) directed at two different tumor antigens on the cell surface. We expect that the binding of such a BAb to normal tissues will be diminished in comparison to that of a monospecific bivalent MAb. For this purpose we have generated a chemically crosslinked BAb directed to the epidermal growth factor receptor (EGFR) 425 epitope and the BR55-2 Lewis Y epitope, both of which are over expressed in various carcinoma cells. As shown in Fig. 3, this heterobispecific antibody binds with high affinity to target cells that co-express both epitopes. The binding affinity of the 425/BR55-2 BAb is somewhat greater than the affinities of F(ab')2 of either parental antibody and about 10-100 fold higher than the affinity of the BR55-2/CD3 or 425/CD3 construct that binds monovalently to target cells. These results indicate that cross-linking of distinct epitopes on the same cells by of BAbs can be accomplished that increase the efficacy of binding of BR55-2. This experiment suggests that homo and heterodimeric species of antibodies that target a variety of breast associated antigens might prove to be better immunotherapeutics. The coming year our plan is to make and test such reagents. In our first set of constructs dimeric and trimeric single chain species of BR55-2 will be made followed by the construction of bispecific antibodies that will include the anti-EGFR antibody 425 and an anti-neu antibody. The scFv's will be constructed and expressed in bacteria to facilitate genetic manipulation necessary to produce the variety of antibody-form derivatives discussed in this proposal and to allow for rapid modifications of determinants which may affect protein folding, binding, and/or bioactivity. Additional advantages of bacterially produced antibody forms over standard hybridoma techniques include: increased stability and consistency of protein production, high protein yields, and increase ease of culturing. Ultimately this approach has the greatest flexibility and potential. In the coming year we plan on making these constructs as described in the following underlined sections.

Figure 3 Synergistic binding of BR55-2 bisepcific antibodies

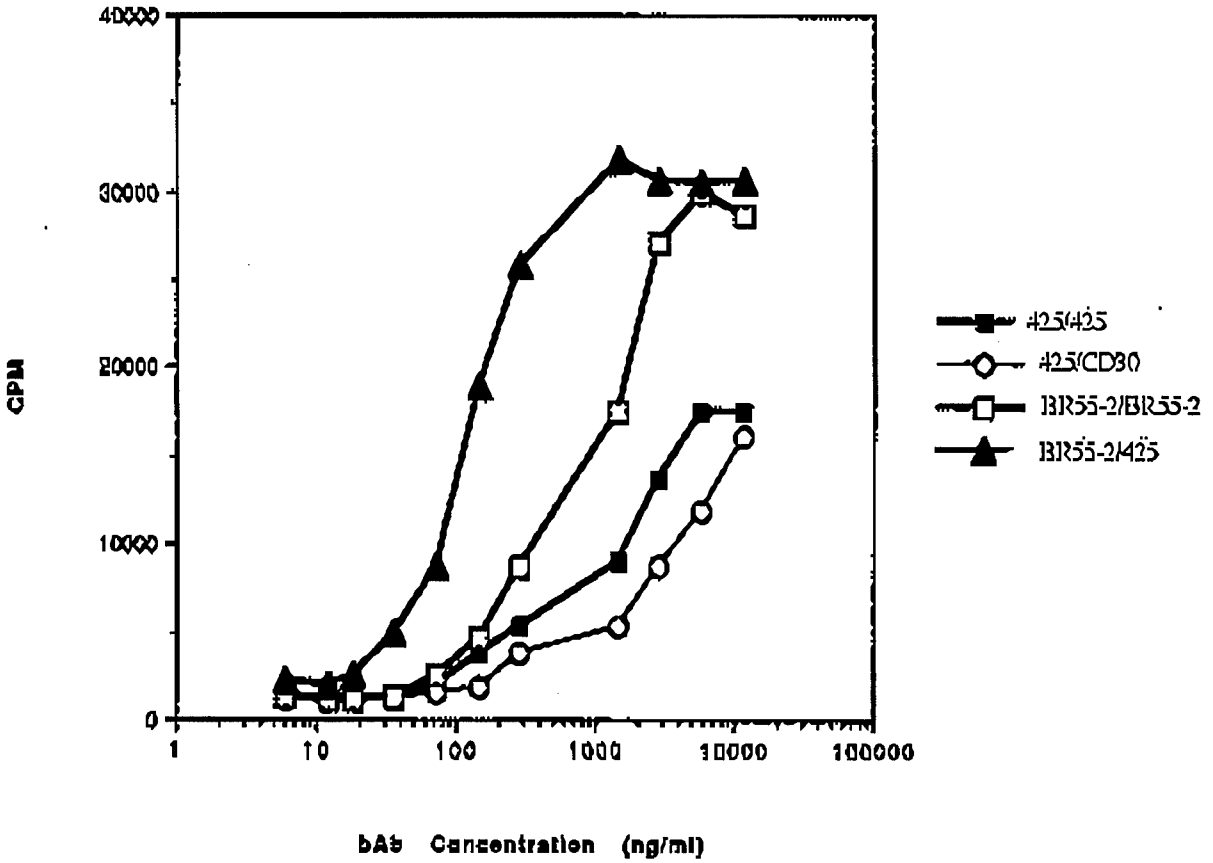

Figure 3: Binding of chemically crosslinked BAbs to MCF-7 breast cells as determined in indirect radioimmunoassay. Enhanced target cell recognition of heterobispecific BR55-2/425 is shown in comparison to 425/425 and BR55-2/BR55-2 F(ab')2 and BR55-2/anti-CD3 F(ab')2.

Expression of scFv fragment of hu-BR 55 -2 mimic: The scFv fragment has been initially cloned into the vector pCANTAB 5E and named as Amhk 13 and expressed in the E. Coli strain HB2151 (Pharmacia). To express the protein, transformed cells are cultured overnight growing in glucose containing media at 28C then changed to glucose-free media with 1 mM IPTG and continued to incubate at the same condition for another 20hrs. The cells are pelleted and sonicated on ice. Both culture supernatant and pellet lysate supernatant were tested using ELISA. Our previous result showed that this scFv fragment is not secretable and mostly formed as an inclusion body, which is solubilized in 6M guanidine hydrochloride pH 7.0 and then tested by ELISA as well.

Construction of dimeric and/or trimeric scFv molecules: Overall, the structure of the dimeric recombinant DNA molecule will contain the following components in order from N-terminus to C terminus: the 5'-Sfi I - scFv fragment, linker, scFv- streptavidin (SA) - Cystein - (His)6 - stop codon-Not 1-3'. the 5'-Sfi I - scFv fragment and the scFv- streptavidin - Cystein - (His)6 - stop codon-Not 1-3' fragment are generated separately. The whole linker sequence is divided into two and incorporated into the relative primer for annealing the two fragments. 5'-Sfi I - scFv fragment is amplified individually through PCR using our clone Amhk 13 as template. The 3'-primer designed for this amplification contains a portion of the linker sequence at the 5' end which is going to be annealed to the rest of the linker sequence which was built into the 5'primer for the amplification of the scFv- streptavidin - Cystein - (His)6 - stop codon-Not 1-

3' fragment. To generate the scFv- streptavidin - Cystein - (His)6 - stop codon-Not 1-3'fragment, we amplify the scFv first with a 3' primer which contains the 5' end sequence of SA. We then amplify the streptavidin Cystein - (His)6 - stop codon-Not 1-3'fragment with a 5'primer containing the 3'sequence of the scFv fragment and a 3' primer containing the entire tail of Cystein - (His)6 - stop codon-Not 1-3'. The two fragments are then annealed to each other to form the second fragment, i.e. the scFv- streptavidin (SA) Cystein - (His)6 - stop codon-Not 1-3' fragment. The final construct contains Sfi I and Not I restriction sites at its 5' end and 3' end which facilities itself to be ligated into the expression vector PCANTAB 5E. To generate the trimeric molecule from the dimeric molecule, another PCR amplification of the scFv fragment needs to be performed with Sfi I sites built into both the 5' primer and the 3' primer. This product is annealed to the N-terminus of the dimeric scFv molecule then ligated into the same expression vector. Under this construction, the Pel B sequence is no longer applied.

Expression of the dimeric and/or trimeric scFv molecules: PCANTAB 5E expression vector contains a gene Ill signal sequence. So our expressed product could be either secreted into the culture media or into the periplasmic layer or stays in the cell cytosols. To determine the expression pattern, cell culture supernatant, periplasmic extract and whole cell extract are need to be tested. In brief, to prepare the periplasmic extract, we resuspend the cell pellet in 1x TES buffer, then add an equal volume of ice-cold 115 x TES and vortex. Incubate on ice for 30'. Spin the whole contents in a 1.5 ml tube at 14,000 rpm at 40C for 10'. Collect the supernatant which contains the scFv fragment from the periplasmic layer. The whole cell extract is made by ultrasonication. When a positive clone has been selected, we will do a time course for determining the optimal expression. The time course is going to be carried out at 28C at which it is believed that the formation of the inclusion body is minimized. To maximize the expression, we use baffled flasks. When functional assay shows that the expressed product does exert the expected function, we will further subclone the fragment and transform it through electroporation into Pichia yeast expression cells. At this point, the (His)6 tag will be removed from the dimeric or trimeric fragments. A multi-copy featured expression will also be performed using a unique expression vector to increase the expression yield.

Peptide mimicry of breast associated carbohydrate antigens

Very few groups are investigating carbohydrate based vaccines or carbohydrate based immunotherapy. One major reason for this is that carbohydrate antigens are expensive and very difficult to synthesize. Further, expression of tumor-associated carbohydrate antigens is by no means specific to tumors. Crucial issues are expression of antigen density, multivalency, reactivity threshold of antibody binding, and efficient production of antibody having a strong complement-dependent or T cell dependent cytotoxic effect on tumor cells without damage to normal tissues. Studies on cancer vaccine development depend on many factors for success that include: 1) Selection of carbohydrate epitopes; 2) Design and assembly of epitopes coupled to macromolecular complex as an efficient immunogen; 3) establishment or availability of a good animal model; 4) Evaluation of immune response in animals; tumor rejection without damage to normal tissues; and 5) careful clinical application.

Since carbohydrate antigens are generally weakly immunogenic in humans, only short lived IgM responses have been historically observed. The importance of adjuvant sublimation is highlighted in such studies to offset the relatively weak immunogenicity of the carbohydrate structures (9-18). In addition, antibodies to carbohydrates are typically of low affinity and the notion of how cellular immunity is modulated by carbohydrates is unclear.

The notion of using peptide mimics of carbohydrates to induce anti-carbohydrate immune responses parallels the use of anti-idiotypic antibodies as immunogens. Peptides that mimic carbohydrates might be used to augment naturally available immunoglublins to tumor antigens. It is now also clear that humans with cancer have, in their draining lymph nodes, precursors of cytotoxic T cells that can be stimulated in vitro to react against their tumors (19). Peptide formulations might trigger such precursors. Subsequently peptides that mimic tumor associated carbohydrates would be of importance as novel agents for adjuvant therapy.

We have shown that a synthetic peptide can mimic the capsular polysaccharide of *N. meningitis* serogroup C (MCP) in that it induces an anti-MCP immune response (20). This peptide was derived from an anti-idiotypic antibody which was capable of inducing an anti-MCP idiotype. Subsequently, we showed that a large immunogen can be reduced to a smaller fragment that retains its biological activity. This MCP mimicking peptide bears some homology with other peptides that mimic carbohydrates identified from phage display peptide libraries (Table 1) involving a Planar-X-Planar sequence motif. All proteins which interact with α-amylase have WRY residues implicated in this interaction (20). Recently, Hoess et al (21) have identified an 8 amino acid peptide expressed on phage capable of inhibiting Lewis Y carbohydrate-antibody binding consisting of the sequence tract PWLY. A peptide which binds ConA has been shown to have a similar configuration, namely YPY (22, 23). These peptides demonstrate the preference of aromatic groups separated by an intervening residue. All these sequences resemble the peptide we have identified as a mimic of the group C meningococcal polysaccharide. The immunological presentation of the putative motifs,(i.e. short or longer peptides, presentation in a helix or beta bend) might mimic overlapping epitopes on otherwise different carbohydrate structures. We have found that sera and monoclonals developed from immunizations with peptide forms of the putative P1, and P2 motifs (Table 1) cross-react with Ley and Leb as assessed by ELISA.

Table 1 Peptide motifs that mimic carbohydrate structures

Peptide	Carbohydrate	Structure
YYPY (P1)	Mannose	methyl-α-D-mannopyranoside
WRY	Glucose	α(1-4)glucose
PWLY	Lewis Y	Fucα1→2Galβ1→4(Fucα1→3)GlcNAc
YYRYD (P2)	Group C Polysaccharide	α(2-9)sialic acid

The sequence similarities among the putative motifs suggest that antibodies raised to this peptide set might cross-react with similar subunits expressed on what are otherwise dissimilar carbohydrate structures. To highlight this possibility, we have recently determined the molecular recognition properties of the tetrasaccharide LeY antigen to anti-LeY antibodies (6) and in figure 4 show that the LeY tetrasaccharide structure is similar to the core structure of MCP. In this orientation, hydroxyl groups (light spheres) on the cFuc residue (Fucα1-3GlcNAc) are spatially conserved with those (dark colored) of the α9 sialic residue of MCP. While the methyl groups on dFuc (Fucα1-2Gal) and α9 sialic subunits are spatially apart, it is possible that these functional groups might still participate in binding to cross-reactive antibodies. Similarly, reactivity with LeY might extend to Leb (Figure 1a in Thurin-Blaszczyk, 1996 #451] see manuscript #1 in appendix). Superposition of LeY and Le^b structures indicates that inspite of the change of glycosidic linkage from β1-3 to β1-4 in the type 1 and 2 chains, resulting conformational features of the respective sugar moieties are still shared forming a common topography. The only effective difference is the position of the N-acetyl and hydroxymethyl groups projected on opposite sides of the type 1 and 2 difucosylated structures.

These possible structural similarities suggest that anti-sera raised to the peptide putative motifs might cross-react with a variety of subunits representative of Lewis antigens (manuscript # 2 appendix). The immunological presentation of the putative motifs, (i.e. short or longer peptides, presentation in a helix or beta bend) might mimic overlapping epitopes on otherwise different carbohydrate structures. To test this idea, Balb/c mice were immunized with peptides representative of the motif YYRYD (P1), and YYPYD (P2). To enhance their immunogenicity, the peptides were complexed to hydrophobic meningococcal group B outer membrane proteins referred to as proteosomes. The Peptides were synthesized with the addition of a 3 amino acid spacer and a Lauroyl group. The meningococcal outer membrane proteins or proteosomes

Figure 4. Superposition of LeY and MCP structures highlighting spatial equilvance of functional groups

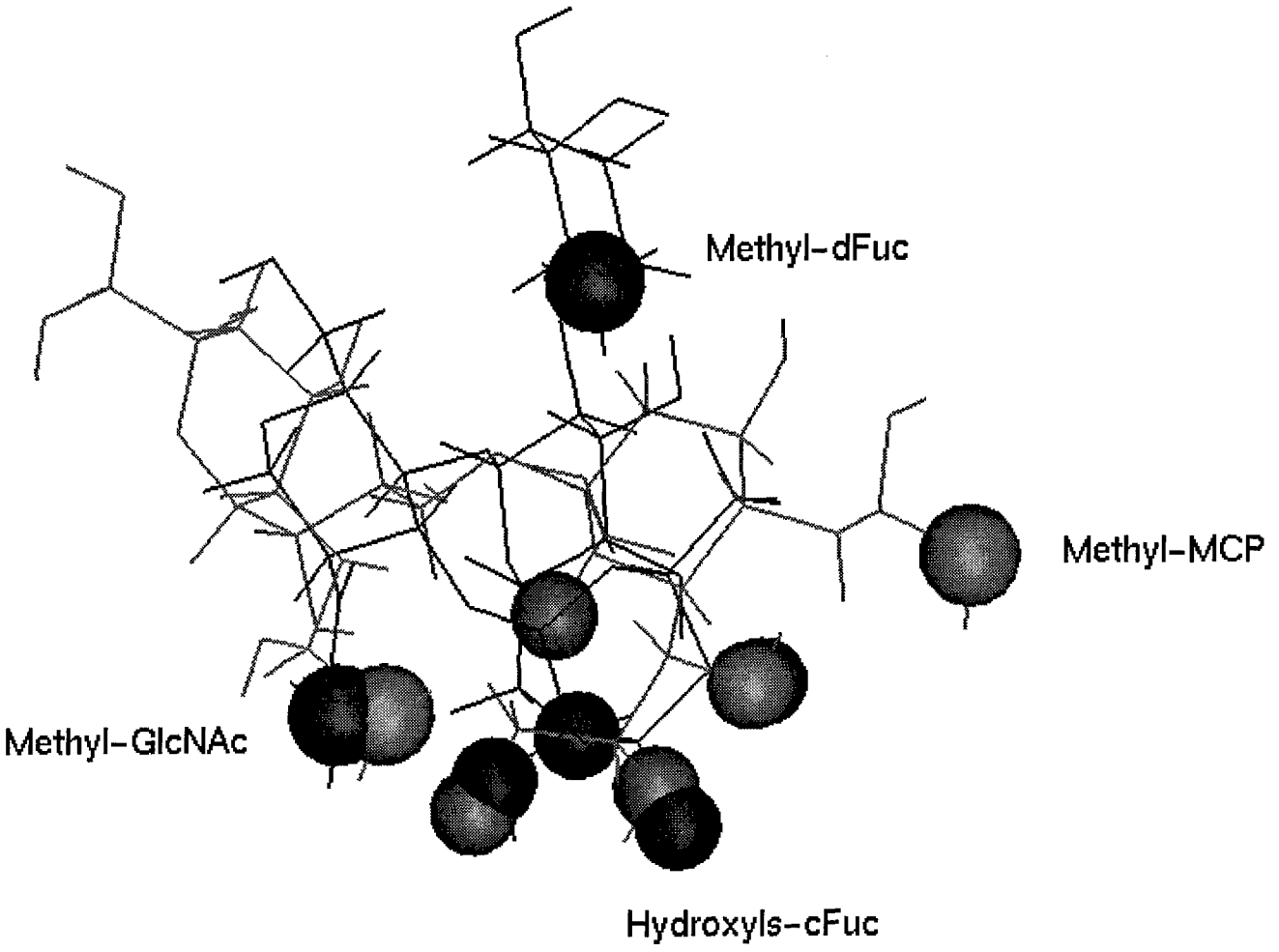

Figure 5. Titration of anti-peptide sera with multivalent Lewis Y and Leb synthetic probes

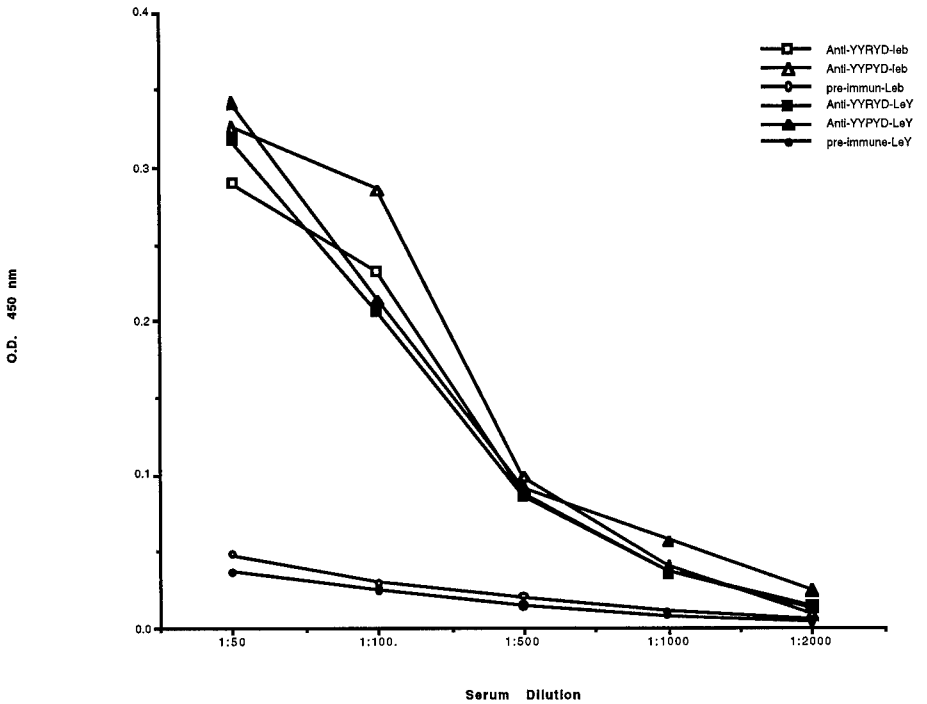

were prepared and complexed to the Lauroyl-C-YGG-Peptides in a 1mg:1mg ratio (20). Sera were collected 1 week after the last immunization, pooled and tested for reactivity with LeY and Leb. We have found that sera developed from immunizations with the putative P1, and P2 motifs (Table 1) react with the two multivalent probes, with the IgG reactivity going out to 1:2000 (figure 5). Control pre-immune sera and sera generated against proteosomes alone and a HIV-1 gp120 derived peptide (24) was not reactive with either synthetic probe.

To further evaluate the reactivity of the sera for breast associated carbohydrate forms, ELISA assays were performed with plates coated with various synthetic carbohydrate subunit probes (Figure 6). As a positive control, the monoclonal antibody BR55-2 which displays specificity for LeY was used. As a negative control, the monoclonal antibody ME361, which displays specificity for the GD2/GD3 gangliosides, was used (25). For BR55-2, selective binding was observed for LeY. ME361 was not reactive with any of the synthetic probes. It was observed that the anti-peptide sera (1:100 titer) was reactive with respective carbohydrate probes above the FCS background binding. Preferences for antisera against the YPY motif include Fucα1-3GlcNAc representative of LeY, and Lex, the Led (H type 1) structure Fucα1-2Galβ1-3GlcNAc representative of Leb, and the disaccharide Galβ1-4Glc. For the YRY motif, reactivity again was observed for all of the synthetic probes, with the disaccharide Galβ1-4Glc displaying the highest reactivity. The antisera reacted with both H type 1 and H type 2 (Fucal-2Galb1-4GlcNAc) structures, with the type 1 structure displaying slightly more activity. This may reflect interaction with the common Fucα1-2Gal structure found on type 1 and type 2 structures or functional groups that are shared within the common topography of these two chains . Reactivity was observed for the TF representative subunit Galβ1→3GalNAc, and the Leb and Lea Fucα1→4GlcNAc subunit. These data suggest that there is a large degree of overlap in the potential carbohydrate structures being recognized by the antisera which was expected since the peptides mimic a wide range of singular

carbohydrate subunits. We are presently examining peptides isolated from phage display that are reactive with BR55-2 (see later section)

Figure 6 Breast associated carbohydrate forms reactive with peptide antisera

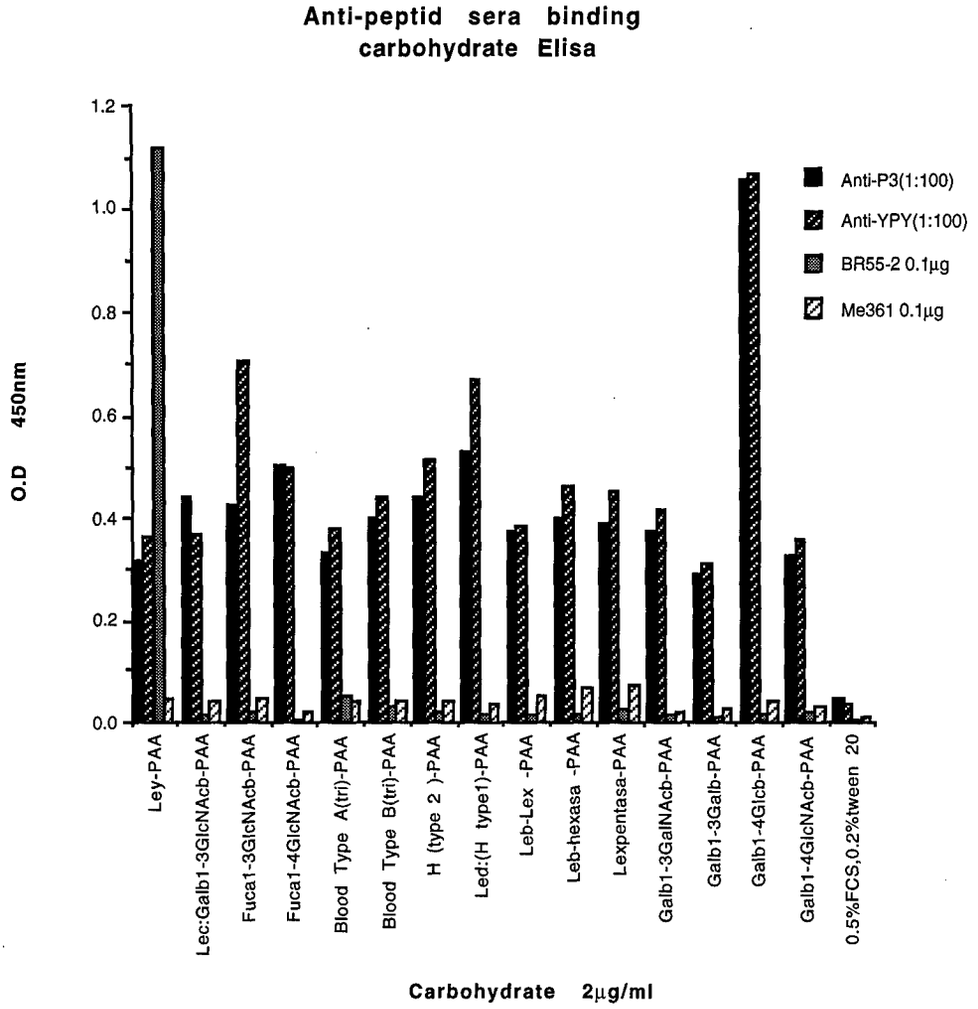

Cross-reactive immune responses with tumor cells

We have evaluated the ability of sera to peptides containing the respective P1, and P2, and putative motifs to bind to representative tumor cells as evaluated by FACS assay (Table 2). Again, positive control monoclonals were BR55-2 and ME361. Normal mouse sera (NMS) and sera generated against proteosome alone were also used as a controls. We found that murine sera elicited against these peptides bind to human breast carcinoma and melanoma cells. We also tested sera raised to a YYRYD related motif YYRGD (referred to as P3). The RYD sequence has been shown to be a mimic for the adhesion motif RGD (26) and its conformational properties correlate with bioactive RGD compounds (27). The anti-peptide sera to the YRGD motif was found to bind to both the human breast cancer cell line SKBR3 and the human melanoma line WM793 to a lesser extent than the other two anti-peptide sera, with all three anti-peptide sera displaying preferential binding to SKBR3. Sera from both Balb/c and C57/BL6 immunized mice reacted in similar fashion indicating that the immune response was not H-2^b or H-2^d dependent (data not shown). Most importantly, none of the sera reacted with normal breast cells indicating that these sera only react with cells that express high levels of respective carbohydrate antigens.

Table 2 Binding of Various Anti-Carbohydrate Sera to Different Cells As Measured by FACS

Cell Line	Anti P1 (YYPY)	Anti P2 (YYRYD)	Anti P3 (YYRGD)
SKBR3	240.6	275.6	166.7
HS578 Bst (normal breast)	17.8	19.9	22.4
WM793	145.5	172.4	42.3
NIH3T3 Murine Fibroblasts	20.9	21.8	41.7

Background fluorescence (Mean Fluorescence) associated with non-specific mouse sera is 24.2, 25.2, and 23.7 for SKBR3,and NIH 3T3 cells, respectively. Background for the human melanoma line was on average 24.4. (Final Sera Concentration: 1:50)

The ability of the peptides to mimic carbohydrate fragments or subunits is further observed from consideration of treating cells with neuraminidase. Treating SKBR3 cells with neuraminidase did not significantly affect the binding of BR55-2 nor any of the antisera as assessed by FACs (Figure 7a). Treatment of WM793 human melanoma line with neuraminidase increased the mean fluorescence for the antisera binding (Figure 7b). As a positive control, treatment of WM793 resulted in decreased binding of ME361. The increase of binding of the anti-sera to WM793 is interpreted as exposing otherwise encryptic epitopes on the cell surface after sialic acid removal. Presumably elimination of sialic acid results in exposure of GalNAc units which is a major constituent of many carbohydrate types including those on the SKBR3 cell line as part of the Lewis Y antigen. Conformational properties of particular carbohydrate subunits overlap in their conformations resulting in the spatial disposition of similar functional groups which might be mimicked.

We have also examined the ability of the sera to mediate complement dependent cytotoxicity (CDC) of the SKBR3 human adenocarcinoma cell line. In fig 8a a we observe that the anti-Lewis Y antibody BR55-2 mediates CDC at high Ab concentrations approaching 80% at 100ug. The negative control antibody ME361 which is specific for GD2 does not mediate CDC of SKBR3. In figure 8b we observe that the three lead anti-

Figure 7. Summary of FACs results for antisera binding to breast and melanoma cells. Background (BG) mean fluorescence was subtracted from the mean experimental (exp) value.

Figure 7a.

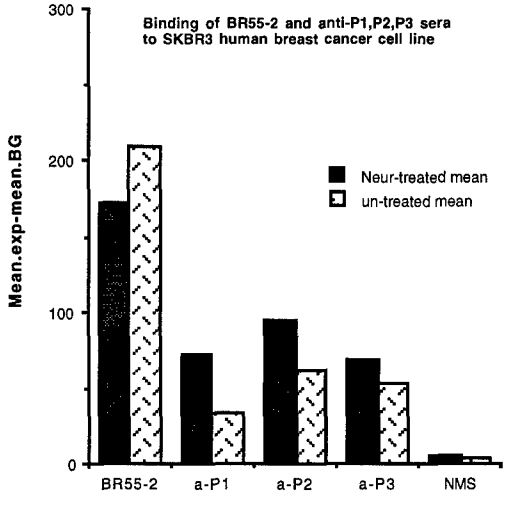

Figure 7b.

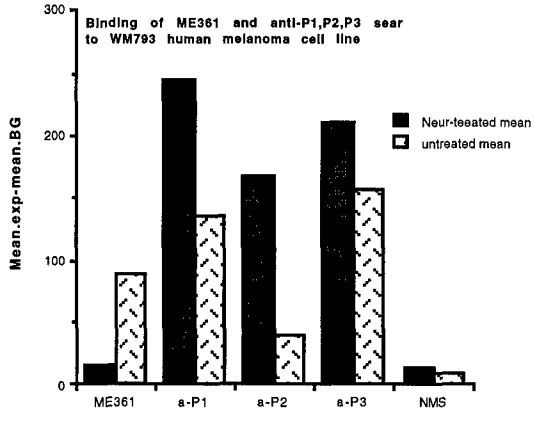

Figure 8 CDC mediated killing of SKBR3 cell line.
a) CDC killing by BR55-2

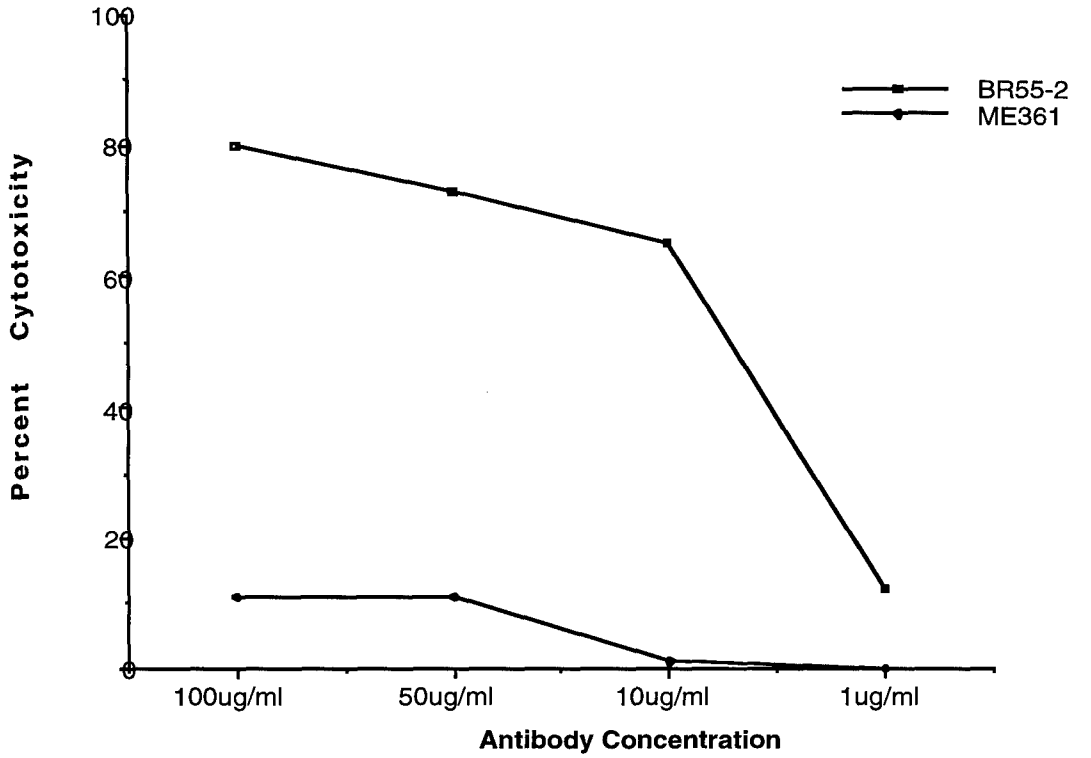

b) CDC killing by anti-peptide sera.

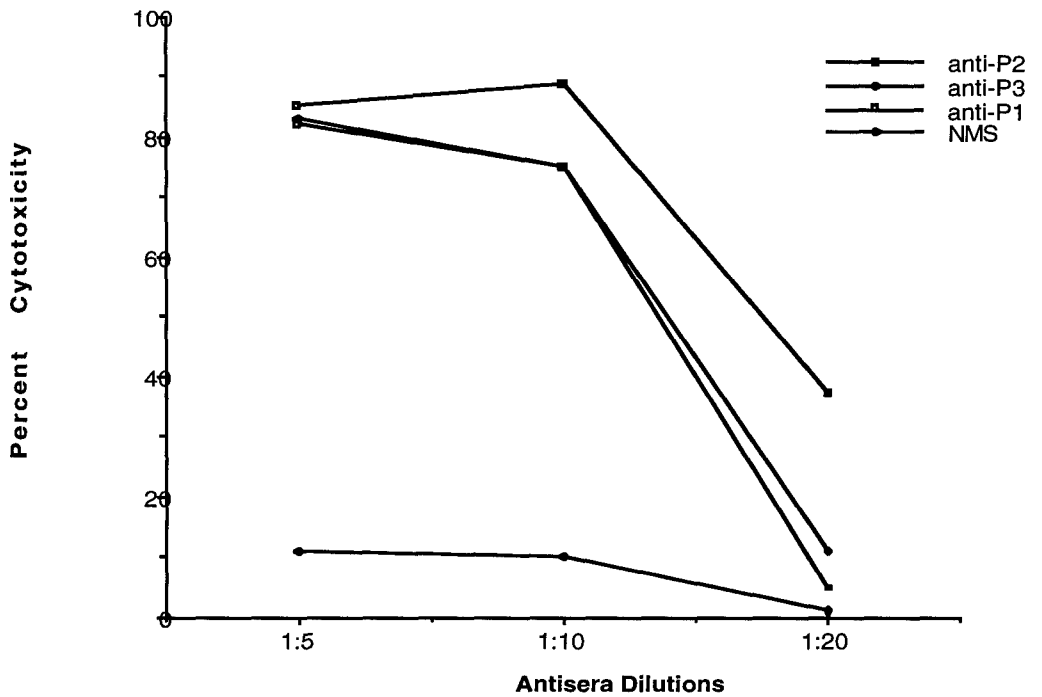

peptide sera mediate CDC of SKBR3 while normal mouse sera (NMS) does not. We are presently examining CDC of other human breast tumor lines.

Immunoprecipitation (IP) of SKBR3 fractions with the anti-peptide polyclonals indicate that the sera displays Immunoprecipitation profiles similar to that of BR55-2, bringing down neoproteins in the range >200,000 < 43,000 (data not shown). These profiles are in fact similar to that observed for anti-LeY antibodies B1 and B3, BR96. We found that treatment of cells with tunicamycin for 2 hrs. decreases carbohydrate expression reactive with BR55-2. Normal mouse sera did not react with any of the neoproteins, consistent with the FACs data. IP with ME361 indicates observable but little reactivity with neoproteins on the SKBR3 cell line. Treatment of SKBR3 cells with tunicamycin for 2 to 16 hrs decreased the reactivity of BR55-2 and the anti-peptide sera.

Phage displayed peptide mimics of Lewis Y

The ability of an antibody to react specifically with a carbohydrate epitope depends on the exposed nature of the terminal subunits and the accessibility of core carbohydrate structures. The role of core carbohydrate structures is to stabilize and impart the spatial disposition of branching terminal subunits. The degree of accessibility of core structures is most likely dependent on the nature and complexity of the branched subunits. In terms of mimicry several possibilities exist. For example, mimicry is dependent on the spatial distribution of carbohydrate functional groups. The more branched a complex carbohydrate is, the more likely the combinatorial spatial disposition of functional groups might lead to cross-reactivity. This result might also decrease the accessibility of core structures. Likewise, the smaller the carbohydrate or less branched and complex, the more likely that the core structure is exposed and the combinatorial spatial disposition of functional groups decreases. In addition, there are multiple ways a carbohydrate epitope can be recognized.

Our modeling studies on BR55-2 and B3 indicate that they contact LeY in a similar fashion, albeit perhaps with differing affinities. In the context of peptide mimicry, of interest is whether peptides mimic the conformational properties of carbohydrates in that they bind to the same amino acid contact sites on the antibody or that they interact with alternative contact sites and mimicry is really the result of steric inhibition. We observed that a peptide identified to bind to B3 does not bind to BR55-2 by ELISA, nor inhibits BR55-2-LeY interaction. When we modeled the mimicking peptide sequence APWLY in the B3 and BR55-2 binding site, we identified a critical distinction between the two antibodies involving position 97 in the heavy change. The Ala (B3) to Asp replacement at this position in BR55-2 precludes this peptide to bind to BR55-2, consistent with the inhibition studies. This facet suggests that peptides identified by phage display can be specific for their isolating antibody. Subsequently, it is possible that peptides identified by phage display that are considered cross-reactive with the anti-CHO antibody, are not necessarily recognized by the same mechanism as their carbohydrate counterparts, even though their binding sites are overlapping or adjacent.

To further examine this point, we have utilized a phage library containing 15 amino acids to screen the anti-Lewis Y antibodies BR55-2 and BR15-6A. The initial choice of using the 15 mer library was predicated on the notion that this length is similar to complementarity determining regions (CDR) in antibodies which confers mimicry capacity to many anti-idiotypic antibodies. Clones were isolated and sequenced (Figure 9) using a new approach to sequencing developed by us (manuscript #3 in appendix).

These sequences can be compared with a putative peptide identified by phage display panning with another anti-LeY antibody, B3 (21). We have tested the APWLYAP peptide for binding to BR55-2 and BR15-6A which proved negative. Nevertheless, the central Planar residue-X-Planar residue tract is represented in families 12, 14-17,21 and 22 for BR55-2 and observed in families 3,4,13 and 20 for 15-6A. In family 22, identified by BR55-2, an inverted tract WPYL is observed in comparison to the sequence PWLY found by B3. A sequence tract of WRY associated with α(1-4) glucose structure is observed in Family 17 of BR55-2. The above sequences were multiply aligned using the program Pileup (Fig 5). We observe that three groups 5&6, 13&14 and 18&19 are equivalent for the two anti-LeY antibodies, suggesting that perhaps these sets might be idiotypically connected since the two antibodies bind to Lewis Y in a non-competing fashion. We have also attempted to de novo design a peptide to selectively react

with BR55-2 using the approach above to place a peptide in the B3 combining site (see below). In our initial attempt we identified a sequence tract SFLL as a possibility. We observed such a tract in families 18 and 19 for BR55-2 and for 15-6A. This result indicates that we can define residues and peptides de novo that are equivalent to those that identified experimentally. It is anticipated that this type of analysis can be used to optimize peptides that are selective for particular antibody subsets, as well as defining peptides that are better mimics of CHO epitopes. Peptides are presently being made covering the various families based upon structural models of the 15 mer loop in comparison with studies on the CDR conformations of the recombinant antibody discussed above. These results indicate a rich source of diversity for peptide mimicry of carbohydrates.

Figure 9 Families for BR55-2 and BR15-6A include the following sequences:

Family	Phage ID	Sequence (1 ... 36)
1	15-6A-posSEQ11	.... .AGVALGSQS YGLHGP
2	BR55-posSEQ09	....T WPVVHGACRA HGHC..
3	15-6A-posSEQ06	..... .GFVLVYTFP SSVCCP.... .....
4	15-6A-posSEQ10	....LAFVWTVA VPPFPPG... .....
5	15-6A-posSEQ16	..... .GLDLLGDVR IPVVRR.... .....
6	BR55-posSEQ15	..... .GLDLLGDVR IPVVRR.... .....
7	BR55-posSEQ02	..... .GLDLLGDVR IPVVAS.... .....
8	BR55-posSEQ28	....SLVSSLD IRVFHRLP.. .....
9	BR55-posSEQ31	.....V GITGFVDPLP LRLL..... .....
10	BR55-posSEQ29	..... GAFSSPRSLT VPLRR..... .....
11	15-6A-posSEQ14	....LRASFFL EAARGSAS.. .....
12	BR55-posSEQ17	....AGRWV FSAPGVRSIL .....
13	15-6A-posSEQ17	.....H GRFILPWWYA FSPS..... .....
14	BR55-posSEQ12	.....H GRFILPWWYA FSPS..... .....
15	BR55-posSEQ30	.....F ARYLFTHWWR LPVD..... .....
16	BR55-posSEQ21	..... .RYLFYSVHP WRVSYS.... .....
17	BR55-posSEQ26	..... ARVSFWRYSS FAPTY..... .....
18	15-6A-posSEQ03	.....I MILLIFSLLW FGGA..... .....
19	BR55-posSEQ34	.....I MILLIFSLLW FGGA..... .....
20	15-6A-posSEQ01	....TVGASFWW LSGGKVP... .....
21	BR55-posSEQ13	.......GRV ASMFGGYFFF SR..... .....
22	BR55-posSEQ14	WPYLRFSPWV VSPLG..... ....
23	BR55-posSEQ10	.......TSV NRGFLLQRVS HP..... .....
24	BR55-posSEQ32	....ARFR HSTKSAQFVP L.....

Molecular mimicry of Lewis Y

In our studies we observed that the model of BR55-2 emphasizes the role played by the fucose methyl groups facing the floor of the antibody combining site. These methyl groups might be mimicked by methyl group containing amino acid residues in a designed peptide or anti-idiotypes that compete with Y for anti-Y antibodies. A peptide that mimics the Y antigen has been described (21) that contains such methyl groups. From a structural standpoint, several questions still need to be addressed that are germane to the development of effective peptide mimics of carbohydrates for utility in vaccine or adjuvant formulation, which is our primary interest (20). First, is the binding site of anti-carbohydrate antibodies different than anti-peptide antibodies. Second, why are anti-carbohydrate antibodies often times of low

affinity. In our own efforts to elucidate answers to such questions, we have been examining the structural basis for anti-Lewis Y antibody recognition of Lewis Y mimicking peptides. The nature of LeY binding was also observed to extend to another anti-Y antibody B3 (manuscript #4 in appendix). The tumor cell binding specificity's of B3, and BR55-2 are different. The B3 antibody has been found to bind to the peptide sequence APWLYGPA presented on phage display in which the putative sequence APWLY is critical for binding to the antibody (21). In that study a peptide with the sequence APWLYAGP was observed to bind to B3 and inhibit B3 binding to the Y carbohydrate structure. The B3 antibody displays homology with other anti-LeY antibodies, including the recently crystallized antibody BR96 co-crystallized with a nonoate methyl ester LeY tetrasaccharide. As with BR55-2, molecular modeling of B3 complexed with the putative tetrasaccharide core of LeY was performed based upon the BR96 -sugar recognition scheme (6). The B3 model emphasizes key polar and nonpolar interactions contributing to the molecular recognition features for Y that are shared among related anti-Y antibodies, consistent with mapping profiles of lactoseries derivatives reactive with B3 (28). While current procedures for predicting ligand - antibody interactions is limited, mainly due to the conformational flexibility of ligands and antibodies, and the role of solvent in mediating ligand recognition and binding, the utilization of a crystallographically determined starting position can lend to discriminating differences in binding orientations of analogues. Utilizing the positional information of the LeY structure we implemented the program Ligand-Design (LUDI (29) Biosym Technologies) to search a fragment library to guide in the position of the putative APWLY peptide sequence. Optimization of the positioned peptide indicates structural similarity between the carbohydrate tetrasaccharide core of LeY, with similar functional groups on the B3 structure in contact with the peptide. This analysis therefore provides a unique perspective of how a peptide sequence fits into the antibody combining site, competing with a native antigen.

In the placement of the B3 reactive putative peptide sequence APWLY, we made use of the program LUDI to identify compounds that potentially interact with the B3 combining site. This program constructs possible new ligands for a given protein of known three-dimensional structure. Small fragments are identified in a database and are docked into the protein binding site in such a way that hydrogen bonds and ionic interactions can be formed with the protein and hydrophobic pockets are filled with lipophilic groups of the ligand. The positioning of the small fragments is based upon rules about energetically favorable non-bonded contact geometry's between functional groups of the protein and the ligand. In this approach the OH-3^c position on the LeY structure was used as the sampling point. To identify possible fragments that are similar to the APWLY sequence, the radius of interaction was set as incrementing radii from 5 to 14 angstroms. Some 269 fragments were identified with the largest radius of interaction, with most redundant for the same set of potential hydrogen bond donors or acceptors on B3. In evaluating the fragments we compared fragments identified by LUDI relative to the APWLY sequence such that the fragments could occupy non-redundant sites and be spatially far enough to accommodate the peptide backbone. In affect one wants to "stitch" the fragments together to form a peptide. In particular LUDI found that a Tyr residue forms a hydrogen bond with Ser at position L31a, that a lipophilic residue representative of a Leu side chain is bounded by residues Tyr H32, His L31, and Asn L31b, a Trp residue forms a hydrogen bond with the B3 backbone carbonyl group at position H98 and another lipophilic residue representative of an Ala side chain is bounded by Ala H97. The APWLY sequence was then modeled such that the corresponding Trp, Tyr, Leu and Ala residues occupied relative positions as the identified LUDI fragments. In the positioning we observed that the AP residues of the peptide tract occupied a similar position as the LeY GlcNAc residue. This positioning indicates that the proline residue mimics the spatial position of the glucose unit of GlcNAc, while the Ala methyl group is positioned similarly as the terminal methyl group of GlcNAc's N- acetyl. Placement of the APWLY peptide in the B3-LeY binding site indicates that the Ala of the peptide interacts with Ala H97 of B3 (Figure 5). BR96 and another related anti-Y antibody, BR55-2, have an Asp residue at this position, while each display homologies in contacting the LeY core antigen (6). We have found that BR55-2 does not bind the APWLYGPA peptide in a series of ELISA assays (unpublished observations) suggesting that Asp H97

might interfere with peptide binding. To test this aspect we substituted an Asp residue into B3 at this position and found that the peptide-B3 interaction was destabilized by 12 Kcal. Calculations for LeY binding with the Ala at this position shows a more favorable energetic for binding (6) suggesting that the Ala at position H97 will enhance carbohydrate binding. This in fact is observed as deduced by mutatgenesis experiments on BR96 (30) and by our own calculations (6).

Conclusions:

The interplay between carbohydrates and proteins is of fundamental importance in a number of different biological processes. In particular, cell adhesion and cell recognition events are often mediated by protein-carbohydrate interactions forming a basis in the etiology of tumors. Aberrant glycosylation may be crucial in tumor progression, since cells acquire competence for metastasis and a faster clonal growth via newly synthesized carbohydrate structures. The carbohydrate expression patterns differ according to clinical features and are also changeable in clinical courses of respective tumors types. The differential exposure at the cell surface of specific carbohydrates may have implications for cell-protein or cell-cell interactions and for antibody-directed tumor detection and therapy. To date, the functional role of the Lewis antigens have not been fully explored. Presumably, these carbohydrates represent functional structures or determinants of molecules controlling cell motility, adhesion and proliferation, functions related to the metastatic potential of human cancers. Subsequently, antibodies that are directed to such antigens might prove useful as therapeutic agents either directly or as carriers for other agents. We have used phage display technology to identify human antibodies that react with Lewis Y and we have compared such sequences with those found by humanizing BR55-2. We are developing constructs for alternative antibody species that might prove useful as reagents to target LeY in passive therapy approaches.

Antibodies are also known to function as surrogates or mimics of ligand binding sites on receptors, binding to both receptor agonists and antagonists. Anti-Idiotypes to BR55-2 can induce anti-LeY responses. We chose BR55-2 and BR15-6A antibodies for phage screening to further identify potential relationships among peptides that mimic LeY. We have identified several peptide families binding to BR55-2 and BR15-6A whose sequences compare well with other our other peptides that mimic carbohydrate structures. We have shown that we can induce anti-carbohydrate immune responses that target breast cancer cells. In the coming year we will synthesize representative peptides and test their ability to induce anti-LeY responses.

Literature Cited

1. Blaszczyk-Thurin M, Thurin J, Hindsgaul O, Karlsson KA, Steplewski Z, Koprowski H. Y and blood group B type 2 glycolipid antigens accumulate in a human gastric carcinoma cell line as detected by monoclonal antibody. Isolation and characterization by mass spectrometry and NMR spectroscopy. J Biol Chem 1987;262(1):372-9.

2. Miyake M, Taki T, Hitomi S, Hakomori S. The correlation of expression of H/Ley/Leb antigens with survival of patients with carcinoma of the lung. Biochemistry 1992;327:14-18.

3. Steplewski Z, Blaszczyk TM, Lubeck M, Loibner H, Scholz D, Koprowski H. Oligosaccharide Y specific monoclonal antibody and its isotype switch variants. Hybridoma 1990;9(2):201-10.

4. Steplewski Z, Lubeck MD, Scholz D, Loibner H, McDonald SJ, Koprowski H. Tumor cell lysis and tumor growth inhibition by the isotype variants of MAb BR55-2 directed against Y oligosaccharide. In Vivo 1991;5(2):79-83.

5. Scholz D, Lubeck M, Loibner H, et al. Biological activity in the human system of isotype variants of oligosaccharide-Y-specific murine monoclonal antibodies. Cancer Immunology, Immunotherapy 1991;33(3):153-7.

6. Thurin-Blaszczyk M, Murali R, Westerink MAJ, Steplewski Z, Co M-S, Kieber-Emmons T. Molecular recognition of the Lewis Y antigen by monoclonal antibodies. Protein Engineering 1996;9:101-113.

7. Kieber-Emmons T, Von Feldt JM, Godillot PA, McCallus D, Weiner D, Williams WV. Isolated heavy chain variable regions derived from patients with active SLE bind DNA. Lupus 1994;in press.

8. Co MS, Baker J, Bednarik K, et al. Humanized anti-Lewis Y antibodies: in vitro properties and pharmacokinetics in rhesus monkeys. Cancer Research 1996;56(5):1118-25.

9. Livingston PO. Construction of cancer vaccines with carbohydrate and protein (peptide) tumor antigens. [Review]. Current Opinion in Immunology 1992;4(5):624-9.

10. Livingston PO, Calves MJ, Helling F, Zollinger WD, Blake MS, Lowell GH. GD3/proteosome vaccines induce consistent IgM antibodies against the ganglioside GD3. Vaccine 1993;11(12):1199-204.

11. Livingston PO, Adluri S, Helling F, et al. Phase 1 trial of immunological adjuvant QS-21 with a GM2 ganglioside-keyhole limpet haemocyanin conjugate vaccine in patients with malignant melanoma. Vaccine 1994;12(14):1275-80.

12. Livingston PO. Approaches to augmenting the immunogenicity of melanoma gangliosides: from whole melanoma cells to ganglioside-KLH conjugate vaccines. [Review]. Immunological Reviews 1995;145(147):147-66.

13. Longenecker BM, Reddish M, Koganty R, MacLean GD. Immune responses of mice and human breast cancer patients following immunization with synthetic sialyl-Tn conjugated to KLH plus detox adjuvant. Annals of the New York Academy of Sciences 1993;690(276):276-91.

14. Longenecker BM, Reddish M, Koganty R, MacLean GD. Specificity of the IgG response in mice and human breast cancer patients following immunization against synthetic sialyl-Tn, an epitope with possible functional significance in metastasis. Advances in Experimental Medicine & Biology 1994;353(105):105-24.

15. Springer GF, Desai PR, Tegtmeyer H, Carlstedt SC, Scanlon EF. T/Tn antigen vaccine is effective and safe in preventing recurrence of advanced human breast carcinoma. Cancer Biotherapy 1994;9(1):7-15.

16. Ravindranath MH, Morton DL. Role of gangliosides in active immunotherapy with melanoma vaccine. [Review]. International Reviews of Immunology 1991;7(4):303-29.

17. Helling F, Shang A, Calves M, et al. GD3 vaccines for melanoma: superior immunogenicity of keyhole limpet hemocyanin conjugate vaccines. Cancer Research 1994;54(1):197-203.

18. Helling F, Zhang S, Shang A, et al. GM2-KLH conjugate vaccine: increased immunogenicity in melanoma patients after administration with immunological adjuvant QS-21. Cancer Research 1995;55(13):2783-8.

19. Apostolopoulos V, McKenzie IF. Cellular mucins: targets for immunotherapy. [Review]. Critical Reviews in Immunology 1994;14(3-4):293-309.

20. Westerink MAJ, Giardina PC, Apicella MA, Kieber-Emmons T. Peptide mimicry of the meningococcal group C capsular polysaccharide. Proc. Natl. Acad. Sci. 1995;92:4021-4025.

21. Hoess R, Brinkmann U, Handel T, Pastan I. Identification of a peptide which binds to the carbohydrate-specific monoclonal antibody B3. Gene 1993;128(1):43-9.

22. Scott JK, Loganathan D, Easley RB, Gong X, Goldstein IJ. A family of concanavalin A-binding peptides from a hexapeptide epitope library. Proceedings of the National Academy of Sciences of the United States of America 1992;89(12):5398-402.

23. Oldenburg KR, Loganathan D, Goldstein IJ, Schultz PG, Gallop MA. Peptide ligands for a sugar-binding protein isolated from a random peptide library. Proceedings of the National Academy of Sciences of the United States of America 1992;89(12):5393-7.

24. Morrow WJ, Williams WM, Whalley AS, et al. Synthetic peptides from a conserved region of gp120 induce broadly reactive anti-HIV responses. Immunology 1992;75(4):557-64.

25. Iliopoulos D, Ernst C, Steplewski Z, et al. Inhibition of metastases of a human melanoma xenograft by monoclonal antibody to the GD2/GD3 gangliosides. Journal of the National Cancer Institute 1989;81(6):440-4.

26. Shattil SJ, Weisel JW, Kieber-Emmons T. Use of monoclonal antibodies to study the interaction between an integrin adhesion receptor, GPIIa-IIIb, and its physiological ligand, fibrinogen. Immun. Meth. 1993;1:53-63.

27. Prammer KV, Boyer J, Ugen K, Shattil SJ, Kieber-Emmons T. Bioactive Arg-Gly-Asp conformations in anti-integrin GPiib-iiia antibodies. Receptor 1994;4:93-108.

28. Pastan I, Lovelace ET, Gallo MG, Rutherford AV, Magnani JL, Willingham MC. Characterization of monoclonal antibodies B1 and B3 that react with mucinous adenocarcinomas. Cancer Research 1991;51:3781-3787.

29. Bohm HJ. LUDI: rule-based automatic design of new substituents for enzyme inhibitor leads. J Comput Aided Mol Des 1992;6(6):593-606.

30. Yelton DE, Rosok MJ, Cruz G, et al. Affinity maturation of the BR96 anti-carcinoma antibody by codon-based mutagenesis. Journal of Immunology 1995;155(4):1994-2004.

Protein Engineering vol.9 no.5 pp.447–459, 1996

Molecular recognition of the Lewis Y antigen by monoclonal antibodies

Magdalena Blaszczyk-Thurin[1], Ramachandran Murali[2], M.A.Julie Westerink[3], Zenon Steplewski[4], Man Sung Co[5] and Thomas Kieber-Emmons[2,6]

[1]The Wistar Institute of Anatomy and Biology, [2]Department of Pathology and Laboratory Medicine, University of Pennsylvania, 36th and Hamilton Walk, Philadelphia, PA 19104-6082, [3]Department of Medicine, Medical College of Ohio at Toledo, [4]Department of Medicine, Thomas Jefferson University, [5]Protein Design Labs, Inc., USA

[6]To whom correspondence should be addressed

The murine monoclonal antibody BR55-2 is directed against the tumor-associated antigen Lewis Y oligosaccharide. The Lewis Y core antigen is a difucosylated structure consisting of four hexose units. Analysis of binding profiles of lactoseries isomeric structures by BR55–2 suggest that the binding epitope includes the OH-4 and OH-3 groups of the β-D-galactose unit, the 6-CH_3 groups of the two fucose units and the *N*-acetyl group of the subterminal β-D-*N*-acetylglucosamine (βDGlcNAc). To elucidate the molecular recognition properties of BR55-2 for the Y antigen, BR55-2 was cloned, sequenced and its three-dimensional structure was examined by molecular modeling. The crystal structure of BR96, another anti-Lewis Y antibody, solved in complex with a nonoate methyl ester Lewis Y tetrasaccharide, and the lectin IV protein in complex with a Lewis b tetrasaccharide core were used as a guide to probe the molecular basis for BR55-2 antigen recognition and specificity. Our modeling study shows that BR55-2 shares similar recognition features for the difucosylated type 2 lactoseries Lewis Y structure observed in the BR96–sugar complex. We observe that a major source of specificity for the Lewis Y structure by anti-Y antibodies emanates from interaction with the β-D-*N*-acetylglucosamine residue and the nature of the structures extended at the reducing site of the fucosylated lactosoamine.

Keywords: anti-carbohydrate antibodies/carbohydrate antigens/Lewis antigens/Lewis Y/molecular modeling

Introduction

Cell-surface carbohydrates play a role in tumor growth, progression and metastases (Hakomori, 1989, 1991). Among the carbohydrate types, the histo-blood group Lewis antigens are highly associated with a number of cancers including human breast, colon, lung and ovarian carcinomas (Fukushi *et al.*, 1986; Itzkowitz *et al.*, 1986; Kim *et al.*, 1986; Blaszczyk-Thurin *et al.*, 1987; Hoff *et al.*, 1989, 1990; Cooper *et al.*, 1991; Tsukazaki *et al.*, 1991; Itzkowitz 1992; Miyake *et al.*, 1992; Murata *et al.*, 1992; Ogawa *et al.*, 1992; Ichihara *et al.*, 1993; Iliopoulos *et al.*, 1993; Kobayashi *et al.*, 1993). The Lewis Y (Y) difucosylated type 2 lactoseries structure, expressed on both glycoproteins and glycolipids, is one tumor-associated carbohydrate structure being explored as a target for monoclonal antibody (MAb)-based imaging and therapy (Trail *et al.*, 1993; Choe *et al.*, 1994). It is postulated that the Y determinant is of key importance for tumor cell growth or maintenance since it mediates internalization and killing with Y-specific MAb (Hellstrom *et al.*, 1990; Pai *et al.*, 1991, 1992; Steplewski *et al.*, 1991; Schreiber *et al.*, 1992 Garrigues *et al.*, 1993).

While a large number of anti-Y antibodies have been generated, their detailed specificity has been studied in only a few cases (Blaszczyk-Thurin *et al.*, 1987; Hellstrom *et al.*, 1990; Pastan *et al.*, 1991; Kitamura *et al.*, 1994). Reactivity patterns of antibodies with synthetic Y determinants might be different when compared with antibody tumor cell binding which depends on the presentation of Y on the tumor cell surface and also the number of hexose subunits defining the Y epitope. We previously described a monoclonal antibody, BR55-2, generated against a human gastric adenocarcinoma cell line, that specifically recognizes the Y determinant (Blaszczyk-Thurin *et al.*, 1987; Steplewski *et al.*, 1990, 1991; Scholz *et al.*, 1991). Monoclonal BR55-2 (IgG3) and its isotype switch variants are found to mediate both antibody-dependent cell-mediated and complement-dependent cytotoxicity and efficiently inhibit tumor growth in xenografted nude mice (Steplewski *et al.*, 1990, 1991). Humanized or chimeric forms of anti-Y antibodies that share some of the properties of BR55-2 are being considered for passive therapy (Kaneko *et al.*, 1993; Kitamura *et al.*, 1994) and BR55-2 is in clinical trials. An increased understanding of the structural basis for antibody recognition of the Y antigen might be exploited to develop improved diagnostic agents and passive and active immunotherapeutics for Y expressing solid tumors.

NMR studies of synthetic Y and Lewis b (Le^b) structures show that the major difference in topography between Le^b and Y molecules is provided by the change of glycosidic linkage from β1→3 to β1→4 in type 1 and 2 chains, respectively (Lemieux *et al.*, 1980; Thogersen *et al.*, 1982; Lemieux and Bock, 1983; Hindsgaul *et al.*, 1985; Rao and Bush, 1988; Cagas and Bush, 1990, 1992; Chai *et al.*, 1992; Strecker *et al.*, 1992). The differences in the glycosidic linkages result in conformers in which the *N*-acetyl and hydroxymethyl groups of the GlcNAc moiety are projected on opposite sides of the type 1 and 2 structures (Figure 1a). Functional groups that are shared or define the common topography between the type 1 and type 2 structures account for their mutual recognition by GS4 (Spohr *et al.*, 1985a). The immunodominant portion of the antigen detected by BR55-2 and other related MAbs is specific for the type 2 Y determinant but not the type 1 isomeric determinant, Le^b. This type 2 specific recognition is in contrast to the lectin IV protein of *Griffonia simplicifolia* (GS4), suggesting that BR55-2 and related MAbs mimic only a portion of the salient recognition features of GS4 for Y.

The aim of the present study was to identify the molecular basis for BR55-2 Y specificity by characterizing the dimensions and similarities of BR55-2 with other anti-Y antibodies. BR55-2 was cloned and sequenced and molecular modeling was

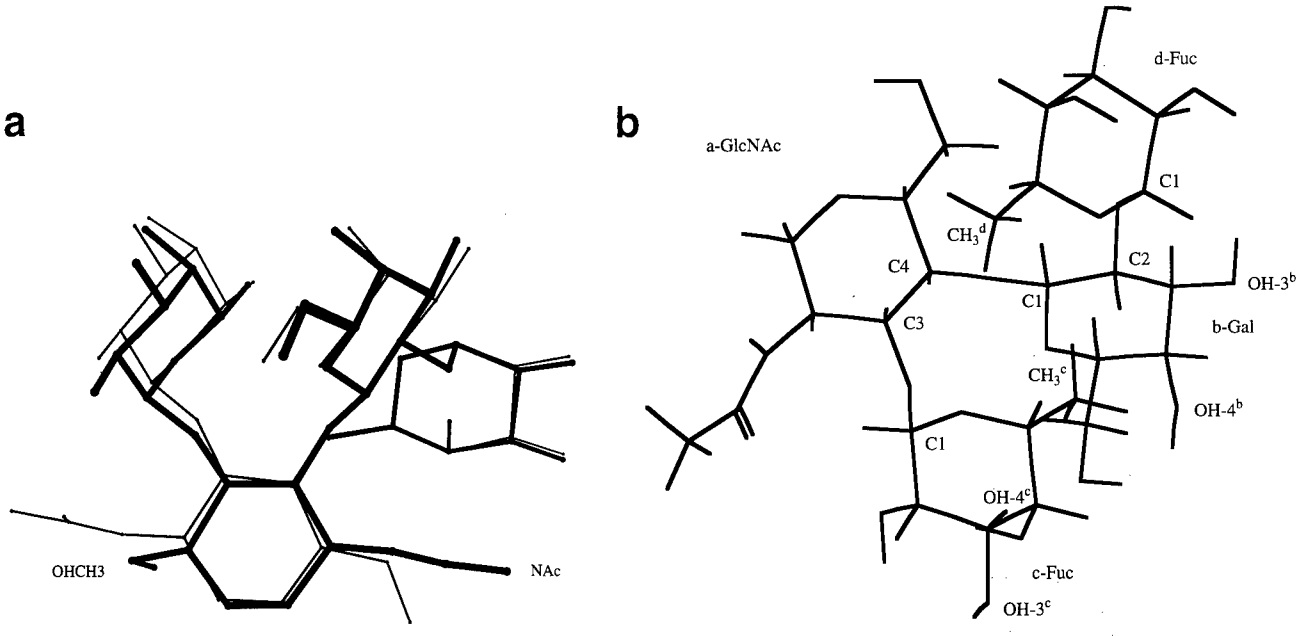

Fig. 1. Similarity in structure and recognition patterns observed for Lewis Y and Le^b structures. (**a**) Superposition of Y (dark line) and Le^b (light line) structures highlighting the *N*-acetyl and hydroxymethyl groups projected on opposite sides of the type 1 and 2 difucosylated structures. Superpositioning indicates that inspite of the change of glycosidic linkage from β1–3 to β1–4 in the type 1 and 2 chains, resulting conformational features of the respective sugar moieties are still shared forming a common topography. (**b**) Stick rendering of the Y tetrasaccharide core, implicating the surface recognized by BR55-2 and lectins by considering mapping information in Table I. The a, b, c, d designations refer to the βDGlcNac, βDGal, αLFuc(1→3) and αLFuc(1→2) units, respectively.

used to elucidate its three-dimensional structure. During the performance of this work the crystal structure of an anti-Y antibody, BR96 in complex with a Y epitope was reported (Jeffrey *et al.*, 1995). Since the crystal coordinates for BR96 are not yet available, molecular modeling of BR55-2 was utilized to identify similarities in the recognition scheme for the Y tetrasaccharide core by BR55-2 based on the BR96–Y co-complex structural features. Potential BR55-2 interaction sites with the putative tetrasaccharide of the Y determinant were identified and further compared with related anti-Y antibodies, B3 (Brinkmann *et al.*, 1991; Pastan *et al.*, 1991; Pai *et al.*, 1991, 1992; Choe *et al.*, 1994), and H18A (Kaneko *et al.*, 1993). The BR55-2 model emphasizes key polar and non-polar interactions contributing to the molecular recognition features for Y that are shared among the related anti-Y antibodies, consistent with results from examination of reactive profiles of lactoseries oligosaccharide probes with BR55-2. We observe that a major source of differential specificity for the type 1 and 2 difucosylated structures emanates from its interaction with the β-D-*N*-acetylglucosamine residue as compared with GS4, which most likely extends to other anti-Y antibodies.

Materials and methods

Cloning and sequencing of the heavy-chain and light-chain variable-domain cDNA for BR55-2

The variable-domain cDNA for the heavy-chain and light-chain of BR55-2 was cloned by the anchored PCR method (Co *et al.*, 1992). First, a total RNA preparation was prepared using the hot phenol method. Briefly, 1×10^7 BR55-2 hybridoma cells were resuspended in 1.2 ml of RNA extraction buffer (50 mM sodium acetate, pH 5.2–1% SDS), vortexed and incubated at room temperature for 2 min. The cell lysates were then incubated with 0.6 ml of phenol, pH 5.2, at 65°C for 15 min, followed by another 15 min incubation on ice. The extract was spun in a microfuge; the aqueous phase was recovered and ethanol precipitated twice. The RNA pellet was resuspended in water and quantitated at OD_{260}. cDNA was synthesized from the total RNA using reverse transcriptase [5 μg total RNA, 40 ng dT_{12-18} (Pharmacia), 200 units of M-MLV reverse transcriptase (BRL), 40 units of RNAsin (Promega), 50 mM Tris–HCl, pH 8.3, 75 mM KCl, 10 mM DTT, 3 mM $MgCl_2$ and 0.5 mM each dNTP in a 20 μl reaction volume]. The G-tailing was achieved with terminal deoxynucleotidyl transferase (TdT) [cDNA, 15 units TdT (BRL), 0.1 M potassium cacodylate, pH 7.2, 2 mM $CoCl_2$, 0.2 mM DTT and 1 mM dGTP in a 20 μl reaction volume]. Under the conditions described, tails generally contained about 20 bases. One half of the G-tailed product was then amplified to generate the V_L gene and the other half amplified to generate the V_H gene, using Taq polymerase. The V_L gene was amplified with the primer TATATCTAGAATTCC-CCCCCCCCCCCCCCC that anneals to the G tail and a primer TATAGAGCTCAAGCTTGGATGGTGGGAAGATG-GATACAGTTGGTGC that anneals to the constant region of the kappa light chain. The V_H gene was amplified with the same C tail primer and a primer TAGAGCTCAAGC-TTCCAGTGGATAGAC(CAT)GATGGGG(GC)TGT(TC)G-TTTTGGC that anneals to the C region of gamma chains. The sequences in parentheses indicate base degeneracies, which were introduced so the primer would be able to recognize all gamma chain isotypes. *Eco*RI and *Hin*dIII sites are included in the upstream and downstream primers for convenient subcloning into pUC18 vector. An alternative set of restriction sites (*Xba*I and *Sac*I) are also included in the primers for the rare event that *Eco*RI and *Hin*dIII sites are present in the variable region genes.

The PCR reactions were performed in a programmable

heating block using 30 rounds of temperature cycling (92°C for 1 min, 50°C for 2 min and 72°C for 3 min). The reaction included the G-tailed product, 1 μg of each primer and 2.5 units of Taq polymerase (Perkin-Elmer Cetus) in a final volume of 100 μl, with the reaction buffer recommended by the manufacturer. The PCR product bands were excised from a low-melting agarose gel, digested with restriction enzymes and cloned into pUC18 vector for sequence determination.

Modeling of BR55-2

We and others have developed procedures for antibody modeling (Fine *et al.*, 1986; Bruccoleri and Karplus, 1987; Shenkin *et al.*, 1987; Bruccoleri *et al.*, 1988; Novotny *et al.*, 1990; Cheetham *et al.*, 1991; Martin *et al.*, 1991; Mas *et al.*, 1992; Nell *et al.*, 1992; Tomiyama *et al.*, 1992; Lohman *et al.*, 1993; Bajorath 1994; Lin *et al.*, 1994) based on the fact that the shapes of heavy and light chains are closely associated with the lengths of complementarity determining regions (CDRs) and that framework (FR) residues play an important role in influencing CDR conformations (Chothia *et al.*, 1992; Tramontano and Lesk, 1992). The conformations of the variable domains of BR55-2 were deduced by comparison with known immunoglobulin crystal structures (Bernstein *et al.*, 1977). Sequence comparisons were used to identify templates for the localized structural folds of the hypervariable or CDR1, CDR2 and CDR3 regions of the heavy and light chains. For modeling of the heavy chain CDR3 region in particular, we utilized both a knowledge-based approach (Blundell *et al.*, 1987) to search for suitable structures that fit a geometry to the base residues of the CDR3 domain (Fine *et al.*, 1986; Shenkin *et al.*, 1987; Martin *et al.*, 1991) and a conformational search procedure (Bruccoleri *et al.*, 1988; Novotny *et al.*, 1990; Mas *et al.*, 1992; Nell *et al.*, 1992). The latter involved using the program AbM (Oxford Molecular)

To determine a base geometry for H-CDR3, the Cα positions of several antibodies of known crystal structure were superimposed to define invariant residue positions. These positions defines the amino-terminal beginning and the carboxyl-terminal end that are shared among the putative CDR3 domains of varying lengths (Tomiyama *et al.*, 1992; Karp *et al.*, 1993; Lohman *et al.*, 1993; Lin *et al.*, 1994). The systematic superpositioning of the CDR3 domain over short sequences defines a consensus region where the base geometry is conserved among the antibody templates. The description of invariant positions effectively reduces the length of the loop to search to those that are representative of a sufficient saturation of conformational space in the crystallographic database; usually six to seven residues in length. The crystallographic database was searched to identify loops of the same size as the CDR3 loop being examined using the program InsightII (version 3.5, Biosym Technologies). The spatially conserved Cartesian positions of the N- and C-terminal regions of CDR3 were held fixed in this search procedure. The 10 best matches were examined using the program InsightII and an appropriate choice was made based upon similarities in positions of side chains at the junctures of the CDR3 loop. As an alternative to this approach we also utilized the automated antibody modeling program AbM which incorporates a knowledge based search, followed by conformational mapping.

The CDRs and the FRs of the templates were mutated to those of the respective antibody heavy and light chains using InsightII or automatically assigned by AbM. For the InsightII-built structures, the side chain angles of the substituted residues were set according to angles identified in a database of side chains. Each CDR and framework region was changed individually, followed by 1000 cycles of energy minimization to eliminate close contacts between atoms. As in our previous studies, the program Discover (version 2.95, Biosym Technologies) was used for conformational calculations with the supplied consistent valence force field (CVFF) parameters. After model building, the respective structures were energy optimized to convergence. Molecular dynamics (MD) at 300 and 600 K was used to alleviate further any close contacts within the antibodies.

Initially a molecular dynamics simulation over 30 ps using the program Discover was performed. The structure was then energy minimized using conjugate gradients to convergence. Following this initial equilibration, the calculation was resumed for another 20 ps at 600 K at constant pressure and then cooled to 300 K over 30 ps. During the second dynamics procedure atoms lying further than 15 Å from all atoms of the CDR loops were held fixed. Non-hydrogen atoms of residues lying in the region 9–15 Å from all CDR loop atoms were harmonically restrained to their initial positions with a force constant of 30 kcal/mol.rad^2. These distance approximations result in fixing or restraining atoms of residues within the framework region of the antibodies. The backbone conformation torsion angles, phi (ϕ) and psi (ψ), of non-CDR loop residues were restrained to their initial values with a force constant of 1600 kcal/mol.rad^2. In addition, a torsional restraint of 10 kcal/mol.rad^2 was employed around the peptide bond. A time step of 1 fs was used. The resulting structure for BR55-2 was energy minimized using conjugate gradients to convergence.

Systematic conformational search of Lewis antigens

Systematic conformational searches over torsional space on both Y and Le^b were performed to relate their binding mode conformations. Utilizing a grid search approach each dihedral angle is stepped through a range of values, and resulting conformations are then steric free. Conformational search calculations were performed using the program Search and Compare (version 2.3.5, Biosym Technologies). The respective units in Y and Le^b were searched over conformational space at 1 or 5° intervals either holding (ϕ,ψ) angles for fixed glycosidic linkages to their binding mode values or allowing all angles to move concomitantly. Glycosidic (ϕ,ψ) angle definitions follow those previously published (Lemieux and Bock, 1983; Mukhopadhyay and Bush, 1991). Angle (ϕ^1,ψ^1) defines rotations about H_1–C_1–O–C_a (ϕ^1), and C_1–O–C_a–H_a (ψ^1). Similarly, (ϕ^2,ψ^2) corresponds to the IUPAC convention in which ϕ^2 corresponds to O ring–C_1–O_1–C'_x, and ψ^2 is defined as C_1–O_1–C'_x–$C'_x - 1$.

Molecular dynamics calculations were also performed for both Le^b and Y tetrasaccharide structures. The structures were first equilibrated at 300 K for 50 ps, followed by 100 ps of molecular dynamics at 300 K. A total of 100 000 conformations were sampled with instantaneous dynamics structures minimized at 1 ps intervals, reducing the number of structures to be examined to 100. The 100 structures were minimized to convergence using conjugate gradients. The differences in populations of the two molecules were analyzed using the Analysis option in InsightII. *In vacuo* calculations were performed with a dielectric of 1 or 80 to monitor electrostatic effects on final conformations.

Docking of Lewis Y to BR55-2

Individual subunits derived from crystal structures of carbohydrate fragments was used to model the putative Y tetrasaccharide core Fucα1→ 2Galβ1→4(Fucα1→)GlcNAc structure. The modeled structure was first energy minimized and compared with published computational (Lemieux and Bock, 1983; Mukhopadhyay and Bush, 1991) and NMR (Cagas and Bush, 1990, 1992) results on Y and Le^b determinants. Residues associated with the CDR loops were identified for possible interaction with the Y determinant based upon BR96 binding to Y (Jeffrey *et al.*, 1995) and Lewis antigen recognition by GS4 (Delbaere *et al.*, 1993). The approach taken in the placement of the Lewis Y core in the antibody combining site was that described previously by us (Lin *et al.*, 1994). The binding surface on the modeled antibodies was first defined as sites accessible to probe spheres of varying radii (1.4–1.7 Å) to identify possible positions which could be occupied by the atoms of the Y structure. The probe spheres were rolled on the binding surface of the models, with the continuum of loci reduced to a set of discrete points by clustering neighboring spheres much like a set of site points (Lin *et al.*, 1994). These site points are localized at atom positions accessible to the probe spheres on each residue on the surface of the antibody. The site points were then used as a guide in the placement of the Y structure. Hydrogen bonding restraints were applied to enhance potential contacts between the respective antibody combining site residues with sugar groups identified in the BR96/LeY structure (Jeffrey *et al.*, 1995), allowing the glycosidic angles of the Y structure to change and the BR55-2 model to adjust to these restraints.

After minimization, a restrained molecular dynamics calculation over 100 ps using the program Discover was performed, preserving the hydrogen bonding constraints. The dynamics run was not intended to be a detailed study, but to alleviate further any close contacts within the antibody and between tetrasaccharide and the antibody. The calculation was initialized and equilibrated for 50 ps at 300 K at constant pressure and resumed for another 50 ps. The resulting structure was energy minimized using conjugate gradients to convergence. In the minimization and dynamics run, no constraints other than the retention of Y-antibody hydrogen bonds were placed on the antibody or binding site. Charges and non-bonded parameters for the Y structure were assigned from atom types from the CVFF parameter list supplied with Discover/InsightII.

Results

Mapping of recognition sites of Lewis binding proteins

Natural oligosaccharides and synthetic probes of Lewis antigens have been used in a variety of studies to map potential recognition sites on lectins and antibodies (Young *et al.*, 1983; Lemieux *et al.*, 1984, 1985; Hindsgaul *et al.*, 1985; Spohr *et al.*, 1985a,b; Blaszczyk-Thurin *et al.*, 1987; Lemieux *et al.*, 1988; Spohr and Lemieux, 1988; Lemieux *et al.*, 1990). Based upon analysis of the binding profiles of lactoseries isomeric structures by BR55-2, we previously identified epitope reactive groups that include the OH-4 and OH-3 groups of the β-D-galactose unit, the 6-CH_3 groups of the two fucose units and the *N*-acetyl group of the subterminal β-D-*N*-acetylglucosamine (βDGlcNAc) (Blaszczyk-Thurin *et al.*, 1987). A similar interaction pattern involving OH-3 and/or OH-4 of the terminal galactose as key polar groups is postulated for the interaction of six other MAbs (Le^a, B blood group, Le^b and I Ma specific antibodies) (Lemieux *et al.*, 1984, 1985, 1988; Spohr *et al.*, 1985b) and lectins [*Ulex europaeus* (Hindsgaul *et al.*, 1985) and GS4 (Spohr *et al.*, 1985a)] (Table I).

Our interpretation of the reactivity patterns (Table I) indicates that $OH\text{-}4^b$, $OH\text{-}3^b$, $OH\text{-}4^c$ and $OH\text{-}3^c$ of the Y molecule might be involved in BR55-2 binding (Figure 1b). A similar hydroxyl group cluster which consists of $OH\text{-}3^b$, $OH\text{-}4^b$ and $OH\text{-}4^c$ is found to be a part of a topography recognized on Le^b and Y determinants by GS4 (Spohr *et al.*, 1985a) and on the H-2 structure recognized by *U.europaeus* lectin I (Hindsgaul *et al.*, 1985). Adjacent to the hydroxyl clusters, a lipophilic surface formed by $CH_3{}^c$ and $CH_3{}^d$ as well as $O\text{-}5^d$ is postulated to interact with both BR55-2 and GS4 (Blaszczyk-Thurin *et al.*, 1987). The $OH\text{-}4^d$ unit might also contribute to the amphiphilic binding surface since it is present at the edge of the proposed epitope for both BR55-2 and GS4. The involvement of the OH-2 group in a-2-fucose recognition of Le^b with MAb and GS4 is also observed. Since GS4 binds to the common surface in both Le^b and Y, this functional group might also be involved in Y recognition by BR55-2.

The acetamido group of the βDGlcNAc residue, part of the binding epitope for Y of BR55-2, is also involved in binding of specific MAbs with Ma I (Lemieux *et al.*, 1984) and Le^b (Spohr *et al.*, 1985b). The specific recognition of the H-2 structure by the lectin *U.europaeus* does not significantly involve the *N*-acetamido group, but does involve the 6-hydroxyl group in the binding reaction (Hindsgaul *et al.*, 1985). On the other hand, MAbs specific for the type 1 Le^a determinant recognize both sides of the β-D-*N*-acetylglucosamine unit with the recognition of CH_2OH being polar in character and that on the acetamido side non-polar (Lemieux *et al.*, 1988).

The nature of the combining site for several anti-Y antibodies that include BR64, BR96 (Hellstrom *et al.*, 1990), BR55-2 (Blaszczyk-Thurin *et al.*, 1987), BR16-5A (Rodeck *et al.*, 1987), B1 and B3 MAbs (Pastan *et al.*, 1991) and AH-6 (Abe *et al.*, 1986) appear to be similar in that they all map to the terminal portion of the Y oligosaccharide. Examination of cross-reactive patterns of the antibodies with synthetic Y probes suggest that they require α-2-fucose for binding and that α-3-fucose increases the binding but is not required. The B1 antibody displays slight cross-reactivity with the type-1 Le^b structure and B-3 binds to di- and tri-fucosylated LeX structures as well as a trifucosyl Le^a/LeX hybrid structure. A distinct group of antibodies recognize only extended Y structures (Kaizu *et al.*, 1986; Kim *et al.*, 1986; Nudelman *et al.*, 1986). These differences in reactivity clearly suggest that Y reactive antibodies recognize different epitopes. This differential specificity might also be extended to interaction with both tumor and normal cells. This difference in the length of the oligosaccharide side chains has important implications for the binding of MAbs to certain cells which have the ability to synthesize extended type 2 chain antigens, such as carcinoma cells.

Sequence and structural similarities between anti-Y antibodies

To define better the functional groups involved in molecular recognition of Y determinants, we cloned and sequenced BR55-2 and compared its sequence/structural properties with several other described anti-Y antibodies, B3 (Brinkmann *et al.*, 1991), H18A (Kaneko *et al.*, 1993) and BR96 (Bajorath, 1994; Jeffrey *et al.*, 1995). The nucleotide sequence and the translated amino acid sequence of the light chain and heavy-

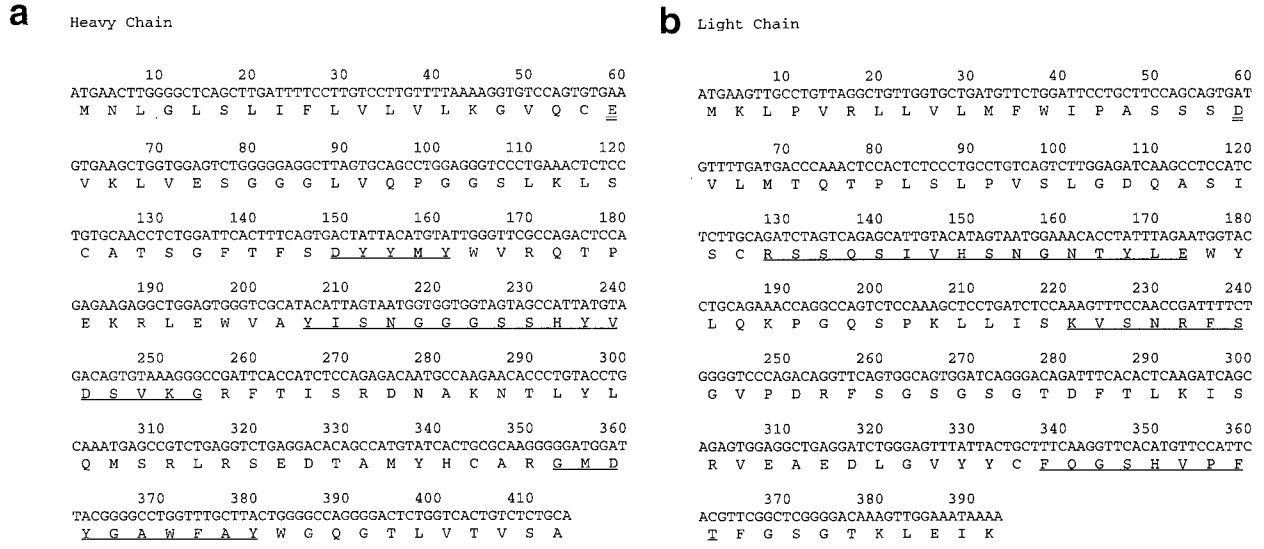

Fig. 2. Nucleic acid and amino acid sequence of (a) the heavy chain and (b) the light chain of BR55-2. The first amino acid of the mature protein is double underlined. CDRs are underlined.

Table I. Summary of functional groups implicated in molecular recognition of Lewis structures with MAbs and lectins[a]

MAb/lectin	βDGalb	α-2-Fucd	α-3,4-Fucc	βDGlcNAca		Ref.[b]
		Key polar interactions			Non-polar interactions	
Type 2						
Y	OH-4b		OH-4c	NAca	6-CH_3c	1
BR55-2	(OH-3b)		OH-3c		6-CH_3d	
H-2, *Ulex europaeus* I	(OH-3b)		OH-4c OH-3c (OH-2c)	OH-6a	6-CH_3c	2
Type 1						
Lea	OH-2b		OH-3c	NAca	6-CH_3c	3
AH8-34	OH-3b			6-OHa		
CF4-C4	OH-3b OH-4b		OH-4c	NAca 6-OHa	6-CH_3c	3
Leb	OH-3b	OH-2d		NAca	6-CH_3c	4
96FR					6-CH_3d	
Type 1 and 2						
Y/Leb	OH-3b	OH-2d	OH-4c		(6-CH_3d)	5
Griffonia simplicifolia B blood group terminal	OH-4b				6-CH_3c OH-3d	6
MAb-1	OH-4b OH-2e*				6-CH_3d 6-CH3e	7
MAb 2	OH-4b OH-2e* OH-3e*				6-CH_3d 6-CH_3e	7
Ma I	OH-4b OH-6b			NAca		8

[a]Atom lower case scripts are those defined in Figure 1. The designation e* refers to the terminal Gal residue of Galα1→3Galβ1→4GlcNAc B blood group structure. Parentheses indicate marginal interactions depending on the number of saccharide units associated with the antigen.
[b]1, Blaszczyk-Thurin *et al.* (1987); 2, Hindsgaul *et al.* (1985); 3, Lemieux *et al.* (1988); 4, Spohr *et al.* (1985b); 5, Spohr *et al.* (1985a); 6, Delbaere *et al.* (1993); 7, Lemieux *et al.* (1985); 8, Lemieux *et al.* (1984).

chain variable domain of BR55-2 is shown in Figure 2. Sequence analysis of BR55-2 shows that VH and V kappa genes are in the VH 7183 family and V kappa C1 family, respectively. Sequence alignment (Figure 3) indicates that the anti-Y antibodies are homologous with each other, except in their heavy-chain hypervariable or CDR regions.

Sequence comparison with known immunoglobulin crystal structures in the Brookhaven Protein database (Bernstein *et al.*, 1977) provide a template for the variable regions of the antibodies (Figure 3). The primary structure of the light chain of the anti-cholera toxin antibody TE33 (1TET) and the autoantibody BV04-01 (1CBV) displayed 96% and 89% identity, respectively, with the BR55-2 light chain (Figure 3). Both of these antibodies have been elucidated by X-ray crystallography as a complex with their respective ligands. Superposition of these two light chains indicates that their CDR conformations are nearly the same except for CDR1 around the sequence tract 'S–N–G' of BVO4-01. The conformational difference appears to be due to an induced conformation in TE33 upon the binding of the cholera toxin

a Light Chain

```
                                10                  20                  31 a b c d e 32
BR55    D V L M T Q T P L S L P V S L G D Q A S I S C R S S Q S I V H S N G N T Y L E W
B3      - - - - - - S - - - - - - - - - - - - - - - - - - - - I - - - - - - - - - - -
H18A    - - - - - - - - - - - - - - - - - - - - - G - G - - - I - T - - - - - - - - -
BR96      -                                                   - - - I - - - N - - - - -
TE33    - - - - - - - - - - - - - - - - - - - - - K - - - - - - - - - S - - - - F - -
BV04    - - V - - - - - - - - - - - - - - - - - - - - - - - - - - - L - - - - - - - H -

                40                  50                  60                  70
BR55    Y L Q K P G Q S P K L L I S K V S N R F S G V P D R F S G S G S G T D F T L K I
H184    - - - - - - - - - - - - - Y - - - - - - - - - - - - - - - - - - - - - - - - - -
B3      - - - - - - - - - - - - - Y - - - - - - - - - - - - - - - - - - - - - - - - - -
BR96                          L   - - -                       -                   -
TE33    - - - - - - - - - - - - - Y - - - - - - - - - - - - - - - - - - - - - - - - - -
BV04    - - - - - - - - - - - - - Y - - - - - - - - - - - - - - - - - - - - - - - - - -

                80                  90                  100
BR55    S R V E A E D L G V Y Y C F Q G S H V P F T F G S G T K L E I K
H184    - - - - - - - - - - - - - - - - - - - - - - - - - - - - - - - -
B3      - - - - - - - - - - - - - - - - - - - - - - - - - - - - - - - -
BR96                          - - - - - - -
TE33    - - - - - - - - - - - - - - - - - I - - - - - - - - - - - - - -
BV04    - - - - - - - - - - - F - S - S T - - - L - - - A - - - - - L -
```

b Heavy Chain

```
                                10                  20                  30
BR55        E V K L V E S G G G L V Q P G G S L K L S C A T S G F T F S D Y Y M
B3          - - - - - - - - - - - - - - - - - - - - - - - - - - - - - - - - - - - - -
H18A        - - - - - - - - - - - - - - - - - - - - - - - - - - - - - - - - - - - - -
BR96                                                                - - - - - - - - -
B13i2       - - Q - - - - - - - - - - K - - - - - - - - - - - A - - - - - - R C A -
Fab17/9     - - Q - - - - - - - - - - K - - - - - - - - - - - A - - - S - - S - G -

                    40                  50  52 a 53            60
BR55        Y W V R Q T P E K R L E W V A Y I S N G G G S S H Y V D S V K G R F
B3          - - - - - - - - - - - - - - - - - - - - D D S - A A - S - T - - - - F
H18A        - - - - - - - - - - P - - - - - - - - - - D I P Y - L - T - - - - F
BR96                                                Q - - D
B13i2       S - - - - - - - - - - - - - - - - G - - S - - S Y T F - P - T - - - - F
Fab17/9     S - - - - - - - D - - - - - - - - T - - - - - - - Y T Y - P - - - - - - F

                70                  80  82 a b c 83             90
BR55        T I S R D N A K N T L Y L Q M S R L R S E D T A M Y H C A R G M D Y
B3          - - - - - - - R - - - - - - - - - - - - - - - - - K - - - - - I - S - - - - L A W
H18A        - - - - - - - - - - - - - - - - - - - - - - - - - K - - - - - - - - Y - - - - K Y -
BR96                  -                                                                 - L - D
B13i2       I - - - N - - R - - - S - - - - - - - - - - - - - - - - - I - - - T - Y S S D
Fab17/9     - - - - - - - - - - - - - - - - - - - - - K - - - S - - - - -

                100
BR55        G A W F A Y W G Q G T L V T V S A
B3          - - - - - - - - - - - - - - - - S
H18A        - - - - - - - - - - - - - - - - -
BR96        - - - - - -
B13i2       P F Y - D - - - - - - T L - - - S
Fab17/9
```

Fig. 3. Sequence alignment of (**a**) the light and (**b**) the heavy chains of BR55-2, B3, H18A and BR96, among themselves and with template crystal structures as identified by Blast search of the protein crystallographic database on the NCBI BLAST server. Dashes indicate identities with respect to BR55-2. Numbering corresponds to that of Kabat *et al.* (1987). Only a partial sequence has been presented for BR96 (Bajorath, 1994). The structure of the light chain of TE33 (Brookhaven code 1TET (Bernstein *et al.*, 1977)) was used as a template for the modeling of BR55-2 and B3 light chain. For the heavy chain the B13i2 structure (2IGF) was used as the template. This structure displayed equivalent length CDRs with respect to the anti-Y antibodies. The antibody 17/9 has a longer CDR3 region than the anti-Y antibodies.

peptide to TE33. Subsequently these structures appear to reflect conformational changes that might be evident upon ligand binding. In the modeling of BR55-2 we utilized the TE33 template for the light chain, but the CDR1 conformation of BV04-01.

For the heavy chain of BR55-2, we identified two immunoglobulin templates, 17/9 (1HIM) and B13i2 (2IGF) which are co-complexed with peptides derived from their respective antigens, displaying 78% and 69% identity, respectively, with BR55-2 up to CDR3. Superpositioning of these structures indicates that they display nearly the same conformations up to the CDR3 region (residues 1–95) with an r.m.s. of 0.47 Å, suggesting CDR1 and CDR2 conformations have undergone similar conformational transitions, if any. This aspect is of relevance in considering that the CDR2 of 17/9 and BR55-2 each display three glycines (Figure 3) which in principle can adopt unusual ϕ/ψ angles. In comparison with B13i2, which displays a 'G–G–S' sequence for residues 53–55, the canonical conformations are equivalent for 17/9 and B13i2.

To model the CDR3 region of the BR55-2 heavy chain, we first examined CDR3 folding patterns of several crystallographicaly known immunoglobulins. Analysis of immunoglobulin crystal structures indicates that CDR3 loop regions can adopt conformations that fall into two general classes which have been referred to as kinked and unkinked (Mas *et al.*, 1992), despite their considerable variability in length, sequence

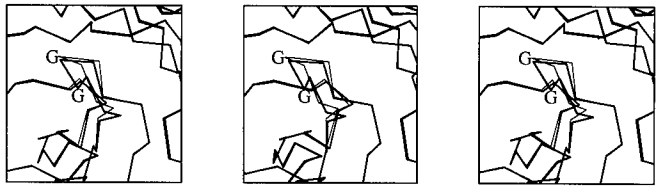

Fig. 4. Stereoview of BR55-2 looking down the binding site emphasizing the sequence-dependent transition of the CDR3H loop. The difference between the structures is the position of the Gly as indicated (see text). This figure was drawn using MOLSCRIPT (Kraulis, 1991).

Table II. Model of CDR3 VH utilizing least-squares fitting to define invariant residues

Antibody designation	Conserved structure	Putative loop	Conserved structure	R.m.s. (Å)
B13i2	CTR	YSSDPFY	FDYWGQG	
BV04–01	CVR	DQTGTAW	FAYWGQG	0.60
1DBM	CTR	GDYVNWY	FDVWGAG	0.53
H18A	CAR	GKYYGAW	FAYWGQG	
B3	CAR	GLAWGAW	FAYWGQG	
BR55-2	CAR	GMDYGAW	FAYWGQG	

and conformation. Conformational search procedures applied to CDR3 clearly suggest that these are the only conformations available to the base of the loop (Mas *et al.*, 1992). It has been suggested that packing of residues at the loop base can be used to differentiate between these structures (Mas *et al.*, 1992).

Based upon the sequence similarities found in B13i2 with the anti-Y antibodies, we utilized this kinked base geometry template and searched for additional loops in the database (Table II). In splicing each loop of seven residues identified from the search into the B13i2 template (Table II), and heating the system to 600 K and then cooling to 300 K, we found that the CDR3 loops approached the conformation of the B13i2 loop. In each of the starting conformations the replaced Gly residue at position 5 in the putative loop did not adopt the conformation analogous to the proline in the B13i2 template (Figure 4). A major difference in the two conformation types was centered on Gly H99 (Figure 4). In effect, the substituted Gly at position 5 in the B13i2 template points downward, whereas the substituted Gly in the second conformer type points upward (Figure 4). Analysis of the low-energy form of the preferred AbM-generated structure displayed correspondence to the second conformer type, indicating that conformational searching leads to structure types identified by the molecular dynamics calculations.

We found that the B13i2 loop was energetically favorable on average by 4 kcal/mol. This finding is probably related to the starting bias in the choice of the B13i2 template. Analysis of VH:VL interfaces indicate that the structure of the CDR3 region and the VL:VH association are interdependent as residues at the C-terminal end of CDR3 form part of the VH:VL interface. However, if we take a different approach and consider the degree of sequence homology for the CDR3 loop of BV04.1 compared with BR55-2, the BV04.1 displays a conformation in which the Trp residue at position H100a is orientated differently with respect to the center of the antigen binding site relative to the calculated low-energy forms. This orientation is similar to that observed in the BR96 crystal structure (Jeffrey *et al.*, 1995), suggesting that perhaps hydrophobic interactions involved in DNA and sugar interactions are similar. These results further suggest that sequence similarities are perhaps a more important consideration for modeling than energetics alone and that multiple starting geometries should still be considered. Subsequently we choose the BV04.1 loop for CDR3.

Docking of Y

Using site point information as a guide, we examined the respective CDR domains for residue types implicated in binding the difucosylated Y structure as determined by the co-complex of BR96. Previous studies have implicated tracts such as YYMY and YYGY as potential regions for carbohydrate interactions (Hoess *et al.*, 1993). The YYMY sequence tract is found in CDR1 of the heavy chain in BR96, B3 and BR55-2 (Figure 3b) and is implicated in BR96 binding to Y. We positioned the Y fragment within the BR55-2 binding site, relying upon distance difference maps between the Y structure and the site points and also the reported contacts in the BR96 co-crystal structure.

In the placement of Y we performed a restrained molecular dynamics calculation using the reported contacts for BR96 with the cFuc functional group contacts. This model is shown in Figure 5a and summarized in Table III. In this model O-7[a] can potentially form a hydrogen bond with the backbone NH group of Tyr H33 as observed in BR96, while a bifurcated hydrogen bond is observed between His L31 and OH-3[b] and OH-4[b]. Tyr H35 forms a hydrogen bond with OH-6[b]. Unlike the crystal structure we observe a hydrogen bond between OH-2[c] and Asp H97. In the crystal structure Asp97 is interacting with the nonoate methyl ester group attached to βDGlcNAc. Our Y structure does not account for this functional moiety (Figure 1b). We also observe hydrogen bonds with dFuc functional groups which are not reported for the crystal structure.

To evaluate the model further we examined alternative placements of Y based upon the GS4 lectin structure in complex with Le[b]. In these models (Figure 5b–d) site points associated with residues displaying homology with GS4-Le[b] contact residues were identified and used as a guide in the placement of the Y structure. We observed a range of possible polar and non-polar arrangements illustrated in Figure 5b–d. We identified several variations of a putative binding mode for BR55-2 in which many of the contacts were conserved in GS4 and the other anti-Y antibodies. In particular, we observed a potential bifurcated hydrogen bond between Asn L31b and OH-3[b] and OH-2[d] (Figure 5b and d) which mimics Asn135 binding to a tetrasaccharide form of Le[b] in GS4. Differences in the glycosidic angles of Y can change the bifurcated hydrogen bond to a single hydrogen bond with OH-2[d] (Figure 5c). The bifurcated hydrogen bonding by Asp89 in GS4 to OH-3[b] and OH-4[b] is potentially mimicked by Ser L31a in the antibodies (Figure 5b–d). In B3 we observe a Trp residue contacting OH-3[d] (Figure 5b), again mimicking that observed for Le[b] binding in GS4, while in BR55-2 this contact involves a Tyr. In BR55-2, B3 and H18A Tyr H33 can bind to OH-4[d] (Figure 5b–d). Again, variations in the Y structure can introduce a hydrogen bond between Ser L31a and OH-2[d] in BR55-2 (Figure 5b and c). This residue is conserved in B3 and mutated to a Thr in H18A (Figure 3a). In BR96 this position is mutated to an Asn (Figure 3a), which presumably can still form a hydrogen bond with OH-2[d].

An electrostatic interaction involving His L93 (assuming a physiological pH of 7.0) and the backbone NH group of

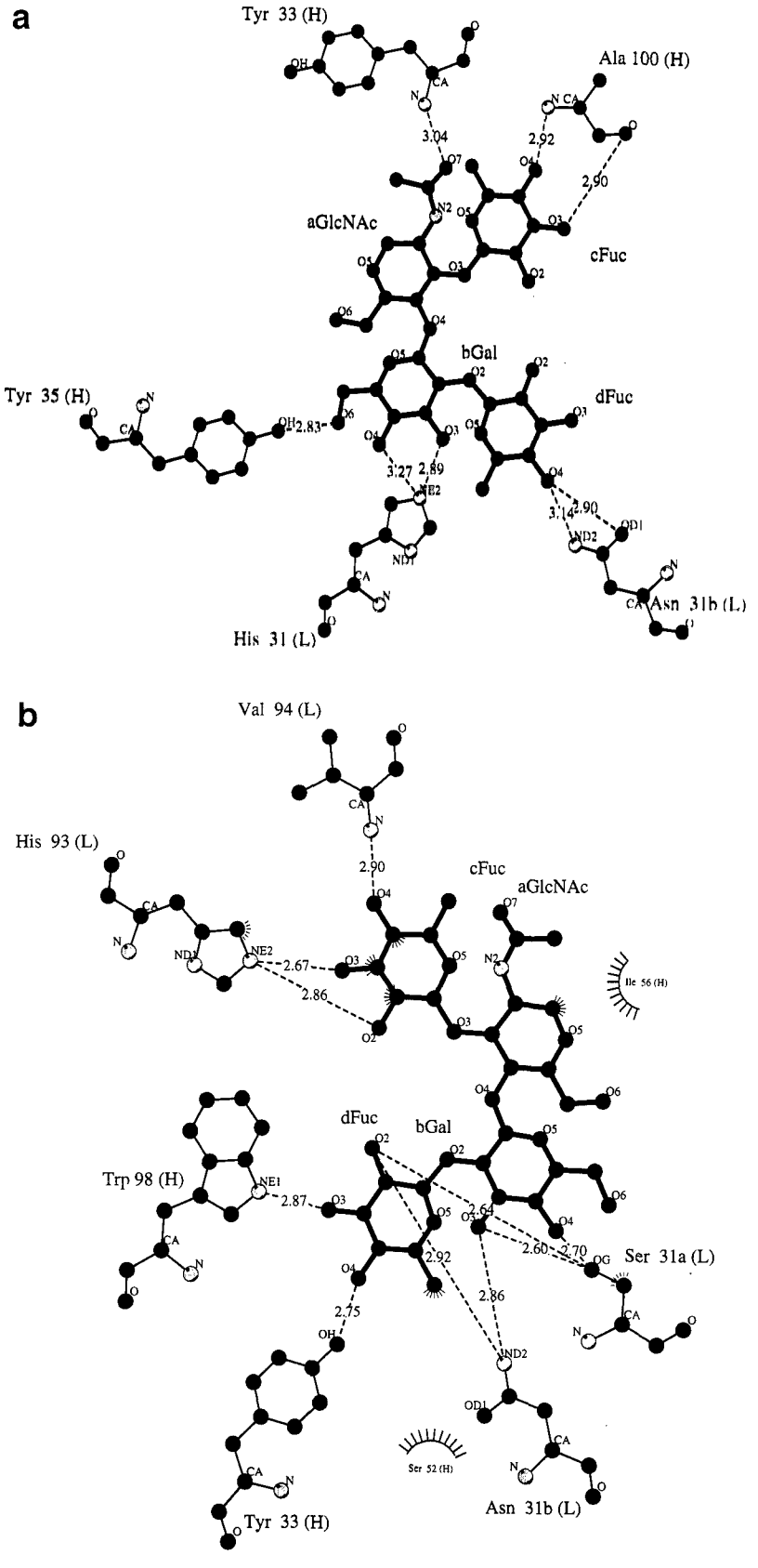

Val L94 potentially stabilizes the polar interactions with the available hydroxyls of cFuc. This interaction can approach hydrogen bonding distances (Figure 5b and c). Val L94 can also interact with cFuc via hydrophobic interactions (Figure 5c) As expected from experimental data (Blaszczyk-Thurin *et al.*, 1987), we observe interactions with the GlcNac residue. Our alternative placement of Y results in a hydrogen bond between Ser H56 in BR55-2 with OH-6[a] (Figure 5b and c).

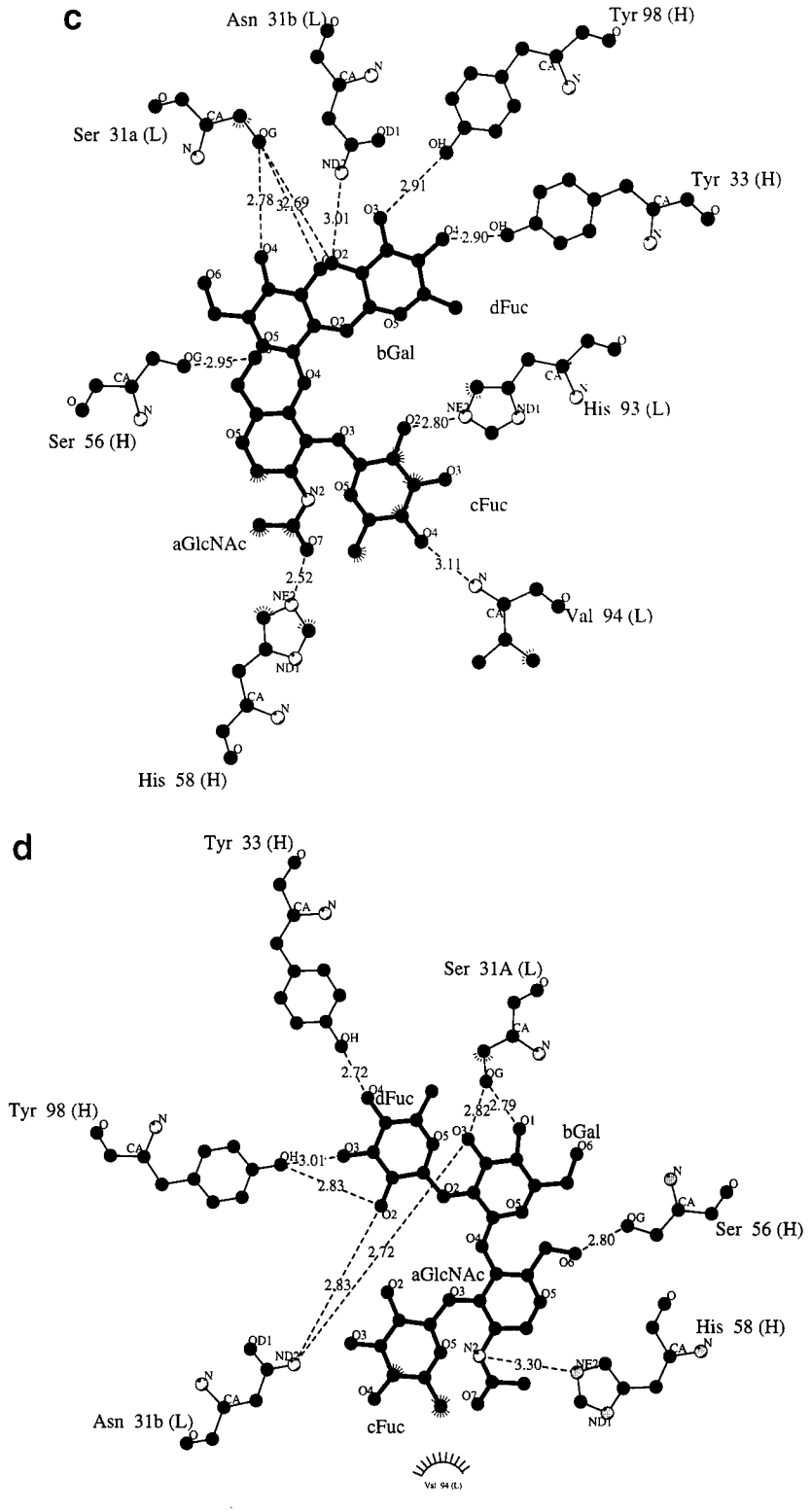

Fig. 5. Summary of hydrogen bonding and hydrophobic interactions identified for Y binding to BR55-2. Hydrogen bonding distances identified by the program LIGPLOT (Wallace *et al.*, 1995) reflect idealized heavy atom distances less than 3.3 Å. Interaction energies for the Y structure for BR55-2 range from –88 kcal/mol (**a**) to –64 kcal/mol (**d**). Model (**a**) corresponds to contacts observed in the BR96-Y crystal structure which are conserved between BR55-2 and BR96. Models (**b**)–(**d**) are those based upon a presumed common topography of Le^b and Y binding to the anti-Y antibodies based upon the GS4 -Le^b crystal complex.

This residue is an Ile in H18A, providing a hydrophobic interaction with GlcNAc (Figure 5b). The acetamido group of GlcNAc is involved in either electrostatic or hydrophobic interactions with residue position H58 in the antibodies. Interactions with either the N-2 or O-7 is dependent on the final conformation of the acetamido group of the GlcNAc residue (Figure 5c and d).

Comparison of interaction energies for the various binding

Table III. Interactions in the carbohydrate-binding site of several anti-Y antibodies and the GS4 lectin[a]

Sugar residue	Sugar atom	GS4	BR55	B3	H18A	BR96	BR96(c)
a-GlcNAc	O-7		*N*-Tyr H33	*N*-Tyr H33	*N*-Tyr H33	*N*-Tyr H33	*N*-Tyr H33
b-Gal	O-3	Asp89, Gly107, Asn135	His L31	His L31	His L31	His L31	His L31
	O-4	Asp89	His L31	HisL31	His L31	HisL31	
	O-6		Tyr H35	Tyr H35	Tyr H35	Tyr H35	Tyr H35
c-Fuc	O-3	Arg48, Gly222	*N*-Ala H100	*N*-Ala H100	*N*-Ala H100	*N*-Ala H100	*N*-Ala H100
	O-4	Ser49, Ser49, Gly222	*O*-Ala H100	*O*-Ala H100	*O*-Ala H100	*O*-Ala H100	*O*-Ala H100
	O-2		Asp H97	Ala H97	Tyr H97	Asp H97	
d-Fuc	O-2	Asn135, Trp138	Ser L31a	Ser L31a	Thr L31a	Asn L31a	
	O-3	Trp138					
	O-4		Asn L31b	Asn L31b	AsnL31b	Asn L31b	

[a]The designations a, b, c, d refer to the βDGlcNac, βDGal, αLFuc(1→4) or αLFuc(1→3) and αLFuc(1→2) units, respectively. BR96(c) designates those contacts observed in the BR96 co-complex. Contact sites in BR55-2 are highly conserved among the anti-Y antibodies.

Table IV. Comparison of ϕ/ψ glycosidic torsion angles (°) in Lewis b

(a)

Linkage type	MD average value[a] ϕ^2,ψ^2	MD fluctuation[a] ϕ^2,ψ^2	NOE result[b] ϕ^2,ψ^2	Crystal ϕ^2,ψ^2	CVFF ϕ^2,ψ^2
dFuc(1→2)bGal	–75, 138	±10.6, ±9.7	–80 (±10), 140 (±10)	–67, 137	–72, 135
bGal(1→3)aGlcNAc	–61, –110	±8.9, ±9.7	–70 (±10), –100 (±10)	–64, –99	–70, –107
cFuc(1→4)aGlcNAc	–62, 148	±13.3, ±9.7	–70 (±10), 140 (±10)	–63, 148	–73, 140

(b)

Linkage	ϕ^1,ψ^1 (crystal)	ϕ^1,ψ^1 (HSEA)	ϕ^1,ψ^1 (CVFF)	$\delta\ \phi^1,\psi^{1c}$
bGal(1→3)aGlcNAc	56/21	55/10	50/13	5/3
cFuc(1→4)aGlcNAc	55/30	55/25	46/21	9/4
dFuc(1→2)bGal	50/17	45/15	47/16	2/1

[a]Molecular dynamics (MD) angle values extracted from literature (Mukhopadhyay and Bush, 1991).
[b]NMR angle values extracted from literature (Cagas and Bush, 1990, 1992). Crystal angle values for Leb are from Delbaere *et al.* (1993). CVFF values (consistent valence force field) are minimized conformations from averaged conformers from grid search.
[c]Absolute angle difference between HSEA and CVFF calculations. HSEA angle values are from hard-sphere exomeric–anomeric calculations (Lemieux and Bock, 1983). CVFF angle values are minimized conformations from averaged conformers from grid search.

mode schemes in Figure 5a–d indicates that the binding mode scheme in Figure 5a was more stable than that observed in Figures 5b–d by 22–27 kcal/mol. Comparison of the models in Figure 5a–d indicates significant differences obtained by analogous computations but different assumptions as to how Y might bind to BR55-2. These results indicate that BR96, BR55-2 and B3 interact with the core tetrasaccharide structure of Y in a similar fashion, which is different from the binding topography of GS4 binding to Y and Le^b.

Comparison of binding mode conformations

Since there is no information reported for the Y structure in the BR96 co-complex, we were interested in how the binding mode conformation of Y, as calculated here, compares with that observed by NMR and theoretical calculations (Lemieux and Bock, 1983; Spohr and Lemieux, 1988; Mukhopadhyay and Bush, 1991). As a basis we compared the dihedral angles of the Y tetrasaccharide with those of Le^b as found in complex with GS4 and with unbound forms established by computational or NMR approaches (Table IV). Molecular dynamics calculations (Table IVa, columns 1 and 2) of unbound Le^b structures indicate that low-energy conformers fluctuate about 10° and are within 3–4 kcal/mol around a single minimum energy conformation represented by NMR results (Table IVa, column 3), HSEA (Table IVb, column 2) calculations and with the Le^b structure observed in GS4 (Table IVa, column 4, and Table IVb, column 1). A converged structure for Le^b (Table IVa, column 5 and Table IVb, column 3), which started from an average of low-energy conformers identified from a grid search, was found to be within this range of angle fluctuations.

To determine the extent to which final minimized models are dependent on the starting conformation, we used the HSEA conformer (Table IVb, column 2) as a starting geometry. Minimization of this geometry resulted in the same conformer (Table IVa, column 5, and Table IVb, column 3) as that starting from the binding mode conformation of Le^b in GS4 (Table IVa, column 4, and Table IVb, column 1). The HSEA-derived starting conformation in Table IVb (column 2) was found to be only 0.8 kcal/mol above the converged conformer (Table IVa, column 5, and Table IVb, column 3), with the Le^b binding mode conformation 2.8 kcal/mol above the converged structure. These calculations confirm that the binding mode of Le^b for GS4 and the HSEA-derived structure are local minimas within the range of fluctuations for the glycosidic angles observed from MD calculations (Mukhopadhyay and Bush, 1991).

Performing similar calculations for the Y structure, it was found that averaged low-energy forms identified from a grid search, and also the HSEA starting conformation (Table V,

Table V. Comparison of ϕ/ψ glycosidic torsion angles (°) in Lewis Y structures[a]

Linkage	ϕ^1,ψ^1 (HSEA)	ϕ^1,ψ^1 (CVFF)	ϕ^1,ψ^1(BM)
bGal(1→3)aGlcNAc	55/10	49/12	46/14
cFuc(1→4)aGlcNAc	50/25	46/22	45/25
dFuc(1→2)bGal	50/10	48/17	50/19

[a]HSEA angle values are from hard-sphere exomeric–anomeric calculations (Lemieux and Bock, 1983). CVFF is a minimized structure from average conformation identified in grid search and is a low-energy structure starting from column 1. BM is BR55-2 binding mode conformation in Figure 5a.

column 1), led to a converged conformer (Table V, column 2) similar to that found for the Le^b structure (Table IVa, column 3) for the representative units. Minimization of the binding mode conformation (Table V, column 3) also led to the converged structure in column 2. The binding mode structure (Figure 5a) (Table V, column 3) was 1.5 kcal/mol above its optimized structure. In comparison, the HSEA conformation (Table V, column 1) was less stable, being 2.3 kcal/mol above its optimized structure shown in column 2. Minimization of binding mode structures in Figure 5b–d resulted in converged structures either representative of that in Table V (column 2) or higher energy conformers.

To examine further the Y specificity of BR55-2, we superimposed the corresponding structure for Le^b on the BR55-2 binding mode Y structure observed in Figure 5a. The binding mode conformation for Le^b in complex with GS4 is not very different from that based upon NMR and theoretical calculations. Minimization of the Le^b–BR55-2 complex resulted in a recognition scheme less stable (14 kcal/mol) than the Y-BR55-2 complex, with the majority of the contribution coming from loss of van der Waals interactions involving the *N*-acetamido group.

Discussion

Structures from lactoseries reactive antibodies (Table I) and crystal structures of BR96 and GS4 have defined potential sites on Lewis structures that might dictate specificity. Comparison of calculated and NMR-derived conformers of precursors of type 1 (Galβ1→3GlcNAc) and type 2 (Galβ1→4GlcNAc) chains show that they display very similar topographical features (Figure 1a). Spohr *et al.* (1985a) have shown that the binding of these structures by GS4 should occur at the termini of the molecule involving the common surface to both structures based on a large number of chemically modified structures related to Le^b and Y human blood group determinants. These interactions are to some extent retained by anti-Y antibodies but important differences are observed.

The major sugar moieties, (bGal, cFuc and dFuc) are stabilized by hydrogen bonds and hydrophobic interactions (Table III). Residue types that form hydrogen bonds with the hexose subunits are different in GS4 in binding to bGal functional groups, but a potential bifurcated hydrogen bond is observed in BR55-2 involving OH-3 and OH-4 as implicated in GS4. A hydrogen bond is observed involving OH-6 which is however absent in GS4 binding. For cFuc, backbone hydrogen bonds are observed to contribute to GS4 binding as observed in BR55-2 and BR96. For dfuc, our model for BR55-2 (Figure 5a) implicates both OH-2 and OH-4 as forming hydrogen bonds.

Based on the oligosaccharide specificity of lectins and antibodies that distinguish between the difucosylated type 1 and 2 lactoseries structures, it appears that a critical recognition feature for type 1 and 2 chains is an involvement of the 6-CH_2OH and/or acetamido group of the GlcNAc residue with the antibody combining site. The involvement of the β-D-*N*-acetylglucosamine residue in the binding epitope for Y-specific MAbs was postulated previously (Blaszczyk-Thurin *et al.*, 1987). In the BR96 crystal structure and BR55-2 model (Figure 5a), this moiety forms a hydrogen bond involving the O-7 group, and provides an enhanced stability over its isosteric homolog Le^b. These differences and those reflective of the nature of the structures extended at the reducing site of the fucosylated lactosoamine probably translate into different affinities for Y by these antibodies. Mutation of Asp97 by Ala in BR96 indicates enhanced tumor cell binding (Jeffrey *et al.*, 1995). This residue is native to B3 (Table III). An intermolecular interaction energy calculation of a substituted Ala at position 97 in the BR55-2 model indicates an enhanced hydrophobic interaction with the CH_3 group of the *N*-acetamido moiety (data not shown). Subsequently, the interaction of the βDGlcNAc residue with Y-specific antibodies is a driving mediator in their specificity as well as the number of hexose subunits comprising the Y structure that are recognized by the respective antibodies.

Anti-Y antibodies differ in their recognition of epitopes on the Y antigen. Based upon the crystal structure of the BR96–Y tetrasaccharide complex and the relative sequence similarities between the anti-Y antibodies examined here, it is apparent that the MAb binding groove of Y-specific MAbs is sufficiently large to bind four monosaccharide units of the Y determinant. Further binding studies to determine specificity and cross-reactivity, and also simple docking studies with other than Y conformers which are recognized by some MAbs (such as H-2, LeX and Le^b), will provide information on the different conformational epitopes presented to Y-specific MAbs, elucidating contact points that might participate in the formation of the carbohydrate–protein complexes. Although the specificity of either BR55-2 or BR96 MAbs was not tested against difucosylated extended Y or trifucosylated Y conformer structures, the analysis of the BR96–Y complex shows that trifucosylated structures extended at the reducing site with a fucosylated lactosamine unit are accommodated in the binding groove of some MAbs. Similarly, we conclude from our model that BR55-2 might bind to the additional trisaccharide unit, similar to the BR96 geometry. The antibody AH-6 was previously shown to bind equally well to Y hexaosylsceramide, difucosylated Y octaosylceramide and trifucosylated nonaosylceramide (Nudelman *et al.*, 1986), suggesting that the epitope is limited to the Y hexasaccharide or the extension at the reducing part of the oligosaccharide is incorporated into the binding groove without influencing antibody binding.

Structural studies on Lewis antigens have generally substantiated that conformations are determined mainly by steric repulsion brought about by changes in the glycosidic dihedral angles. Molecular dynamics calculations on Lewis antigen structure prototypes indicate the lack of spontaneous conformational transitions to other minima during the simulations, suggesting that these oligosaccharides maintain well defined conformations with relatively long lifetimes (Mukhopadhyay and Bush, 1991). These results further indicate that hard-sphere or rigid-geometry calculations, albeit in the absence of solvent, provide a good picture of the steric repulsion that modulates the conformational properties of the Lewis antigens.

Our minimizations, starting from binding mode geometries, were found to converge to such conformations. Subsequently, the binding mode conformation for BR55-2, and presumably also for BR96, is in excellent agreement with expectations for the Y structure derived from consideration of both MD (Mukhopadhyay and Bush, 1991) and NMR (Cagas and Bush, 1990, 1992) studies.

Current procedures for predicting ligand–antibody interactions are limited, mainly owing to the conformational flexibility of ligands and antibodies and the role of solvent in mediating ligand recognition and binding. Comparison of the models in Figure 5a–d, which are reflective of different assumptions about the interaction of Y with the Y binding proteins, indicate that modeling and intermolecular energy calculations can discriminate differences in binding orientations. Intermolecular interaction calculations for the structures in Figure 5b–d were within 5 kcal/mol of each other, with the model in Figure 5a 22 kcal/mol more stable than the most stable alternative model (Figure 5d). While the general features of Y recognition is retained in the BR55-2 model (Figure 5a) in comparison with the BR96 crystal structure, the notion of induced fit upon Y binding as representative of the crystal structure of BR96 involving CDR3 of the heavy chain was not predictive within our calculations. This is an obvious limitation to predictive approaches in elucidating recognition of ligands by antibodies. In addition, the comparison of the various models indicates that BR55-2 and BR96 do not faithfully mimic Y recognition by the GS4 lectin, binding to a different topography on the Y antigen. The recognition of different functional groups on trifucosylated Y structures most probably explains differences in the efficacy of anti-Y antibodies.

In summary, the sequence and structural analysis presented here indicates that BR55-2, B96 and, to some extent, H18A and B3, share similarities in binding the putative Y tetrasaccharide core. An understanding of the three-dimensional basis for the molecular recognition of Y by these and related antibodies can be applied for future diagnosis in tumor progression and micrometastasis and also active immunotherapy. Further structural studies of Y antigen forms binding to anti-Y antibodies will provide information relevant to vaccine design strategies and improved immunotherapeutics.

Acknowledgments

We thank Matthew Kieber-Emmons for assistance with sequence analysis and model building. This work was supported by the USAMRMC (DAMD17-94-J-4310) Breast Cancer Program. Computer equipment support from The Cancer Center of the University of Pennsylvania is also gratefully acknowledged.

References

Abe,K., Hakomori,S. and Ohshiba,S. (1986) *Cancer Res.*, **46**, 2639–2644.
Bajorath,J. (1994) *Bioconj. Chem.*, **5**, 213–219.
Bernstein,F.C. *et al.* (1977) *J. Mol. Biol.*, **112**, 535–542.
Blaszczyk-Thurin,M., Thurin,J., Hindsgaul,O., Karlsson,K.A., Steplewski,Z. and Koprowski,H. (1987) *J. Biol. Chem.*, **262**, 372–379.
Blundell,T.L., Sibanda,B.L., Sternberg,M.J. and Thornton,J.M. (1987) *Nature*, **326**, 347–352.
Brinkmann,U., Pai,L.H., FitzGerald,D.J., Willingham,M. and Pastan,I. (1991) *Proc. Natl Acad. Sci. USA* **88**, 8616–8620.
Bruccoleri,R.E. and Karplus,M. (1987) *Biopolymers*, **26**, 137–168.
Bruccoleri,R.E., Haber,E. and Novotny,J. (1988) *Nature*, **335**, 564–568.
Cagas,P. and Bush,C.A. (1990) *Biopolymers*, **30**, 1123–1138.
Cagas,P. and Bush,C.A. (1992) *Biopolymers*, **32**, 277–292.
Chai,W., Hounsell,E.F., Cashmore,G.C., Rosankiewicz,J.R., Feeney,J. and Lawson,A.M. (1992) *Eur. J. Biochem.*, **207**, 973–980.
Cheetham,J.C.,Raleigh,D.P., Griest,R.E., Redfield,C., Dobson,C.M. and Rees,A.R. (1991) *Proc. Natl Acad. Sci. USA* **88**, 7968–7972.
Choe,M., Webber,K.O. and Pastan,I. (1994) *Cancer Res.*, **54**, 3460–3467.
Chothia,C., Lesk,A.M., Gherardi,E., Tomlinson,I.M., Walter,G., Marks,J.D., Llewelyn,M.B. and Winter,G. (1992) *J. Mol. Biol.*, **227**, 799–817.
Co,M.S., Avdalovic,N.M., Caron,P.C., Avdalovic,M.V., Scheinberg,D.A. and Quenn,C. (1992) *J. Immunol.*, **148**, 1149–1154.
Cooper,H.S., Malecha,M.J., Bass,C., Fagel,P.L. and Steplewski,Z. (1991) *Am. J. Pathol.*, **138**, 103–110.
Delbaere,L.T., Vandonselaar,M., Prasad,L., Quail,J.W., Wilson,K.S. and Dauter,Z. (1993) *J. Mol. Biol.*, **230**, 950–965.
Fine,R.M., Wang,H., Shenkin,P.S., Yarmush,D.L. and Levinthal,C. (1986) *Proteins*, **1**, 342–362.
Fukushi,Y., Orikasa,S., Shepard,T. and Hakomori,S. (1986) *J. Urol.*, **135**, 1048–1056.
Garrigues,J., Garrigues,U., Hellstrom,I. and Hellstrom,K.E. (1993) *Am. J. Pathol.*, **142**, 607–622.
Hakomori,S. (1989) *Adv. Cancer Res.*, **52**, 257–331.
Hakomori,S. (1991) *Curr. Opin. Immunol.*, **3**, 646–653.
Hellstrom,I., Garrigues,H.J., Garrigues,U. and Hellstrom,K.E. (1990) *Cancer Res*, **50**, 2183–2190.
Hindsgaul,O., Khare,D.P., Bach,M. and Lemieux,R.U. (1985) *Can J. Chem.*, **63**, 2653–2658.
Hoess,R., Brinkmann,U., Handel,T. and Pastan,I. (1993) *Gene*, **128**, 43–49.
Hoff,S.D., Matsushita,Y., Ota,D.M., Cleary,K.R., Yamori,T., Hakomori,S. and Irimura,T. (1989) *Cancer Res.*, **49**, 6883–6888.
Hoff,S.D., Irimura,T., Matsushita,Y., Ota,D.M., Cleary,K.R. and Hakomori,S. (1990) *Arch. Surg.*, **125**, 206–209.
Ichihara,T. *et al.* (1993) *Cancer*, **71**, 71–81.
Iliopoulos,D. *et al.* (1993) *Digest. Dis. Sci.*, **38**, 155–160.
Itzkowitz,S.H. (1992) *J. Cell. Biochem., Suppl.*, **16G**, 97–101.
Itzkowitz,S.H. *et al.* (1986) *Cancer Res.*, **46**, 2627–2632.
Jeffrey,P.D., Bajorath,J., Chang,C.Y., Yelton,D., Hellstrom,I., Hellstrom,K.E. and Sheriff,S. (1995) *Nature Struct. Biol.*, **2**, 466–471.
Kabat,E.A., Wu,T.T., Reid-Miller,M., Perry,H.M. and Gottesman,K.S. (1987) *Sequences of Proteins of Immunologic Interest.* United States Department of Health and Human Services, Public Health Service, National Institutes of Health, Bethesda, MD.
Kaizu,T., Levery,S.B., Nudelman,E., Stenkamp,R.E. and Hakomori,S. (1986) *J. Biol. Chem.*, **261**, 11254–11258.
Kaneko,T. *et al.* (1993) *J. Biochem (Tokyo)*, **113**, 114–117.
Karp,S.L., Kieber-Emmons,T., Sun,M.J., Wolf,G. and Neilson,E.G. (1993) *J. Immunol.*, **150**, 867–879.
Kim,Y.S., Yuan,M., Itzkowitz,S.H., Sun,Q.B., Kaizu,T., Palekar,A., Trump,B.F. and Hakomori,S. (1986) *Cancer Res.*, **46**, 5985–5992.
Kitamura,K. *et al.* (1994) *Proc. Natl Acad. Sci. USA*, **91**, 12957–12961.
Kobayashi,K., Sakamoto,J., Kito,T., Yamamura,Y., Koshikawa,T., Fujita,M., Watanabe,T. and Nakazato,H. (1993) *Am. J. Gastroenterol.*, **88**, 919–924.
Kraulis,P.J. (1991) *J. Appl. Chem.*, **24**, 946–950.
Lemieux,R.U. and Bock,K. (1983) *Arch. Biochem. Biophys.*, 221, 125–134.
Lemieux,R.U., Bock,K., Delbaere,L.T.J., Koto,S. and Rao,V.S. (1980) *Can. J. Chem.*, **58**, 631–653.
Lemieux,R.U., Wong,T.C., Liao,J. and Kabat,E.A. (1984) *Mol. Immunol.*, **21**, 751–759.
Lemieux,R.U., Venot,A.P., Spohr,U., Bird,P., Mandal,G., Morishima,N., Hindsgaul,O. and Bundle,D.R. (1985) *Can. J. Chem.*, **63**, 2664–2668.
Lemieux,R.U., Hindsgaul,O., Bird,P., Narasimhan,S. and Young,W.W.J. (1988) *Carbohydr. Res.*, **178**, 293–305.
Lemieux,R.U., Szweda,R., Paszkiewicz,H. E. and Spohr,U. (1990) *Carbohydr. Res.*, **205**, C12–C18.
Lin,C., Kieber-Emmons,T., Villalobos,A.P., Foster,M.H., Wahlgren,C. and Kleyman,T.R. (1994) *J. Biol. Chem.*, **269**, 2805–2813.
Lohman,K.L., Kieber-Emmons,T. and Kennedy,R.C. (1993) *Mol. Immunol.*, **30**, 1295–1306.
Martin,A.C., Cheetham,J.C. and Rees,A.R. (1991) *Methods Enzymol.*, **203**, 121–153.
Mas,M.T., Smith,K.C., Yarmush,D.L., Aisaka,K. and Fine,R.M. (1992) *Proteins*, **14**, 483–498.
Miyake,M., Taki,T., Hitomi,S. and Hakomori,S. (1992) *Biochemistry*, **327**, 14–18.
Mukhopadhyay,C. and Bush,C.A. (1991) *Biopolymers*, **31**, 1737–1746.
Murata,K., Egami,H., Shibata,Y., Sakamoto,K., Misumi,A. and Ogawa,M. (1992) *Am. J. Clin. Pathol.*, **98**, 67–75.
Nell,L.J., McCammon,J.A. and Subramaniam,S. (1992) *Biopolymers*, **32**, 11–21.
Novotny,J., Bruccoleri,R.E. and Haber,E. (1990) *Proteins*, **7**, 93–98.

Nudelman,E., Levery,S.B., Kaizu,T. and Hakomori,S. (1986) *J. Biol. Chem.*, **261**, 11247–11253.
Ogawa,H., Inoue,M., Tanizawa,O., Miyamoto,M. and Sakurai,M. (1992) *Histochemistry*, **97**, 311–317.
Pai,L.H., Batra,J.K., FitzGerald,D.J., Willingham,M.C. and Pastan,I. (1991) *Proc. Natl Acad. Sci. USA*, **88**, 3358–3362.
Pai,L.H., Batra,J.K., FitzGerald,D.J., Willingham,M.C. and Pastan,I. (1992) *Cancer Res.*, **52**, 3189–3193.
Pastan,I., Lovelace,E.T., Gallo,M.G., Rutherford,A.V., Magnani,J.L. and Willingham,M.C. (1991) *Cancer Res.*, **51**, 3781–3787.
Rao,B.N. and Bush,C.A. (1988) *Carbohydr. Res.*, **180**, 111–128.
Rodeck,U., Herlyn,M., Leander,K., Borlinghaus,P. and Koprowski,H. (1987) *Hybridoma*, **6**, 389–401.
Scholz,D., Lubeck,M., Loibner,H., McDonald,S.J., Kimoto,Y., Koprowski,H. and Steplewski,Z. (1991) *Cancer Immunol. Immunother.*, **33**, 153–157.
Schreiber,G.J., Hellstrom,K.E. and Hellstrom,I. (1992) *Cancer Res.*, **52**, 3262–6.
Shenkin,P.S., Yarmush,D.L., Fine,R.M., Wang,H.J. and Levinthal,C. (1987) *Biopolymers*, **26**, 2053–2085.
Spohr,U. and Lemieux,R.U. (1988) *Carbohydr. Res.*, **174**, 211–237.
Spohr,U., Hindsgaul,O. and Lemieux,R. U. (1985a) *Can. J. Chem.*, **63**, 2644–2652.
Spohr,U., Morishima,N., Hindsgaul,O. and Lemieux,R.U. (1985b) *Can. J. Chem.*, **63**, 2659–2663.
Steplewski,Z., Blaszczyk,T.M., Lubeck,M., Loibner,H., Scholz,D. and Koprowski,H. (1990) *Hybridoma*, **9**, 201–210.
Steplewski,Z., Lubeck,M.D., Scholz,D., Loibner,H., McDonald,S.J. and Koprowski,H. (1991) *In_Vivo*, **5**, 79–83.
Strecker,G., Wieruszeski,J.M., Michalski,J.C. and Montreuil,J. (1992) *Biochem. J.*, **287**, 905–909.
Thogersen,H., Lemieux,R.U., Bock,K. and Meyer,B. (1982) *Can. J. Chem.*, **60**, 44–57.
Tomiyama,Y. *et al.* (1992) *J. Biol. Chem.*, **267**, 18085–18092.
Trail,P.A. *et al.* (1993) *Science*, **261**, 212–215.
Tramontano,A. and Lesk,A.M. (1992) *Proteins*, **13**, 231–245.
Tsukazaki,K., Sakayori,M., Arai,H., Yamaoka,K., Kurihara,S. and Nozawa,S. (1991) *Jpn. J. Cancer Res.*, **82**, 934–941.
Wallace,A.C., Laskowski,R.A. and Thornton,J.M. (1995) *Protein Engng*, **8**, 127–134.
Young,W.J. *et al.* (1983) *J. Biol. Chem.*, **258**, 4890–4894.

Received August 17, 1995; revised January 25; accepted January 26, 1996

In Press Hybridoma

#2

Peptide Mimicry of Adenocarcinoma Associated Carbohydrate Antigens

Thomas Kieber-Emmons[+1], Ping Luo[+], Jianping Qiu [+], Michael Agadjanyan[+], Lisa Carey[+] ,Wendy Hutchins*, M.A. Julie Westerink*, Zenon Steplewski[**]

Department of Pathology and Laboratory Medicine[+], University of Pennsylvania, Philadelphia PA. 19104 Department of Medicine*, Medical College of Ohio at Toledo, Toledo OH. Department of Medicine[**], Thomas Jefferson University, Philadelphia PA.

[1]Please Address All Correspondence to:

Thomas Kieber-Emmons
Department of Pathology and Laboratory Medicine
Philadelphia PA, 19104
Phone Number: 215-898-2428
FAX Number:215-898-2401

Abstract

Carbohydrate antigens have been identified as significant antigens in many human tumors either by analyzing antibodies in patients sera or by using monoclonal antibodies, of either mouse or human origin. Three carbohydrate epitopes present on cancer-associated mucins [sialy-Lewis A (SLA), sialy-Lewis X (SLX) and siayl-Tn (STn)] may have functional significance in metastasis. Subsequently, these antigens are considered as targets for active specific immunotherapy. Carbohydrates, as T cell independent antigens, often elicit diminished immune responses. To overcome this drawback, carbohydrates are typically coupled to protein carriers to elicit IgG responses as opposed to low affinity IgM responses which often times accompanies carbohydrate based immunizations. In addition, some complex carbohydrates are difficult to synthesize. Moreover, this latter aspect is further magnified if one considers that clustering of epitopes on neoglycoproteins must be emulated in the synthesis process, leading to multiple presentation or tandem repeats of the synthetic carbohydrate immunogen. Here, we examine the hypothesis that peptides that mimic carbohydrates might be developed to induce immune responses that target and mediate the killing of tumor cells, particularly breast cancer cells in an adjuvant type setting. We have found that carbohydrate mimicking peptides retain carbohydrate like conformations, inducing anti-carbohydrate immune responses against breast tumor cells, mediating their killing by a complement-dependent mechanism.

Introduction

Cell surface carbohydrates undergo dramatic changes in cancer, playing a crucial role in cell-cell communication, cell growth and differentiation (1). Aberrant glycosylation of tumors relative to their normal counterparts, represents a phenotypic feature associated with different human malignancies (1, 2). This phenomenon is demonstrated repeatedly at frequencies higher than those of oncogenes and suppressor genes in various tumors. Aberrant glycosylation influences tumor progression, since cells acquire competence for metastasis and faster clonal growth via newly synthesized carbohydrate structures.

Several types of altered glycosylation have been described in human carcinomas and are prevalent in mammary adenocarcinoma (some common ones illustrated in Figure 1): 1) enhanced expression of GlcNAcβ1→6Manβ1→6 units appear to correlate with progression of human mammary carcinoma (3, 4); 2) the T and Tn structures, Galβ1→3GalNAcα and GalNAcα, respectively, are powerful histologic markers in diagnosis and prognosis, occurring as surface antigens on most primary human breast carcinomas and their metastases, and are able to elicit both humoral and cell-mediated immunity (5-7); 3) the Thomsen Friedenreich (TF) antigen is an important disaccharide panadenocarcinoma antigen which targets antibodies for tumor killing (8); 4) human breast carcinomas express the histo-blood group antigen H (type 2) Fucα1→2Galβ1→4Galβ1 on the globoside backbone (9); 5) sialylated derivatives of type 1 and 2 Lewis antigens such as sialyl-Le^a (SLA) NeuAcα2→3Galβ1→3(Fucα1→4) GlcNAcβ1→3Galβ1→4 Glcβ1→R and sialyl-LeX (SLX) NeuAcα2→3Galβ1→4(Fucα1→3)GlcNAcβ1→3Galβ1→4Glcβ1→R are tumor-associated gangliosides and are observed more frequently than their respective nonsialylated forms in breast adenocarcinomas (10); 6) The accumulation of α-fucosylated derivatives of lactoseries type 1 and 2 structures such as Lewis Y (LeY), Fucα1→2Galβ1→4(Fucα1→3)GlcNAcβ1→3Galβ1→4 Glcβ1→R, H-2 and Lewis b (Le^b) is closely associated with adenocarcinoma development and correlates inversely with patient survival with primary lung adenocarcinoma (11-13).

Epidemiological studies have shown that patients expressing SLA, SLX, STn, Lewis X (LeX) and LeY structures on their primary tumors have markedly lowered survival rates. STn formulations have been shown to induce immune responses to breast cancer and formulations are in clinical trails (13, 14). Immune responses to some Lewis antigens is expected to be weaker in humans compared to other

mammals. From a vaccine perspective, responses to carbohydrates as Tumor Associated Antigens (TAAs) are notorious in eliciting diminished immune responses, with predominately IgM antibodies displaying relatively low affinity for carbohydrates (15, 16). Immune responses can be enhanced however by coupling carbohydrates to carrier proteins and adjuvants which is perceived to recruit T cell help (15, 17-26). While these results show promise for active specific immunotherapy with carbohydrate formulations they point out the limitations of this approach. These include: difficulty in antigen purification or synthesis, the utility of carbohydrate carrier-protein coupling strategies which might prove to be impractical for broad application, and the lack of persistent high titer cytotoxic antibodies in many patients. These difficulties might be further magnified by considering that neoglycoconguates in which the carbohydrate structures are clustered together might make better immunogens (8, 27). It is argued that such structures would more closely resemble the arrangement of carbohydrate epitopes on the cell surface- either glycolipid aggregates, multiantennary N-linked chains or clustered O-linked oligosaccharides on mucins. Despite this widely held view there is little experimental support for this concept. The most convincing evidence for this concept is from examining the specificity of mAbs raised to cells or other sources. For example, in a recent study it was shown that a clustered neoglycoprotein antigen consisting of STn substituted on a tri-serine peptide, which in turn is coupled to KLH, gave an antibody response in mice that recognized clustered epitopes and natural forms of STn (27). Despite these promising results, synthetic routes for developing clustered carbohydrate epitopes is not straight forward.

Carbohydrates that influence the metastatic potential of tumor cells are not restricted to just tumors. Adhesion of pathogens and toxins to host cell plasma membrane is mediated by glycoconjugates. Subsequently, the distribution of carbohydrates lend to cross-reactivity of antibodies for common saccharide subunits among bacteria, viruses and tumor cells. Immunochemical studies of sialylated lipo-oligosaccharides (LOS) of the Gram-negative bacteria Neisseria gonorrhoeae and Neisseria meningitidis suggest that structural characteristics of these LOS might relate to their roles during pathogenesis. The carbohydrate moieties of the LOS of pathogenic Neisseria mimic carbohydrates present in glycosphingolipids of human cells (28). Such studies indicate that the pathophysiology of processes such as infection and neoplasia are profoundly affected by the same or similar carbohydrate forms.

We have shown that antibodies induced by a peptide mimic of the major C polysaccharide (MCP) of N. meningitidis can induce antibodies that react with MCP and protect mice from lethal challenge with N. meningitidis (29). MCP is a polymer of α(2→9)sialic acid. Structural analysis of MCP suggests that its conformation is similar to subunits associated with carbohydrate forms associated with breast tumors. Here, we show that peptides that mimic carbohydrate subunits can induce humoral responses that cross-react with representative synthetic carbohydrate probes associated with breast tumors, and with tumor cells, mediating complement dependent cytotoxicity (CDC) of human breast cell lines.

Materials and Methods

Preparation of Peptide-proteosome complex. Peptides were synthesized with the addition of a tripeptide YGG spacer, and a cysteine at the amino terminus conjugated to a lauroyl group (Bio-Synthesis, Lewisville TX). The meningococcal outer membrane proteins or proteosomes were prepared and complexed to the Lauroyl-C-YGG-Peptides as described by Lowell et al. (30, 31) in a 1mg:1mg ratio, combining the components in the presence of detergent. The detergent was removed by extensive dialysis (30, 31). Proteosomes were prepared from outer membrane complex vesicles from group B meningococci, strain M99, by ultra-centrifugation and soluble in detergent buffer (32). The lauroyl group allows for hydrophobic complexing of the peptide to the proteosomes while the cysteine at the N terminus appears essential for immunogenicity apparently cross-linking multiple epitopes (30, 31).

Preparation of Antibodies Against Carbohydrate-Mimicking Peptides. For generation of polyclonal sera Balb/c mice (n=4 per group) 4-6 weeks of age, were immunized i.p. on a weekly basis for 3 weeks with 50ug of peptide-proteosome complex. Sera was collected within 7 and 14 days after the last immunization and analyzed for binding against synthetic carbohydrate probes by ELISA and against breast cells using FACs analysis.

ELISA assays. Solid phase ELISA was performed to asses the binding activity of sera induced by the carbohydrate mimicking peptides to a variety of carbohydrate synthetic probes incorporated into ployacrylamide matrix, (creating 30Kd multivalent polymers (purchased from Glycotech)). Immunlon 2 plates were coated with the Fucα1-4GlcNAc, LeY, Galβ1-3Gal, Galβ1-3GalNAc, Sialyl-Lea, Lea, Sialyl-Lex, Lex, Lex pentasaccharide and Leb-hexasaccharide overnight at 4^{o}C. The plates were blocked with

0.5%FCS / 0.2% tween, 200 µl / well, 37°C, for 1hr. Serial dilutions of the respective anti-sera was added and resolved with 100 µl / well of 1 : 10000x Goat-anti-Mouse IgG isotype matched-HRP (Sigma) diluted in blocking buffer, incubated at 37°C for 1hr. OD_{450nm} was read using a Dynatech MR5000 ELISA reader.

FACS analysis: For the preparation of cells, 10ml of FACS buffer was added and the cells were washed, scrapped and transferred to 15 ml. centrifuge tubes. Viable cells were counted by trypan blue. Cells were diluted to 2 $X10^6$/ml and 100ul used for each sample. Primary sera (10ul) was added to the sample tubes and incubated on ice for 30 min. washed twice with 1 ml FACS buffer and centrifuged for 2 minutes at 1500 rpm. 10 ul of FITC Ab (goat anti-mouse IgG FITC labeled (Sigma) diluted 1:20 with PBS) was added to the sample and incubated on ice for 30 min. and again washed twice with FACS buffer. Cells were fixed using 2% paraformaldelhyde, followed by FACS measurement.

Complement-dependent cell cytotoxicity (CDC). Briefly, sera was tested for its ability to bind to tumor lines and modulate CDC. Ten ul of each Cell line ($4X10^4$ cells per ml) were added to duplicate wells of a microtiterplates to which was added 20ul of serially diluted sera, and incubated for 45 min on ice. 20ul of rabbit complement 1:2 was added and allowed incubate for 4 hrs at 37°C. The medium was discarded and 50 ul methanol fix was added and allowed to incubate for 10 min. This procedure was repeated, once again for 5 min. The number of viable cells was determined by Giemsa stainning. 2% Giemsa stain in methanol was added and allowed to fix for 25 min, then rinsed in distilled water. Plates were counted under a light microscope. The percent of cytotoxicity (PC) was calculated with the formula: Percentage cytoxicity=[1-(number of cells in well treated with antibody and complement / number of cells in well treated with medium only)] x 100. Control wells did not contain antisera.

Results

The induction of anti-carbohydrate immune responses by peptides. We have recently shown that the peptide, CARIYYRYDGTAY, (derived from an anti-idiotypic antibody that mimics the major C polysaccharide (MCP) of N. meningitis) when complexed to proteosomes induces an anti-MCP antibody response in Balb/c mice that is protective in nature (29). The major Ig fraction upon immunization was found to be IgM, with IgG coming up later (29). This peptide bears some homology with other peptides

that mimic carbohydrates involving a Planar-X-Planar sequence motif (Table 1). In particular, Hoess et al (33) have identified an 8 amino acid peptide expressed on phage capable of inhibiting LeY carbohydrate-antibody binding consisting of the sequence tract PWLY. The sequence similarities among the putative motifs suggest that antibodies raised to this peptide set might cross-react with similar subunits expressed on what are otherwise dissimilar carbohydrate structures. For example, antibodies that recognize MCP might cross-react with the sialyic acid portions of SLX and SLA. It is also possible that anti-peptide sera reactive with MCP reacts with the tetrasaccharide core of LeY since the peptide motif that mimics LeY bears similarity with the peptide motif that mimics MCP (Table 1 and Figure 1).

The possible structural similarities suggest that anti-sera raised to the peptide putative motifs might cross-react with a variety of subunits representative of Lewis antigens. The immunological presentation of the putative motifs, (i.e. short or longer peptides, presentation in a helix or beta bend) might mimic overlapping epitopes on otherwise different carbohydrate structures. To test this idea, Balb/c mice were immunized with peptides representative of the motif YYPYD (P1), YYRYD (P2), and the tract YYRGD (refrred to as P3). To enhance their immunogenicity, the peptides were complexed to hydrophobic meningococcal group B outer membrane proteins referred to as proteosomes. The Peptides were synthesized with the addition of a 3 amino acid spacer and a Lauroyl group. The meningococcal outer membrane proteins or proteosomes were prepared and complexed to the Lauroyl-C-YGG-Peptides in a 1mg:1mg ratio (29). Sera were collected 1 week after the last immunization and tested for reactivity against MCP and carbohydrate probes of Lewis antigens or their subunits.

For ELISA assays, plates were coated with synthetic carbohydrate probes and allowed to react with the respective antisera (Figure 2). As a positive control, the monoclonal antibody BR55-2 which displays specificity for LeY was used (34, 35). The monoclonal antibody ME361, which displays specificity for the GD2 ganglioside, was used as a negative control (36). For BR55-2, selective binding was oberved for LeY with some reactivity for the Galβ1$\rightarrow$3GlcNAc structure representative of the TF antigen. We also observed binding with the related core structure Galβ1$\rightarrow$4GlcNAc shared between LeY and LeX (data not shown). However, this core structure is appearently not seen by BR55-2 when present in the LeX-pentasaccharide. ME361 was not reactive with any of the synthetic probes. It was observed that the anti-

peptide sera (1:200 titer) was reactive with respective carbohydrate probes above the FCS background binding, suggesting commonalties in recognition of functional groups among the subunits as indicated in figure 1. Antisera to the YYRGD motif was consistently 2 fold above the FCS background, followed by sera to the YYRYD motif displayong about 11/2 times above background. Sera generated against the YYPYD motif was observed to range between 2 to 6 fold above FCS reactivity. These data suggest that there is a large degree of overlap in the potential carbohydrate structures being recognized by the antisera which was expected since the peptides mimic a wide range of individual carbohydrate subunits.

FACS analysis of Tumor cells with anti-peptide sera. The extent of cross-reactivity of the sera among the synthetic probes suggest that the sera should bind to breast cells. The ability of the sera to bind to breast cells was evaluated by FACS analysis. We found that murine sera elicited against the peptides bind to the human breast line SKBR3 expressing high a level of lactoseries structures (Table 3), but little binding to the normal human breast line HS578. Some cross-reactivity of the anti-P3 sera to NIH3T3 cells was observed, but its specificity for SKBR3 was 4 fold higher. Some binding was also observed for the WM793 human melanoma cell line. For the melanoma cell line, some differences among the sera was displayed. These data suggest that the antisera for the most part recognize overly expressed carbohydrate antigens on human breast tumors, with diminished reactivity for normal breast and control cell lines.

We also examined the ability of synthetic probes to inhibit the binding of the sera to SKBR3 cells. Figure 3 summarizes represents one experiment in which the ability of LeY and Lea to inhibit the respective sera from binding to SKBR3 cells was assessed by FACS analysis. The positive control antibody BR55-2 is LeY inhibitiable by over 50% within the concentration range used. Normal mouse serum (NMS) is about background levels as observed previously (Table 2). While the antisera to YYRYD and YYRGD motifs are not inhibitable at the concentartions used for LeY and Lea, antisera to the YYPYD motif is inhibitiable by the LeY probe over the concentration used. These data suggest that the anti-YYPYD sera is sensitive to low concentrations of the LeY probe, similarly to the anti-LeY antibody BR55-2.

Mediated Cytotoxicity. We next examined the ability of the sera to mediate complement dependent cytotoxicity (CDC) of the SKBR3 human adenocarcinoma cell line. In fig 4a we observe that the anti-

Lewis Y antibody BR55-2 mediates CDC at high antibody concentrations, approaching 80% at 100ug. The negative control antibody ME361 did not mediate CDC of SKBR3. In figure 4b we observe that the three lead anti-peptide sera mediate CDC of SKBR3 about the same, while normal mouse sera did not. This result was observed for the MCF7 line as well (data not shown). Whie the antisera was observed to bind to the human melanoma WM793 lineas assesed by FACS (Table 2), we did not observe CDC killing of this cell line (data not shown). These data suggest that the peptides can induce immune responses that target tumor cells, mediating their killing in vitro. The relatively low titers for effective killing might be the result of the density of carbohydrate epitopes on the cell. More faithful peptide mimics of the respective mucin epitopes, clustered in a fashion to mimic the high carbohydrate density, might prove more effective in mediating killing.

Discussion

Mucins are attracting great interest as potential targets for immunotherapy in the development of vaccines for cancers (e.g., breast, pancreas, ovary, and others) as there is (1) a 10-fold increase in the amount in adenocarcinomas; (2) an alteration in expression where they become ubiquitous, and (3) due to altered glycosylation, new epitopes appear on the cell surface that are absent in normal tissues (37). Several investigators have shown that the expression of the STn epitope on mucins is associated with a poor prognosis in several human cancers suggesting that STn may have functional significance in metastasis. Immunization with STn formulations have resulted in the observation that immunized patients can mediate complement dependent cytotoxicity that parallel those observed with murine monoclonal antibodies (5, 24, 25). This suggests that antibodies recognize the cancer-associated disaccharide NANA alpha (2-->6)GalNAc. Evidence of a clinical response was noted in immunized breast cancer patients, with other patients showing prolonged disease stability (5, 24, 25). By the same token, the difucosylated neolactoseries structure Lewis Y, associated with several human tumors such as breast, lung and gastrointestinal carcinomas (1-4, 9-11, 38) is also specifically detected by MAbs. These MAbs have unique properties among MAbs specific for solid tumors, i.e., they are rapidly internalized and can effectively utilize human effector mechanisms (both cellular and complement-dependent) for tumor cell

destruction and inhibit tumor growth in nude mice xenografted with human tumor cells (34, 39, 40). However, there is no evidence that Lewis Y is immunogenic in man.

As anti-carbohydrate antibodies reactive with carbohydrates associated with solid tumors (Figure 1) mediate complement dependent cytotoxicity, we wanted to examine whether peptides that mimic carbohydrate forms can induce antibodies that are reactive with breast tumor associated carbohydrates and whether this antisera can mediate breast tumor killing in vitro. Mice were immunized with peptide proteosome complexes and sera was found to be reactive with representative breast associated carbohydrates (Figure 2). It was further observed that the sera bound to SKBR3 cells in FACS analysis, with diminished reactivity with normal breast cells (Table 2). This activity is inhibitiable by select synthetic probes (Figure 3). We also found that the sera mediates complement dependent cytotoxicity of the SKBR3 human adenocarcinoma cell lines at about 1:15 dilution (Figure 4). The SKBR3 line expreses high levels of the LeY antigen, which can be targeted by both anti-LeY MAbs (Figure 4a) and by the peptide antisera(Figure 4b). Based upon our present analysis the YYPY motif appears to better mimic the LeY antigen subunits than the other motifs, since antisera to this motif is close to 40% inhibitable at 0.5 ug of synthetic probe (Figure 3).

Very few groups are investigating carbohydrate based vaccines or carbohydrate based immunotherapy. One major reason for this is that carbohydrate antigens are expensive and very difficult to synthesize. Further, expression of tumor-associated carbohydrate antigens is by no means specific to tumors. Crucial issues are expression of antigen density, multivalency, reactivity thresold of antibody binding, and efficient production of antibody having a strong complement-dependent or T cell dependent cytotoxic effect on tumor cells without damage to normal tissues. Studies on cancer vaccine development depend on many factors for success that include: 1) Selection of carbohydrate epitopes; 2) Design and assembly of epitopes coupled to macromolecular complex as an efficient immunogen; 3) Establishment or availability of a good animal model; 4) Evaluation of immune response in animals; tumor rejection without damage to normal tissues; and 5) careful clinical application.

Since carbohydrate antigens are generally weakly immunogenic in humans, only short lived IgM responses have been historically observed. The importance of adjuvant sublimation is highlighted in such

studies to offset the relatively weak immunogenicity of carbohydrate structures (6, 15, 17-21, 23-25). In addition, antibodies to carbohydrates are typically of low affinity and the notion of how cellular immunity is modulated by carbohydrates antigens is unclear. Subsequently, protein antigens have been viewed as more viable for vaccine development and genetic vaccination is the most recent trend in such studies. The notion of using peptide mimics of carbohydrates to induce anti-carbohydrate immune responses parallels the use of anti-idiotypic antibodies as immunogens. Peptides that mimic carbohydrates might be used to augment naturally available immunoglublins to tumor antigens. It is now also clear that humans with cancer have, in their draining lymph nodes, precursors of cytotoxic T cells that can be stimulated in vitro to react against their tumors (37). Peptide formulations might trigger such precursors. Subsequently peptides that mimic tumor associated carbohydrates would be of importance as novel agents for adjuvant therapy.

Acknowledgment

This work was funded by the USAMRMC (DAMD17-94-J-4310) Breast Cancer Initiative.

References

1. Hakomori S. Possible functions of tumor-associated carbohydrate antigens. Current Opin. Immunol. 1991;3:646-653.

2. Hakomori S. Aberrant glycosylation in tumors and tumor-associated carbohydrate antigens. Adv. Cancer Rres. 1989;52:257-331.

3. Dennis JW, Laferte S. Oncodevelopmental expression of GlcNAcβ1,6Manα1,6 Manα1-branched asparagine-linked oligosaccharides in murine tissues and human breast carcinoma. Cancer Res. 1989.;49:945-950.

4. Hiraizumi S, Takasaki S, Ochuchi N, et al. Altered glycosylation of membrane glycoproteins associated with human mammary carcinoma. Jap. J. Cancer Res. 1992;83:1063-1072.

5. MacLean GD, Reddish M, Koganty RR, et al. Immunization of breast cancer patients using a synthetic sialyl-Tn glycoconjugate plus Detox adjuvant. Cancer Immunology, Immunotherapy 1993;36(4):215-22.

6. Springer GF, Desai PR, Tegtmeyer H, Carlstedt SC, Scanlon EF. T/Tn antigen vaccine is effective and safe in preventing recurrence of advanced human breast carcinoma. Cancer Biotherapy 1994;9(1):7-15.

7. Toyokuni T, Hakomori S, Singhal AK. Synthetic carbohydrate vaccines: synthesis and immunogenicity of Tn antigen conjugates. Bioorganic & Medicinal Chemistry 1994;2(11):1119-32.

8. Adluri S, Helling F, Ogata S, et al. Immunogenicity of synthetic TF-KLH (keyhole limpet hemocyanin) and sTn-KLH conjugates in colorectal carcinoma patients. Cancer Immunology, Immunotherapy 1995;41(3):185-92.

9. Bremer EG, Levery SB, Sonnino S, et al. Characterization of a glycosphingolipid antigen defined by the monoclonal antibody MBR1 expressed in normal and neoplastic epithelial cells of human mammary gland. J. Biol. Chem. 1984;259:14773-14777.

10. Nakagoe T, Fukushima K, Hirota M, et al. Immunohistochemical expression of blood group substances and related carbohydrate antigens in breast carcinoma. Jpn. J. Cancer Res. 1991;82:559-568.

11. Blaszczyk-Thurin M, Thurin J, Hindsgaul O, Karlsson KA, Steplewski Z, Koprowski H. Y and blood group B type 2 glycolipid antigens accumulate in a human gastric carcinoma cell line as detected by monoclonal antibody. Isolation and characterization by mass spectrometry and NMR spectroscopy. J Biol Chem 1987;262(1):372-9.

12. Rodeck U, Herlyn M, Leander K, Borlinghaus P, Koprowski H. A mucin containing the X, Y, and H type 2 carbohydrate determinants is shed by carcinoma cells. Hybridoma 1987;6:389-401.

13. Miyake M, Taki T, Hitomi S, Hakomori S. The correlation of expression of H/Ley/Leb antigens with survival of patients with carcinoma of the lung. Biochemistry 1992;327:14-18.

14. Ma XC, Terata N, Kodama M, Jancic S, Hosokawa Y, Hattori T. Expression of sialyl-Tn antigen is correlated with survival time of patients with gastric carcinomas [see comments]. European Journal of Cancer 1993;.

15. Ravindranath MH, Morton DL. Role of gangliosides in active immunotherapy with melanoma vaccine. [Review]. International Reviews of Immunology 1991;7(4):303-29.

16. Mond JJ, Lees A, Snapper CM. T cell-independent antigens type 2. [Review]. Annual Review of Immunology 1995;13(655):655-92.

17. Helling F, Shang A, Calves M, et al. GD3 vaccines for melanoma: superior immunogenicity of keyhole limpet hemocyanin conjugate vaccines. Cancer Research 1994;54(1):197-203.

18. Helling F, Zhang S, Shang A, et al. GM2-KLH conjugate vaccine: increased immunogenicity in melanoma patients after administration with immunological adjuvant QS-21. Cancer Research 1995;55(13):2783-8.

19. Livingston PO. Construction of cancer vaccines with carbohydrate and protein (peptide) tumor antigens. [Review]. Current Opinion in Immunology 1992;4(5):624-9.

20. Livingston PO, Calves MJ, Helling F, Zollinger WD, Blake MS, Lowell GH. GD3/proteosome vaccines induce consistent IgM antibodies against the ganglioside GD3. Vaccine 1993;11(12):1199-204.

21. Livingston PO, Adluri S, Helling F, et al. Phase 1 trial of immunological adjuvant QS-21 with a GM2 ganglioside-keyhole limpet haemocyanin conjugate vaccine in patients with malignant melanoma. Vaccine 1994;12(14):1275-80.

22. Livingston PO, Wong GY, Adluri S, et al. Improved survival in stage III melanoma patients with GM2 antibodies: a randomized trial of adjuvant vaccination with GM2 ganglioside. Journal of Clinical Oncology 1994;12(5):1036-44.

23. Livingston PO. Approaches to augmenting the immunogenicity of melanoma gangliosides: from whole melanoma cells to ganglioside-KLH conjugate vaccines. [Review]. Immunological Reviews 1995;145(147):147-66.

24. Longenecker BM, Reddish M, Koganty R, MacLean GD. Immune responses of mice and human breast cancer patients following immunization with synthetic sialyl-Tn conjugated to KLH plus detox adjuvant. Annals of the New York Academy of Sciences 1993;690(276):276-91.

25. Longenecker BM, Reddish M, Koganty R, MacLean GD. Specificity of the IgG response in mice and human breast cancer patients following immunization against synthetic sialyl-Tn, an epitope with possible functional significance in metastasis. Advances in Experimental Medicine & Biology 1994;353(105):105-24.

26. Ifversen P, Martensson C, Danielsson L, Ingvar C, Carlsson R, Borrebaeck CA. Induction of primary antigen-specific immune reponses in SCID-hu-PBL by coupled T-B epitopes. Immunology 1995;84(1):111-6.

27. Zhang S, Walberg LA, Ogata S, et al. Immune sera and monoclonal antibodies define two configurations for the sialyl Tn tumor antigen. Cancer Research 1995;55(15):3364-8.

28. Mandrell RE, Apicella MA. Lipo-oligosaccharides (LOS) of mucosal pathogens: molecular mimicry and host-modification of LOS. [Review]. Immunobiology 1993;187(3-5):382-402.

29. Westerink MAJ, Giardina PC, Apicella MA, Kieber-Emmons T. Peptide mimicry of the meningococcal group C capsular polysaccharide. Proc. Natl. Acad. Sci. 1995;92:4021-4025.

30. Lowell GH, Smith LF, Seid RC, Zollinger WD. Peptides bound to proteosomes via hydrophobic feet become highly immunogenic without adjuvants. Journal of Experimental Medicine 1988;167(2):658-63.

31. Lowell GH, Ballou WR, Smith LF, Wirtz RA, Zollinger WD, Hockmeyer WT. Proteosome-lipopeptide vaccines: enhancement of immunogenicity for malaria CS peptides. Science 1988;240(4853):800-2.

32. Zollinger WD, Mandrell RE, Griffiss JM, Altieri P, Berman S. Complex of meningococcal group B polysaccharide and type 2 outer membrane protein immunogens in man. J. Clin. Invest. 1979;63:836-848.

33. Hoess R, Brinkmann U, Handel T, Pastan I. Identification of a peptide which binds to the carbohydrate-specific monoclonal antibody B3. Gene 1993;128(1):43-9.

34. Scholz D, Lubeck M, Loibner H, et al. Biological activity in the human system of isotype variants of oligosaccharide-Y-specific murine monoclonal antibodies. Cancer Immunology, Immunotherapy 1991;33(3):153-7.

35. Steplewski Z, Blaszczyk TM, Lubeck M, Loibner H, Scholz D, Koprowski H. Oligosaccharide Y specific monoclonal antibody and its isotype switch variants. Hybridoma 1990;9(2):201-10.

36. Iliopoulos D, Ernst C, Steplewski Z, et al. Inhibition of metastases of a human melanoma xenograft by monoclonal antibody to the GD2/GD3 gangliosides. Journal of the National Cancer Institute 1989;81(6):440-4.

37. Apostolopoulos V, McKenzie IF. Cellular mucins: targets for immunotherapy. [Review]. Critical Reviews in Immunology 1994;14(3-4):293-309.

38. Springer GF. T and Tn, general carcinoma autoantigens. Science 1984;224:1198-1206.

39. Steplewski Z, Lubeck MD, Scholz D, Loibner H, McDonald SJ, Koprowski H. Tumor cell lysis and tumor growth inhibition by the isotype variants of MAb BR55-2 directed against Y oligosaccharide. In Vivo 1991;5(2):79-83.

40. Lubeck MD, Kimoto Y, Steplewski Z, Koprowski H. Killing of human tumor cell lines by human monocytes and murine monoclonal antibodies. Cellular Immunology 1988;111(1):107-17.

41. Scott JK, Loganathan D, Easley RB, Gong X, Goldstein IJ. A family of concanavalin A-binding peptides from a hexapeptide epitope library. Proceedings of the National Academy of Sciences of the United States of America 1992;89(12):5398-402.

42. Oldenburg KR, Loganathan D, Goldstein IJ, Schultz PG, Gallop MA. Peptide ligands for a sugar-binding protein isolated from a random peptide library. Proceedings of the National Academy of Sciences of the United States of America 1992;89(12):5393-7.

Figure Legends

Figure 1. Common adenocarcinoma associated carbohydrate structures.
Figure 2. ELISA profiles of synthetic carbohydrate probes with the anti-peptide sera.
Figure 3. Inhibition of binding of antisera to SKBR3 cells.
Figure 4. CDC mediated killing SKBR3 cell line. a) CDC killing by BR55-2; b) CDC killing by anti-peptide sera.

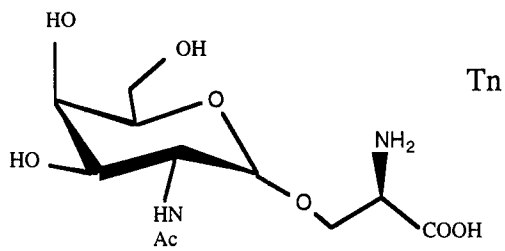

Tn (αGalNAc-O-Ser)

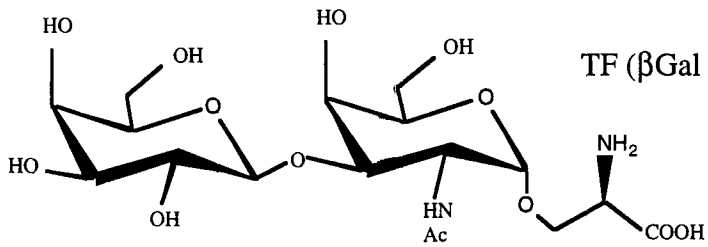

TF (βGal 1-3 αGalNAc-O-Ser)

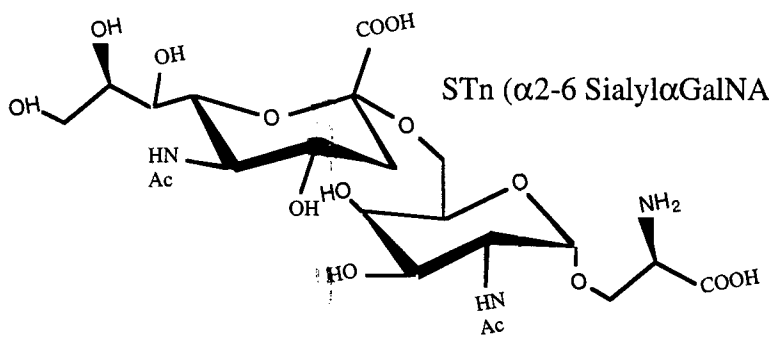

STn (α2-6 SialylαGalNAc-O-Ser)

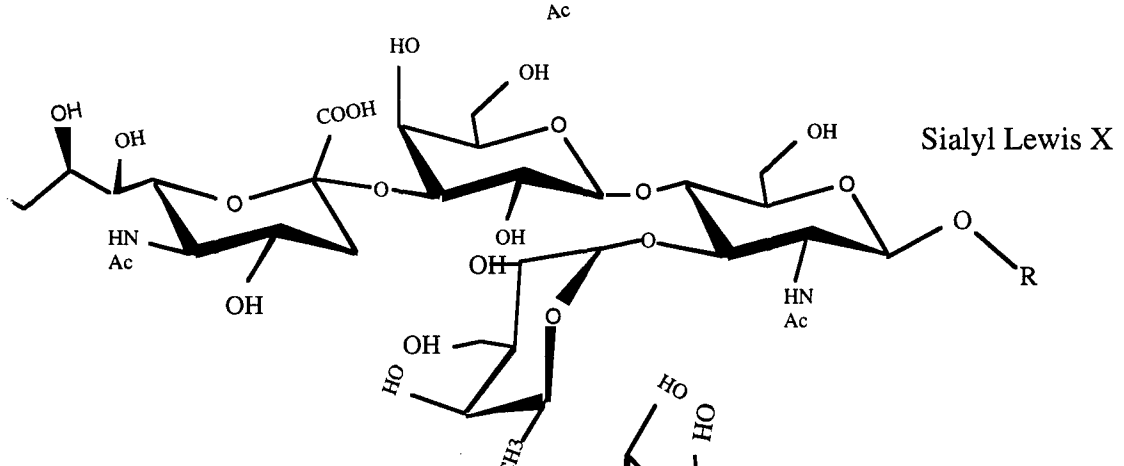

Sialyl Lewis X

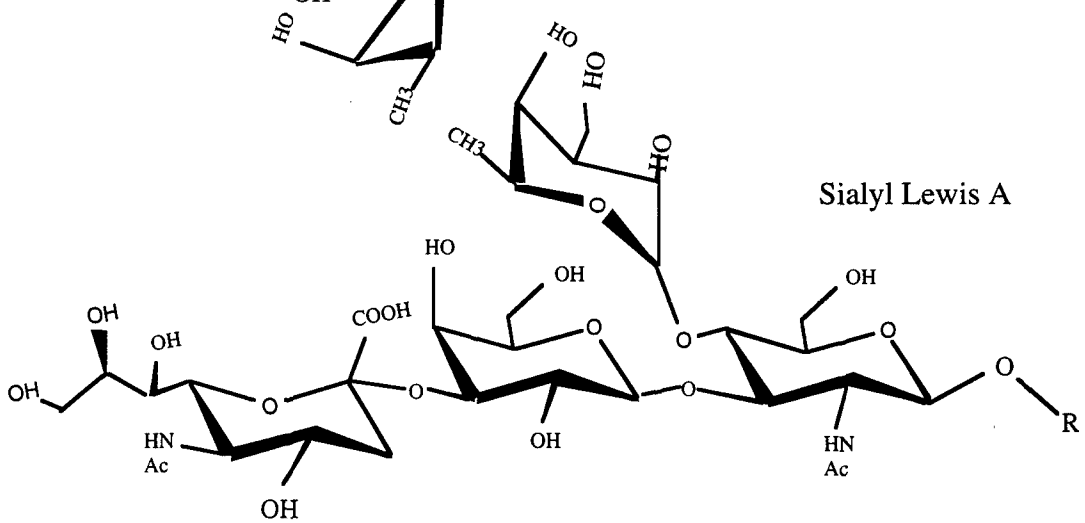

Sialyl Lewis A

Table 1

Peptide	Carbohydrate	Structure	Reference
YYPY (P1)	Mannose	methyl-α-D-mannopyranoside	(41, 42)
WRY	Glucose	α(1→4glucose	
PWLY	Lewis Y	Fucα1→2Galβ1→4(Fucα1→3)GlcNAc	(33)
YYRYD (P2)	Group C Polysaccharide	α(2→9)sialic acid	(29)

Figure 2

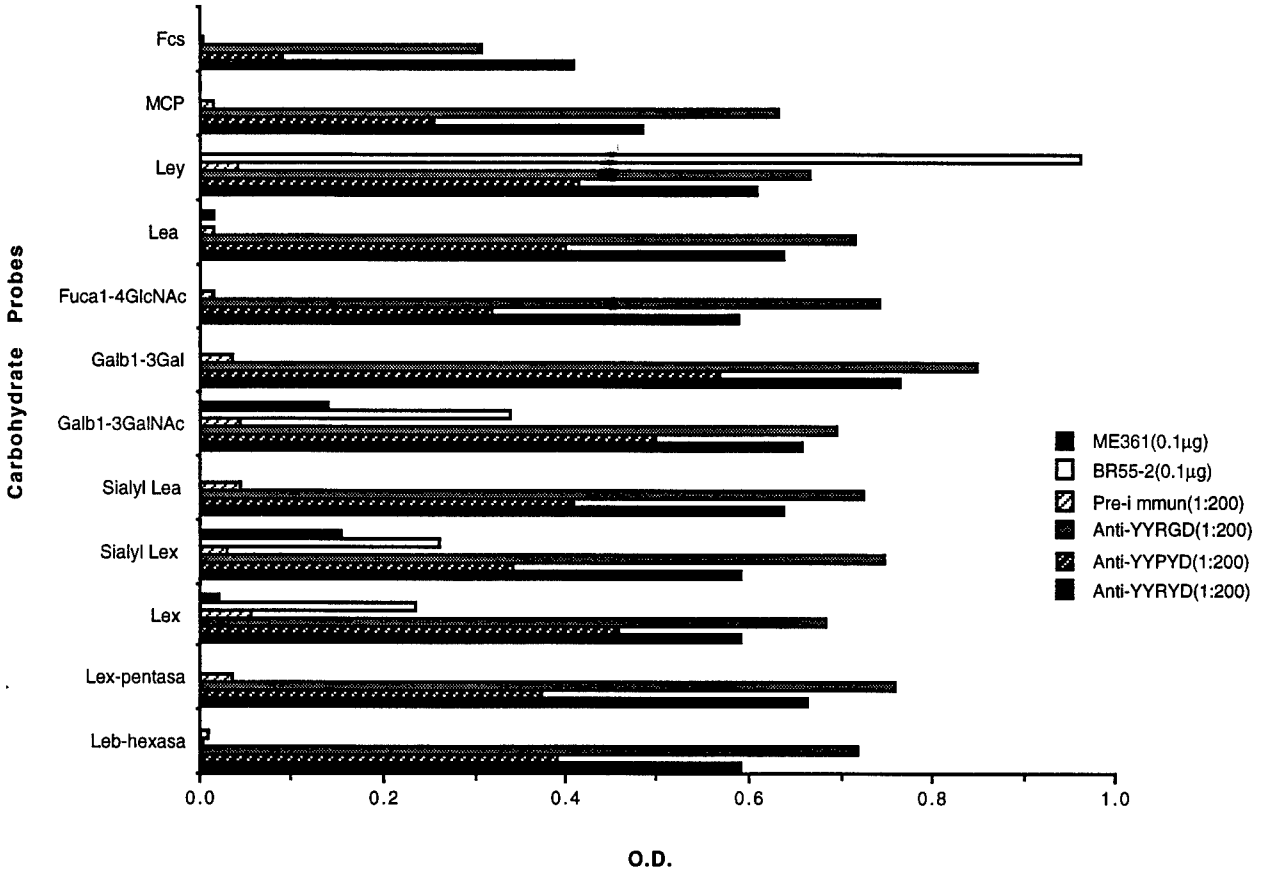

Table 2 Binding of the Anti-Peptide Sera to Different Cells As Measured by FACS

Cell Line	Anti P1 (YYPY)	Anti P2 (YYRYD)	Anti P3 (YYRGD)
SKBR3	171.0	120.0	101.0
HS578 Bst (normal breast)	17.8	19.9	22.4
WM793	145.5	172.4	42.3
NIH3T3 Murine Fibroblasts	20.9	21.8	41.7

Representative FACS experiment. Final sera concentration was 1:50. Background fluorescence (Mean Fluorescence) associated with non-specific mouse sera is 24.2, 25.2, and 23.7 for SKBR3, and NIH 3T3 cells, respectively. Background for the human melnoma line WM793 was on average 24.4.

Figure 3

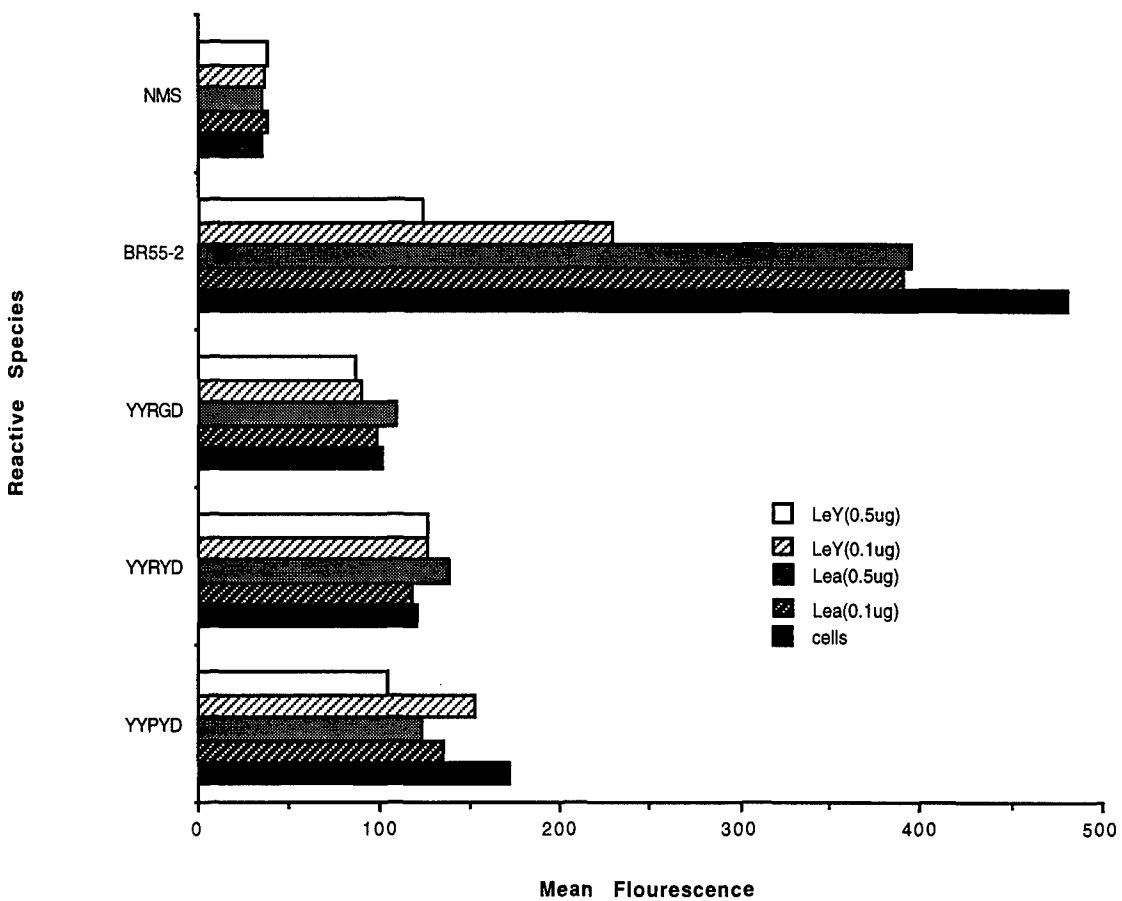

Figure 4 a

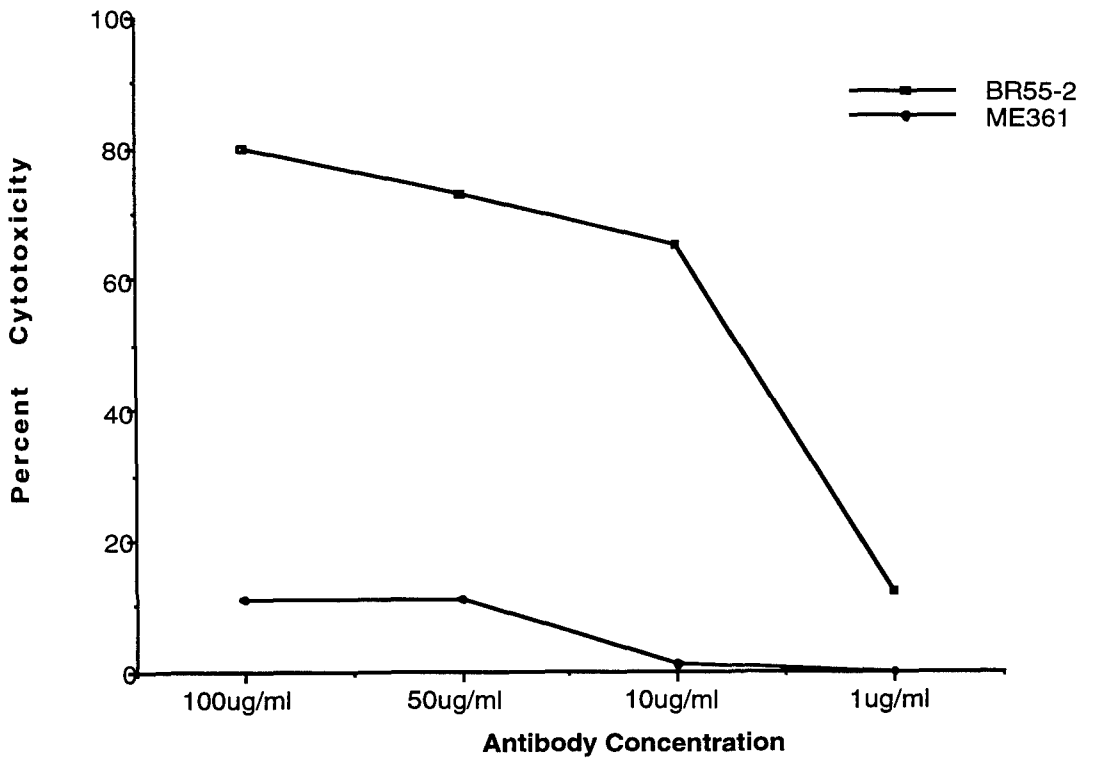

Figure 4b

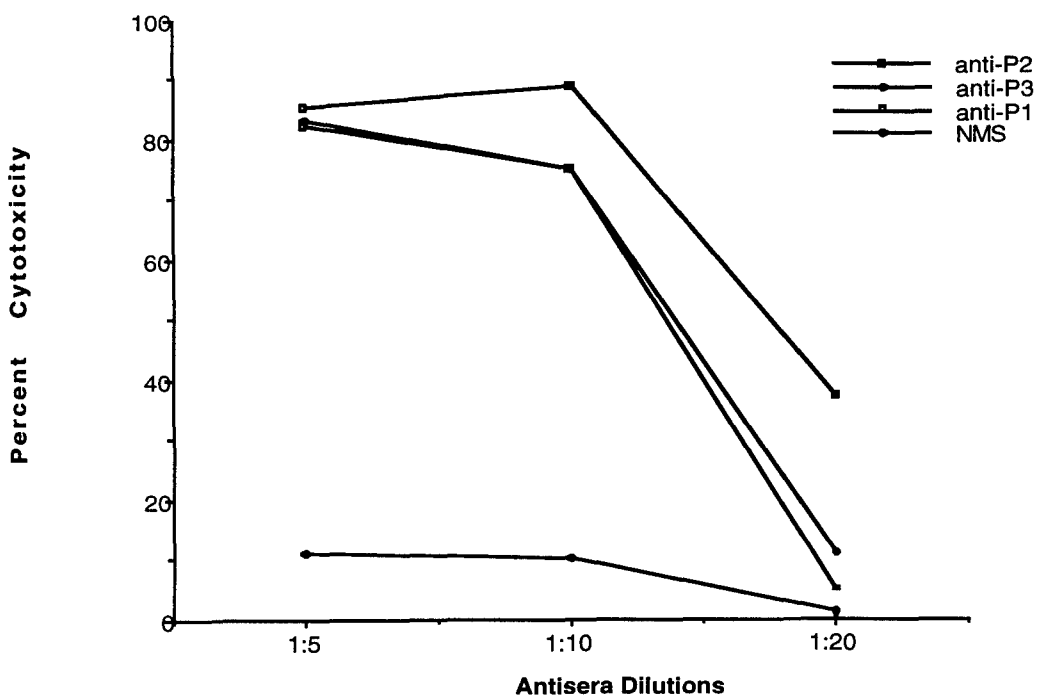

Manuscript Submitted for Publication

#3

Non-Radioactive ΔTaq Cycle Sequencing for Filamentous Phage DNA

Kay words: ΔTaq DNA polymerase; Cycle DNA sequencing; Filamentous phage library

Jianping Qiu[1], Huanying Zhou[2], Joseph F. Aceto[1], Thomas Kieber-Emmons[1+]; Department of Pathology and Laboratory Medicine, School of Medicine, University of Pennsylvania[1]; Department of Neuroscience, School of Medicine, University of Pennsylvania[2]

+Address all correspondence to:
Thomas Kieber-Emmons, Ph.D.
Department of Pathology and Laboratory Medicine
Room 280, John Morgan Building
36th and Hamilton Walk
Philadelphia, PA 19104-6082
Phone: (215) 898-2428
Fax: (215) 898-2401

Abstract

We describe a rapid non-radioactive double-stranded phage DNA sequencing method using ΔTaq polymerase in cycle reaction for phage peptide-display library screening. This procedure is specific, rapid, sensitive and safe for the sequencing of large numbers of peptide phage display colonies. In addition, thermal cycle sequencing with this chemiluminescent image detection protocol provides an inexpensive method for completing a large amount of sequencing reactions. Consequently, this method is especially useful for those extensively working on peptide mimics using phage display libraries.

Introduction

Phage display libraries have become an important tool in biotechnology. Phage peptide display libraries have been extensively used in investigating unknown peptide fragments with certain specific bioactivities [1, 5, 6]. Although limited length DNA fragments need to be sequenced (usually spanning from 18-45 bp of interest), sequencing large numbers of phage clones for this purpose is an arduous task. Mutational studies, holding fixed consensus residues identified by comparing a large number of phage sequences, adds to the volume of sequencing required. Phage DNA is usually more difficult to sequence however than that from typical plasmid DNA due to its tedious purification and possible interference from secondary structure of the DNA. Subsequently, it has become an important topic to develop a simple yet reliable sequencing method especially when large numbers of clones need to be examined [2].

To offset the prolonged exposure to radio-nucleotides during large phage sequence studies, we have developed a non-radioactive ΔTaq cycle sequencing protocol, displaying the following features: 1). Many samples can be handled at a time. One can start with 50-100 single phage colonies. Rather than using 96 well plates for phage proliferation, we found that single microtube culturing eliminated cross contamination among phage colony samples; 2). the phage DNA template preparation method is clean and fast. No contaminated DNA and RNA from host cells is observed on 1% agarose gel; 3). The method is fast. The optimized cycling sequencing protocol has made double-stranded phage DNA sequencing accomplished in less than 90 min., with reliable and reproducible results; 4). One can directly sequence double-stranded phage DNA starting with a very low amount of DNA; 5). The method leads to a fast exposure time: 8-20 min; 6). ΔTaq polymerase generates a much lower background than that by the Taq enzyme; 7). The method eliminates radioactive materials without sacrificing sensitivity and resolution. The described four lane sequencing approach has advantages over a two lane sequencing strategy [2] in that the percentage of readable clones is significantly increased (100%) compared to an estimated 76% from a two lane approach [2]. In addition, cross contamination risk from the two lane protocol is high and more hidden hands-on work is involved. Another practical advantage is sample size. When DNA template is less sufficient, the two lane sequencing method suffers from weaker band reading than that using our four lane strategy.

Materials and Methods

Phage DNA Preparation: To prepare phage DNA, we inoculated 1 ml terrific broth containing 100 µg Kanamycin / ml and 20 µg Tetracycline/ ml with each single phage pIII15 colony in a 1.5 ml tube, shaked at 300 rpm at 37°C overnight and then spun at 7,000 rpm, at 4°C, for 10 min. Supernatant was then transferred to clean tubes to which 2 ul of RNase A (USB, Cat # E701942, 12U/µl) was added for a final concentration of 24 U/ ml. This was followed by the addition of 2 ul DNAase I (BMB, Cat # 776 785, 10 U/ ul). The solution was vortexed briefly, quickly spun down and incubated at 37°C for 60 min. PEG/ NaCl solution (16.7%/ 3.3 M) was then added to the supernatant to a final volume of 15% and kept at -20°C for 1hr. The solution was centrifuged at 12,000 rpm at 4°C for 15 min., with the supernatant aspirated off as much as possible. The residual amount of solution was briefly spun again and aspirated. The pellet was resuspended in 0.2 ml of TBS buffer, spun at 12,000 rpm for 5 min. at room temperature and the supernatant was transferred to a clean 1.5 ml tube. The DNA was extracted by adding 0.2 ml of phenol:chloroform (3:1)/ tube and briefly vortexed and spun for 4 min at Rt. The top aqueous layer was transferred to a clean 1.5 ml tube. The extraction was performed three times. 0.2 ml chloroform was added to each vial, vortexed briefly and spin for 4 min at Rt. After removal of the top aqueous layer, 0.1 volume of 5 M sodium acetate (pH 5.5) and 2.5 volumes of 100% ethanol was added, vortexed and left at -70°C for 30 min. The sample was microcentrifuged at 10,000 xg for 15 min. at 4°C, the supernatant aspirated, and washed with 1 ml of 90% ethanol/ tube. After removal of the supernatant, the residual volume was spin again and the supernatant aspirated again. The pellet was air dried for 20 min. The final DNA was salt-free, phenol and PEG free and ready for cycle DNA sequencing.

Primer design and biotinylation : Primer 1797 was designed using the Program Oligo 5.0™ (NBI) with the full length sequence of the FUSE 5 phage vector. The primer was synthesized on an Applied Biosystems Cyclon Oligo Synthesizer 450. Total primer length is 27mer with Tm = 78°C: 3'-GTAGCATTCCACAGACAGCCCTCATAG-5' (52% G+C, 48% A+T). The synthesized primer was then cartridge purified (Applied Biosystems, #400771). Biotinylation was performed using USB Kit # 72350, modifying the procedure slightly. We mixed 20 µl of cartridge purified Primer 1797 (0.25 nmol/ µl) in a 0.5 ml tube containing 230 µl of Kinase Reaction Mix (Table 1). The tube was incubated at 37°C 1 hr.

then inactivated at 70°C 10 min., 30 µl of 1M KPO_4, pH 8.0 was added to the 250 µl reaction mix. Coupling was performed with the addition of 25 µl 20 mM N-Iodoacetyl-N'-Biotinylhexylenlodiamine or NIBH (USB, cat.#72353) in Dimethyl Formamide (DMF). After mixing well, the reaction was incubated at 50°C for 1 hr. During this period, 5 Sephadex G-25 columns were equilibrated according to the manufacture's specifications (BMB, cat # 1273 922). Briefly, the column was removed from the storage bag and gently invert several times to resuspend the medium. After removal of the top cap followed by removal the bottom tip (to avoid creating a vacuum and uneven flow of the buffer), the buffer was allowed to drain by gravity and discarded. The columns were washed using 4X column volume of Column Washing Buffer (Table 1). The column was placed in a collection tube, and centrifuged at 1100 x g for 2 min using a swinging-bucket rotor. The collection tubes were discarded along with the eluted buffer. With the column in an upright position, the DNA sample (up to 50 µl) was applied to the center of the column bed to avoid applying the sample to the sides of the column and subsequent loss of nucleotides. Total volume was kept below 50 µl so as to avoid overloading the column and consequent flow through of nucleotides, contaminating the DNA sample. The column was placed in the second collection tube and maintained in an upright position. Any change in the position of the column causes back flow of the DNA sample, resulting in reduced recovery. The column was then centrifuged for 4 min at 1100 xg. at Rt and the eluate saved from the second collection tube. This contained the purified DNA sample.

ΔTaq Cycle Sequencing : Cycle sequencing was completed according to previously described protocol with all reaction mixes kept on ice until needed [4]. Template DNA was dissolved with 12 µl dH_2O in a 0.5 ml tube. Sets of 0.5 ml tubes labeled with G.A.T.C. were prepared and 4 µl of each terminal mix (G.A.T.C.) was added into each tube. All tubes were capped until needed. ΔTaq Enzyme (25-30 units/ul) was diluted with 6 µl ice-cold Dilution Buffer (Table 1). The diluted enzyme was used within 8 hrs. For each DNA template 2 µl of the diluted enzyme was added. In a 0.5 ml tube, a master mix was made containing the following for each DNA sample: 2 µl Reaction buffer (USB); 1µl biotinylated primer 1797 (1pmol / µl in water); 2 µl diluted ΔTaq enzyme. The master mix was mixed well by pipetting and 5 µl transferred to each DNA template tube and mixed well. 4 µl of this mixture was transferred to each set of G,A,T,C tubes, mixed well by pipetting, and then spin down. 10 µl of light mineral oil was added to

each tube then spin down again. The sequencing cycle reaction was completed at 95°C, 30 sec; 72°C, 60 sec for 47 cycles using an MJ Research thermal cycler. 4 µl of stop solution (Table 1) was added to each tube, spun down, the tube tapped and spun down again. If electrophoresis was not run immediately, samples were kept at -20°C.

Gel Running : Electrophoresis was completed as previously described [3]. Typically we use 6 % denaturing sequencing gel with 1X TBE running buffer for sequencing. Samples are usually heated at 95°C for 3 min just before use, then chilled on ice. Loading amount: 4 µl/ lane; Running condition: Power supply: Stratagene FeatherVolt 2000. Prerun the gel at 70 W constant power until the gel temperature reaches 48 to 50°C. Total running time: 2 hrs.

Sequencing Image Detection: The DNA was transferred to the Nylon Membrane according to the following protocol. Hybond nylon membrane (Amersham) and several sheets of 3 MM filter paper were cut slightly larger than the area of the gel to be transferred. The membrane was prewet with dH_2O in a clean tray. The short glass plate with the inside surface siliconized was removed from the gel . With clean rinsed gloves, the membrane was placed on the gel leaving no air bubbles. It was important not to move the membrane once in contact with the surface. If necessary, air bubbles are rolled out with a clean 25 ml pipette. With 2 sheets of 3 MM paper laying on top of the membrane and a short glass plate onto sheets, a 2 kg weight was placed onto the glass plate. Transfer occurred at Rt. for 1 to 1.5 hrs. After the transfer, the membrane was carefully removed from the gel, air dried, and placed in a development bag for storage at 4°C.

Detection of DNA Sequence: 1X blocking buffer (0.3 ml/ cm^2) was placed into the bag, and all air removed. The bag was sealed with a clip and agitated for 30 min on an orbital shaker at 100 rpm. SAAP (streptavidin-alkaline phosphatase conjugate) was added in a 1:2000 to 1:4000 volume directly to the blocking buffer (Table 1) and mixed immediately by inverting the bag several times. Again all air was removed and the bag sealed with a clip. The bag was agitated for 10 min to 30 min at Rt at 100 rpm with the incubation time varying based on the batch of SAAP. The bag was then drained completely and any liquid removed by rolling with a 25 ml pipette. The membrane was rinsed once with 0.5 ml/ cm^2 dH_2O and then washed with 0.5 ml/ cm^2 1X wash buffer A resealed, and agitated for 10 min at 100 rpm (x3). The

membrane was rinsed briefly with dH_2O by adding 0.5 ml/ cm^2 dH_2O to the bag, agitated 3 min at 100 rpm, drained, and replaced with 0.5 ml/ cm^2 1X wash buffer B. The bag was resealed, agitated for 5 min at 100 rpm., drained, and stored at 4°C until for the film exposure.

Exposure of Membrane to Film: Using a sterile pipette, 0.01 ml Lumi-Phos 530 / cm^2 was added into a sealed bag containing the membrane. The liquid was distributed over the entire membrane by gently rolling a 25 ml pipette back and forth across the bag for 3 min at Rt. Any remaining solution was removed and the bag sealed with a thermal sealer. The membrane was stored in the dark at Rt for 2 hours followed by immediate exposure to Amersham Hyperfilm (or equivalent) in close contact for 8 to 20 min at Rt.

Results and Discussions

Figure 1 shows that the non-radioactive cycle direct sequencing method presents high quality band resolution. On a 42 x 62 cm film, one can expose up to 30 samples with 4 lanes rather than 2 lanes for each sample. We have compared two approaches in phage DNA preparation. One utilizes asymmetric PCR , the other uses enzymatic disgestion with DNAse I and RNase A. Although one can use asymmetric PCR to amplify a target DNA fragment directly from a single colony, we feel for many entry level operators it is not an easy task to control all parameters, especially the transferring step from the end product after asymmetric PCR reactions to the next cycle sequencing. It is easier to start with inoculating 1 ml media with each single colony in a 1.5 ml tube (Eppendorf) and let them grow overnight. We routinely use 20 U of DNAase I and 24 U of RNase A for 1 ml overnight culture supernatant. Although overgrowing may cause cells to die, hence released cell contents interfere with phage DNA purification, we didn't encounter such a problem. By incubating phage-containing supernatant with DNAase I and RNase A at 37°C for 1 hr., the phage DNA is clean enough for cycle sequencing as checked by 1 % agarose gel (data not shown). We have found these units for the enzymes are the minimal required for a clean prepartion at 37°C, 60 min. We compared the enzymatic preparation method with another approach by directly loading PEG precipitated phage DNA on 1% low melting agarose gel. Although both methods can separate the contaminated DNA and RNA from the DNA of interest, the low melting agarose gel method requires much more hands-on time than the one step enzyme digestion. This is especially important when handling multiple samples. PEG precipitation should be performed after enzyme digestion

rather than before, because even a trace quantity of PEG can diminish enzyme activity. One can also add Proteinase K to the reaction after DNAase and RNase digestion and incubate for another 30 min. Our experience indicated there was no obvious difference. The amount of sodium acetate added is not strict. We used up to 10x the amount in this protocol and the results showed no significant difference in phage DNA precipitation (data not shown). After the last washing with 90% ethanol, it is easier to redissolve the phage DNA pellet by air drying than by speedvac drying.

We especially lengthened the primer from the typical length from 20-22 mers to 27mers to generate a Tm value above 76°C. Our primer has a calculated Tm value of 78°C. Therefore we can merge the annealing step and the extension step into one step by using the same temperature through the entire cycle sequencing reaction. This minimizes possible non-specific annealing during the reaction, dramatically reducing the non-relevant background bands and requiring less time for this step. This effectively excludes the ramp time between annealing and extension, and shortening the ramp time between the denaturing and annealing steps. We have found that the design of a sequencing primer should reflect a Tm value higher than 76°C. In other words, the length of the primer to be used in cycle sequencing should be 26-mer or longer. For those thermal cyclers which have a long ramp time, our design of the primer can efficiently cut the time duration, shortening the entire sequencing time; indirectly prolonging the thermal enzyme activity. We set up two different cycle sequencing programs. One was set up as 95°C, 30 sec; 63°C, 15 sec; 72°C, 60 sec; total 48 cycles. The other was set up as 95°C, 30 sec; 72°C, 60 sec; total 48 cycles. The results indicated that using the second program generated a cleaner background although the band density was slightly lower (data not shown). This was compensated by exposing the film for several minutes longer without sacrificing the resolution and background cleanness. In addition, much less template DNA was required in the sequencing reaction than in other non-cycling methods, because the template was amplified in the reaction. The rapid thermal cycling also helped prevent some sequencing problems due to reannealing of linear double-stranded templates. With the use of a thermostable DNA polymerase, this type of thermal cycling enabled the elongation reaction to be completed at a high temperature destabilizing secondary structures that may interfere with polymerase activity.

We also compared the amount of the sample loaded onto each well. Usually 2.5 ul/ lane generates a much better background than 4.5 ul/ lane without losing band image. Using this protocol, we were able to obtain readable sequences as close as 20 bp from the location of the primer. If closer bps are needed to be read, one can simply add Mn ions to the reaction without interfering with other reaction components. When the parameters were set up as 95°C, 30 sec; 72°C, 75 sec; 50 cycles, the total readable sequences was beyond 1000 bp. In order to obtain sharp bands during the transfer, it was better to use Whatman 3MM filter paper than the normal lab paper towel. The time for transferring ranged 1-1 1/2 hrs at room temperature. Since the sequence of interest in the pIII15 phage display library is only 45 bps long, we only needed to transfer that portion of the bands to the membrane saving transfer material.

While the two lane sequencing strategy suggested for phage display work has some advantages [2], our experience indicates that the readiblae clone percentage (76 %) is much lower than ours (100 %). This means that when 784 clones are prepared for sequencing, about 200 clones are unreadable and hence completely wasted. In addition, cross contamination risk from the two lane protocol is still high and more hidden hands-on work is involved. When the amount of DNA template is less, the two lane sequencing method suffers from visualizing faint bands as opposed to our 4 lane strategy. The transferred membrane can also be stored at 4°C for several days without sacrificing the resolution. It is also possible to get the membrane striped off the DNA for reuse. Finally, Biotinylation at the 5' end of primers complementary to the FUSE 5 vector was performed manually but oligonucleotide synthesis with biotin is the simplest and most practical labeling method.

Acknowledgment

This work was supported by the USAMRMC (DAMD17-94-J-4310) Breast Cancer Program.

References:

1. Felici, F., L. Castagnoli, A. Musacchio, R. Jappelli and G. Cesareni 1991. Selection of antibody ligands from a large library of oligopeptides expressed on a multivalent exposition vector. Journal of Molecular Biology. 222:301-10.

2. Haas, S.J. and G.P. Smith 1993. Rapid sequencing of viral DNA from filamentous bacteriophage. Biotechniques. 15:422-4.

3. Slatko, B. 1991. Protocols for manual dideoxy DNA sequencing. Methods in Nucleic Acids Research. J. Karam, L. Chao, and G. Warr, eds:83-129. CRC Press, Boca Raton, Fla.

4. Slatko, B.E. 1994. Thermal cycle dideoxy DNA sequencing. [Review]. Methods in Molecular Biology. 31:35-45.

5. Smith, G.P. 1991. Surface presentation of protein epitopes using bacteriophage expression systems. [Review]. Current Opinion in Biotechnology. 2:668-73.

6. Smith, G.P. and J.K. Scott 1993. Libraries of peptides and proteins displayed on filamentous phage. Methods in Enzymology. 217:228-57.

Table 1. Composition of Required Solutions

Terrific Broth: 12 g Bacto tryptone, 24 g Bacto yeast extract, 4 ml glycerol, 4 ml glycerol, in 900 dH_2O, autoclave. Add 100 ml of a sterile solution of 0.17 M KH_2PO_4 and 0.72 M K_2HPO_4
PEG/NaCl (16.7%/3.3 M): 16.7 g PEG 8000, 19.3 g NaCl in 100 ml; autoclaved.
10x Kinase Buffer: 0.5 M Tris-HCl (pH 7.5), 100 mM $MgCl_2$, 50 mM dithioerythritol, 1 mM spermidine, 1 mM Na_2EDTA (pH adjusted to 8.0 with NaOH); stored at -20°C
Kinase Reaction mix: 25 µl 10xT4 Buffer, 50 µl 1mM ATPgS, 150 µl dH_2O and 5 µl T4 Kinase (30 U/ µl) in a 250 µl reaction
Column Wash Buffer: Biotinylated DNA purification buffer (pH 7.0), 15 mM Sodium Citrate (pH 7.0), 150 mM NaCl, 0.1% SDS
Terminal mix: 80 µM dGTP, 80 µM dATP, 80 µM dCTP, 80 µM dTTP, 8 µM ddNTP (G,A,T or C), 50 mM NaCl
ΔTaq Dilution Buffer: 10 mM Tris HCl (pH 7.5), 5 mM DTT, 0.5 mg/ml BSA
5x Reaction Buffer: 200 mM Tris HCl (pH 7.5), 100 mM $MgCl_2$, 250 mM NaCl
Stop Solution: 95% Formamide, 20 mM EDTA, 0.05% Bromophenol Blue, 0.05% Xylene Cyanol FF
10x TBE: 108 g Tris base, 55 g Boric acid, 9.3 g $Na_2EDTA\text{-}2H_2O$ in 1000 ml dH_2O
6% Denaturing Sequencing Gel: 5.7 g/ 0.3 g Acrylamide/ Bis-acrylamide, 50 g Urea, 100 ml dH_2O, filter and degass, add 1 ml 10% ammonium persulfate and 25 µl N,N,N',N' Tetramethyl Ethylenediamine (TEMED)
5XBlocking Buffer: 2.5% Na Caseinate, 500 mM NaCl, 250 mM Tris, 0.5% SDS, 0.02% Na Azide. Adjust to pH 10 with NaOH (about 0.08%).
1XBuffer A: 0.1 M NaCl, 50 mM Tris-HCl (pH 10), 0.1 % SDS
1XBuffer B: 0.1 M NaCl, 50 mM Tris-HCl (pH 10)
TBS: 8g NaCl, 0.38g KCl, 3g Tris-Base, 0.015g phenol/red add dH_20 to 800 ml. Adjust pH to 7.4 with HCl. Adjust volume to 1 liter. Autoclave.

Figure Legend

Figure 1. **Typical sequencing gel from Non-Radioactive ΔTaq Phage DNA Sequencing.** Representative phage DNA sample was sequenced using the Biotinylated 1797 primer, with described procedure (see methods). The 4 lane sequenceing gel follows the order GATC, with the arrow on the primer end of the gel, pointing at the G lane. High band resolution is still obtained even after overexposure (15 min for this sample). Similar resolution is observed for ^{32}P (Sequenase Kit V2.0) after 5 hr exposure time (data not shown).

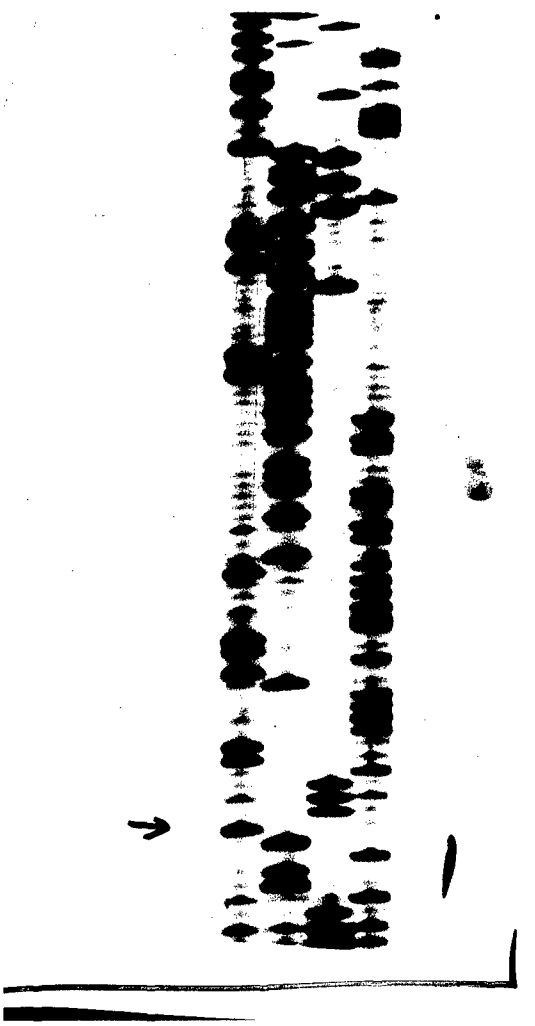

Figure 1

Manuscript Submitted for Publication

#4

Molecular recognition of a Peptide mimic of the Lewis Y antigen

Ramachandran Murali and Thomas Kieber-Emmons+

Department of Pathology and Laboratory Medicine, University of Pennsylvania, Philadelphia PA.

Address all correspondence to:
Thomas Kieber-Emmons, Ph.D.
Department of Pathology and Laboratory Medicine
Room 280, John Morgan Building
36th and Hamilton Walk
Philadelphia, PA 19104-6082
Phone: (215) 898-2428
Fax: (215) 898-2401

Summary
Peptides as mimics of carbohydrate moieties display a distinct advantage in both drug and vaccine design. To further our insight into structural relationships between peptide-mimics and carbohydrate structures, we have analyzed a potential recognition scheme between a murine monoclonal antibody, B3, directed against the tumor-associated antigen Lewis Y oligosaccharide and a peptide identified from phage display screening with B3 in which the putative sequence APWLY was found to be critical for antibody binding. The crystal structure of BR96, another anti-Lewis Y antibody, solved in complex with a nonoate methyl ester Lewis Y tetrasaccharide, was used as a guide to probe the molecular basis for B3-peptide recognition.

The interplay between carbohydrates and proteins is of fundamental importance in a number of different biological processes. The role of carbohydrate structures present on the cell surface is not fully understood but their presence range from influencing tumor growth, progression and metastases, to mediating bacterial and viral attachment (1, 2). Subsequently, the inhibition of these interactions is a possible point of therapeutic intervention for a number of diseases. Carbohydrates have been formulated as vaccines (3-8) and are also considered as pharmacophores (9-11). One of the problems in developing carbohydrate based therapeutics, however, is the difficulty involved in purifying or synthesizing some complex carbohydrate forms. An alternative approach is to develop mimics that could serve the same function, with one being peptides. Peptides that mimic carbohydrate forms have been identified by screening carbohydrate binding proteins against phage display peptide libraries (12-15), and by consideration of protein surrogates, particularly antibodies (16-21). In the vaccine development area, peptides as mimics of carbohydrates have an advantage in that they convert otherwise T cell independent antigens into T cell dependent forms. Peptides can recruit T cell help in eliciting higher affinity antibodies unlike carbohydrate immunogens. This is of particular relevance in the development of neonatal vaccines. In the drug development area, while peptides are not the best pharmaceutical agents of choice, they are easy to work with, and they provide structural concepts that can be tested to further develop small bioactive compounds (22, 23).

From a structural standpoint, several general questions still need to be addressed that are germane to the development of effective peptide mimics of carbohydrates for utility in vaccine or adjuvant formulation, which is our primary interest (21). First, is the binding site of anti-carbohydrate antibodies different than anti-peptide antibodies. Second, why are anti-carbohydrate antibodies often times of low affinity. In our own efforts to elucidate answers to such questions, we report here a molecular basis for mimicry of a peptide surrogate for the Histo blood group antigen Lewis Y. The Lewis Y (LeY) difucosylated type 2 lactoseries structure, Fucα1$\rightarrow$2 Galβ1$\rightarrow$4(Fucα1$\rightarrow$3) GlcNAcβ1$\rightarrow$3Galβ1$\rightarrow$4Glcβ1$\rightarrow$, expressed on both glycoproteins and glycolipids, is one tumor-associated carbohydrate structure being explored as a target for monoclonal antibody (MAb) based imaging and therapy. A peptide with the putative sequence APWLYGPA , as identified by phage display screening with the anti-LeY antibody B3, has been shown to compete with the LeY structure for B3 binding (15).

The B3 antibody displays homology with other anti-LeY antibodies, including the recently reported structure of antibody BR96 with a nonoate methyl ester LeY tetrasaccharide (24). Since the crystal coordinates for the ligated BR96 is not yet available, molecular modeling of B3 complexed with the putative tetrasaccharide core of LeY was performed based upon the BR96 -sugar recognition scheme (25). The B3 model emphasizes key polar and nonpolar interactions contributing to the molecular recognition features for Y that are shared among related anti-Y antibodies (Figure1), consistent with mapping profiles of lactoseries derivatives reactive with B3 (26). While current procedures for predicting ligand - antibody interactions is limited, mainly due to the conformational flexibility of ligands and antibodies, and the role of solvent in mediating ligand recognition and binding, the utilization of a crystallographically determined starting position can lend to discriminating differences in binding orientations of analogues. Utilizing the positioned LeY structure, we implemented the program Ligand-Desgin (LUDI (27) Biosym Technologies) to search a fragment library to guide in the position of the putative APWLY peptide sequence. Optimization of the positioned peptide indicates some structural similarity between the carbohydrate tetrasaccharide core

of LeY, with similar functional groups on the B3 structure in contact with the peptide. This analysis therefore provides a unique perspective of how a peptide sequence fits into the antibody combining site, competing with a native antigen.

Placement of the Lewis tetrasaccharide core antigen in the B3 binding site.

The modeling of B3 followed our previous studies on anti-LeY related antibodies (25). This model of B3 interacting with LeY indicates a high degree of homology in the contact sites between B3 and BR96. We positioned the LeY fragment within the B3 binding site (figure 1), relying upon the reported contacts in the BR96 co-crystal structure (24). Contact sites with the LeY structure are observed to be conserved between BR96 and B3. In the placement of LeY we performed a restrained molecular dynamics calculation using the reported contacts for BR96 with the cFuc functional group contacts. In this restrained calculation, the backbone amide and carbonyl groups of Ala H100 forms hydrogen bonds with OH-3^c and OH-4^c as observed in the crystal structure of BR96. In this placement, $O7^a$ potentially forms a hydrogen bond with the backbone NH group of Tyr H33, also observed in BR96, while a bifurcated hydrogen bond is observed between His L31 and OH-3^b and OH-4^b. In addition, Tyr H35 forms a hydrogen bond with OH-6^b and Asn L31b forms a hydrogen bond with OH-4^d. The orientation of the LeY tetrasaccharide core in B3 highlights a hydrophobic interaction between Ala H97 with the methyl group of GlcNAc. Mutation of the native aspartic acid at this position in BR96 to alanine, results in increased tumor cell binding of BR96 (28).

Peptide placement

In the placement of the B3 reactive putative peptide sequence APWLY, we made use of the program LUDI to identify compounds that potentially interact with the B3 combining site. Some 269 fragments were identified with the largest radius of interaction, with most redundant for the same set of potential hydrogen bond donors or acceptors on B3. In evaluating the fragments we compared fragments identified by LUDI relative to the APWLY sequence such that the fragments could occupy non-redundant sites and be spatially far enough to accommodate the peptide backbone. In affect one wants to "stitch" the fragments together to form a peptide. In particular LUDI found that a Tyr residue forms a hydrogen bond with Ser at position L31a, that a lipophilic residue representative of a Leu side chain is bounded by residues Tyr H32, His L31, and Asn L31b, a Trp residue forms a hydrogen bond with the B3 backbone carbonyl group at position H98 and another lipophilic residue representative of an Ala side chain is bounded by Ala H97. In Figure 2 the placement of these fragments is shown relative to their position with each other within the B3 binding site. The APWLY sequence was then modeled such that the corresponding Trp, Tyr, Leu and Ala residues occupied relative positions as the identified LUDI fragments (Figure 3). In the positioning we observed that the AP residues of the peptide tract occupied a similar position as the LeY GlcNAc residue (Figure 4). This positioning indicates that the proline residue mimics the spatial position of the glucose unit of GlcNAc, while the Ala methyl group is positioned similarly as the terminal methyl group of GlcNAc's N- acetyl. Placement of the APWLY peptide in the B3-LeY binding site indicates that the Ala of the peptide interacts with Ala H97 of B3 (Figure 5). BR96 and another related anti-LeY antibody, BR55-2, have an Asp residue at this position, while each display homologies in contacting the LeY core antigen (25). We have found that BR55-2 does not bind the APWLYGPA peptide in a series of ELISA assays (unpublished observations) suggesting that Asp H97 might interfere with peptide binding. To test this aspect we substituted an Asp residue into B3 at this position and found that the peptide-B3 interaction was destabilized by 12 Kcal. Calculations for LeY binding with the Ala at this position shows a more favorable

energtic for binding (25) suggesting that the Ala at position H97 will enhance carbohydrate binding. This in fact is observed as deduced by mutatgenesis experiments on BR96 (28) and by our own calculations (25). In addition, peptide binding is favored over LeY binding to B3 by 22 Kcal indicating a higher affinity of binding. This difference ia attributable to increaed dispersion interactions between the peptide and antibody.

Discussion

Based upon the crystal structure of the BR96-LeY tetrasaccharide complex and the relative sequence similarities between anti-LeY antibodies, it is apparent that the MAb binding groove of LeY specific MAbs is sufficiently large to bind four monosaccharide units of the LeY determinant and fit a putative peptide surrogate that effectively mimics LeY binding. Structural studies on Lewis antigens have generally substantiated that conformations are determined mainly by steric repulsion brought about by changes in the glycosidic dihedral angles. Molecular dynamics calculations on Lewis antigen structure prototypes indicate the lack of spontaneous conformational transitions to other minima during the simulations, suggesting that these oligosaccharides maintain well-defined conformations with relatively long lifetimes (25). These results further indicate that hard sphere or rigid-geometry calculations, albeit in the absence of solvent, provides a good picture of the steric repulsion that modulate the conformational properties of the Lewis antigens. Subsequently the notion of utilizing a structure based drug design approach to determine a possible binding mode of a carbohydrate surrogate peptide offers a novel approach to confirm the ability of certain peptide residues to participate in contacting a receptor. The search of a fragment library for possible compounds that would fit within the B3 combining site provides a guide to position the side chains of the putative peptide sequence APWLY to effectively compete with the LeY antigen. The binding mode of the peptide does not have to faithfully mimic the antigen in contacting the same functional groups on B3, but may bind in a fashion that provides for steric competition between the peptide and the LeY structure. The extent of potential fragments that we have found to interact with the B3 combining site indicates that there may well be many ways for peptides with differing sequences to interact with B3. In related studies, we have found many potential peptides from phage display screening of the anti-LeY antibody BR55-2 (unpublished). The approach taken here can help to narrow down which peptides to examine first from the many that are identified. While current procedures for predicting ligand-antibody interactions is limited, an understanding of the 3-dimensional basis for the molecular recognition of LeY by B3 and related antibodies can be applied for future diagnosis in tumor progression and micrometastasis as well as active immunotherapy. Further structural studies of LeY antigen forms binding to anti-LeY antibodies will provide information relevant to vaccine design strategies and improved immunotherapeutics. Such analysis coupled with additional information derived from consideration of peptide mimics might also allow for peptides to be developed as immunogens to induce anti-carbohydrate immune responses.

Methods

Model Building and Energy Refinement

The conformations of the variable domains of B3 was deduced by comparison with known immunoglobulin crystal structures (25, 29). Sequence and crystallographic structure comparisons were used to identify templates for the localized structural folds of the hypervariable or CDR1, CDR2 and CDR3 regions of the heavy and light chains. For modeling of the heavy chain CDR3 region in particular, we utilized both a knowledge-based approach to search for suitable structures that fit a geometry to the base residues of

the CDR3 domain and a conformational search procedure (29). The latter involved using the program AbM (Oxford Molecular Inc.)

To determine a base geometry for H-CDR3, the Cα positions of several antibodies of known crystal structure were superimposed to define invariant residue positions. These positions define the amino-terminal beginning and the carboxyl terminal end that are shared among the putative CDR3 domains of varying lengths. The systematic superpositioning of the CDR3 domain over short sequences define a consensus region where the base geometry is conserved among the antibody templates. The description of invariant positions effectively reduces the length of the loop to search to those that are representative of a sufficient saturation of conformational space in the crystallographic database; usually six to seven residues in length. The crystallographic database was searched to identify loops of the same size as the CDR3 loop being examined using the program InsightII (Biosym Technologies version 3.5). The spatially-conserved Cartesian positions of the N and C terminal regions of CDR3 were held fixed in this search procedure. The 10 best matches were examined using the program InsightII and an appropriate choice was made based upon similarities in positions of side chains at the junctures of the CDR3 loop. As an alternative to this approach we utilized the automated antibody modeling program AbM which incorporates a knowledge based search, followed by conformational mapping.

The CDRs and the FRs of the templates were mutated to those of the respective antibody heavy and light chains using Insight II or automatically assigned by AbM. For the InsightII built structures, the side chain angles of the substituted residues were set according to angles identified in a database of side chains. Each CDR and framework region was changed individually, followed by 1000 cycles of energy minimization to eliminate close contacts between atoms. As in our previous studies, the program Discover (version 2.95 Biosym Technologies) was used for conformational calculations with the supplied consistent valence force field (CVFF) parameters. After model building, the respective structures were energy optimized to convergence. Molecular dynamics (MD) at 300 K and 600 K was used to further alleviate any close contacts within the antibodies.

Initially a molecular dynamics simulation over 30 picoseconds using the program Discover was performed. The structure was then energy minimized using conjugate gradients to convergence. Following this initial equilibration, the calculation was resumed for another 20 picoseconds at 600 K at constant pressure and then cooled to 300 K over 30 picoseconds. During the second dynamics procedure atoms lying further than 15 Å from all atoms of the CDR loops were held fixed. Non-hydrogen atoms of residues lying in the region 9 to 15 Å from all CDR loop atoms were harmonically restrained to their initial positions with a force constant of 30 kcal x mol^{-1} x rad^{-2}. These distance approximations result in fixing or restraining atoms of residues within the framework region of the antibodies. The backbone conformation torsion angles, phi and psi, of non-CDR loop residues were restrained to their initial values with a force constant of 1600 kcal x mol^{-1} x rad^{-2}. In addition, a torsional restraint of 10 kcal x mol^{-1} x rad^{-2} was employed around the omega bond. A time step of 1 fs was used. The resulting structure for B3 was energy minimized using conjugate gradients to convergence.

Docking of Lewis Y to B3

Individual subunits derived from crystal structures of carbohydrate fragments was used to model the putative LeY tetrasaccharide core Fucα1→ 2Galβ1→4(Fucα1→3)GlcNAc structure. Residues associated with the CDR loops were identified for possible interaction with the LeY determinant based upon BR96 binding to LeY (24). The

approach taken in the placement of the Lewis Y core in the antibody combining site was that described previously by us (30). The binding surface on the modeled antibodies was first defined as sites accessible to probe spheres of varying radii (1.4 to 1.7 Å) to identify possible positions which could be occupied by the atoms of the Y structure. The probe spheres were rolled on the binding surface of the models, with the continuum of loci reduced to a set of discrete points by clustering neighboring spheres much like a set of site points (30). These site points are localized at atom positions accessible to the probe spheres on each residue on the surface of the antibody. The site points were then used as a guide in the placement of the LeY structure. Hydrogen bonding restraints were applied to enhance potential contacts between the respective antibody combining site residues with sugar groups identified in the BR96/LeY structure (24), allowing the glycosidic angles of the LeY structure to change and the B3 model to adjust to these restraints.

After minimization, a restrained molecular dynamics calculation over 100 picoseconds using the program Discover was performed, preserving the hydrogen bonding constraints. The dynamics run was not intended to be a detailed study, but to further alleviate any close contacts within the antibody and between tetrasaccharide and the antibody. The calculation was initialized and equilibrated for 50 picoseconds at 300 K at constant pressure and resumed for another 50 picoseconds. The resulting structure was energy minimized using conjugate gradients to convergence. In the minimization and dynamics run no constraints other than the retention of LeY-antibody hydrogen bonds were placed on the antibody or binding site. Charges and non-bonded parameters for the Y structure were assigned from atom types from the CVFF parameter list supplied with Discover/InsightII.

Peptide identification

A LUDI search was performed using standard default values and fragment library supplied with the program to identify fragment positions within the B3 binding sit. This program constructs possible new ligands for a given protein of known three-dimensional structure. Small fragments are identified in a database and are docked into the protein binding site in such a way that hydrogen bonds and ionic interactions can be formed with the protein and hydrophobic pockets are filled with lipophilic groups of the ligand. The positioning of the small fragments is based upon rules about energetically favorable non-bonded contact geometry's between functional groups of the protein and the ligand. The center of search was defined using the LeY position. In this approach the OH-3^c position on the LeY structure was used as the sampling point. To identify possible fragments that are similar to the APWLY sequence, the radius of interaction, which defines the size of spheres in which LUDI is to fit appropriate fragments, was set as incrementing radii from 5 to 14 angstroms. Results of the search were compared with the putative peptide sequence side chain types, with those Ludi fragments retained within the B3-Lewis Y binding site which displayed similarities with the putative peptide side chains. The peptide was built using InsightII and positioned relative to the docked Ludi fragments. The peptide backbone and side chain torsional angles were rotated until the side chains of the peptide were approximate to the corresponding LUDI fragments. The peptide-B3 complex was subjected to energy optimization and molecular dynamics simulations as with the LeY-B3 complex.

Acknowledgments

This work was supported by the USAMRMC (DAMD17-94-J-4310) Breast Cancer Program. Computer equipment support from The Cancer Center of the University of Pennsylvania is also gratefully acknowledged.

References

1. Hakomori S. Aberrant glycosylation in tumors and tumor-associated carbohydrate antigens. Adv. Cancer Rres. 1989;52:257-331.

2. Hakomori S. Possible functions of tumor-associated carbohydrate antigens. Current Opin. Immunol. 1991;3:646-653.

3. Helling F, Shang A, Calves M, et al. GD3 vaccines for melanoma: superior immunogenicity of keyhole limpet hemocyanin conjugate vaccines. Cancer Research 1994;54(1):197-203.

4. Houghton AN. On course for a cancer vaccine. [Review]. Lancet 1995;345(8962):1384-5.

5. Kitamura K, Livingston PO, Fortunato SR, et al. Serological response patterns of melanoma patients immunized with a GM2 ganglioside conjugate vaccine. Proceedings of the National Academy of Sciences of the United States of America 1995;92(7):2805-9.

6. Toyokuni T, Hakomori S, Singhal AK. Synthetic carbohydrate vaccines: synthesis and immunogenicity of Tn antigen conjugates. Bioorganic & Medicinal Chemistry 1994;2(11):1119-32.

7. Wessels MR, Paoletti LC, Rodewald AK, et al. Stimulation of protective antibodies against type Ia and Ib group B streptococci by a type Ia polysaccharide-tetanus toxoid conjugate vaccine. Infection & Immunity 1993;61(11):4760-6.

8. Verheul AF, Braat AK, Leenhouts JM, et al. Preparation, characterization, and immunogenicity of meningococcal immunotype L2 and L3,7,9 phosphoethanolamine group-containing oligosaccharide-protein conjugates. Infection & Immunity 1991;59(3):843-51.

9. Berg EL, Magnani J, Warnock RA, Robinson MK, Butcher EC. Comparison of L-selectin and E-selectin ligand specificities: the L-selectin can bind the E-selectin ligands sialyl Le(x) and sialyl Le(a). Biochemical & Biophysical Research Communications 1992;184(2):1048-55.

10. Imai Y, Lasky LA, Rosen SD. Sulphation requirement for GlyCAM-1, an endothelial ligand for L-selectin. Nature 1993;361(6412):555-7.

11. Takada A, Ohmori K, Yoneda T, et al. Contribution of carbohydrate antigens sialyl Lewis A and sialyl Lewis X to adhesion of human cancer cells to vascular endothelium. Cancer Research 1993;53(2):354-61.

12. Scott JK. Discovering peptide ligands using epitope libraries. [Review]. Trends in Biochemical Sciences 1992;17(7):241-5.

13. Scott JK, Loganathan D, Easley RB, Gong X, Goldstein IJ. A family of concanavalin A-binding peptides from a hexapeptide epitope library. Proceedings of the National Academy of Sciences of the United States of America 1992;89(12):5398-402.

14. Oldenburg KR, Loganathan D, Goldstein IJ, Schultz PG, Gallop MA. Peptide ligands for a sugar-binding protein isolated from a random peptide library. Proceedings of the National Academy of Sciences of the United States of America 1992;89(12):5393-7.

15. Hoess R, Brinkmann U, Handel T, Pastan I. Identification of a peptide which binds to the carbohydrate-specific monoclonal antibody B3. Gene 1993;128(1):43-9.

16. Cheung NK, Canete A, Cheung IY, Ye JN, Liu C. Disialoganglioside GD2 anti-idiotypic monoclonal antibodies. International Journal of Cancer 1993;54(3):499-505.

17. Evans SV, Rose DR, To R, Young NM, Bundle DR. Exploring the mimicry of polysaccharide antigens by anti-idiotypic antibodies. The crystallization, molecular replacement, and refinement to 2.8 A resolution of an idiotope-anti-idiotope Fab complex and of the unliganded anti-idiotope Fab. Journal of Molecular Biology 1994;241(5):691-705.

18. Furuya A, Yoshida H, Hanai N. Development of anti-idiotype monoclonal antibodies for Sialyl Le(a) antigen. Anticancer Research 1992;12(1):27-31.

19. Saleh MN, Stapleton JD, Khazaeli MB, LoBuglio AF. Generation of a human anti-idiotypic antibody that mimics the GD2 antigen. Journal of Immunology 1993;151(6):3390-8.

20. Westerink MA, Apicella MA. Anti-idiotypic antibodies as vaccines against carbohydrate antigens. [Review]. Springer Seminars in Immunopathology 1993;15(2-3):227-34.

21. Westerink MAJ, Giardina PC, Apicella MA, Kieber-Emmons T. Peptide mimicry of the meningococcal group C capsular polysaccharide. Proc. Natl. Acad. Sci. 1995;92:4021-4025.

22. Hruby VJ. Strategies in the development of peptide antagonists. Prog Brain Res 1992;92(1):215-24.

23. Jenks S. Mimetics may one day replace peptide antibodies [news]. J Natl Cancer Inst 1992;84(2):79-80.

24. Jeffrey PD, Bajorath J, Chang CY, et al. The x-ray structure of an anti-tumour antibody in complex with antigen [see comments]. Nature Structural Biology 1995;2(6):466-71.

25. Thurin-Blaszczyk M, Murali R, Westerink MAJ, Steplewski Z, Co M-S, Kieber-Emmons T. Molecular recognition of the Lewis Y antigen by monoclonal antibodies. Protein Engineering 1996;9:101-113.

26. Pastan I, Lovelace ET, Gallo MG, Rutherford AV, Magnani JL, Willingham MC. Characterization of monoclonal antibodies B1 and B3 that react with mucinous adenocarcinomas. Cancer Research 1991;51:3781-3787.

27. Bohm HJ. LUDI: rule-based automatic design of new substituents for enzyme inhibitor leads. J Comput Aided Mol Des 1992;6(6):593-606.

28. Yelton DE, Rosok MJ, Cruz G, et al. Affinity maturation of the BR96 anti-carcinoma antibody by codon-based mutagenesis. Journal of Immunology 1995;155(4):1994-2004.

29. Martin AC, Cheetham JC, Rees AR. Molecular modeling of antibody combining sites. Methods Enzymol 1991;203(1):121-53.

30. Lin C, Kieber-Emmons T, Villalobos AP, Foster MH, Wahlgren C, Kleyman TR. Topology of an amiloride binding protein. J. Biol. Chem. 1994;269:2805-2813.

Figure Legends

Figure 1: Hydrogen bond interaction scheme of B3 with the LeY tetrasaccharide core. The position of LeY is based upon sequence similarity between B3 and BR96 whose crystal structure is known in complex with a LeY derivative. The a,b,c,d designation refer to the βDGlcNac, βDGal, αLFuc(1→3) and αLFuc(1→2) units, respectively.

Figure 2. Fragment positions as identified by LUDI sitting in the LeY binding site of B3. These fragments define potential positions of the side chains of the peptide putative sequence APWLY for interaction with B3, competing with the LeY antigen for B3 binding.

Figure 3. Fitting of the putative peptide sequence onto the LUDI defined fragments. The Tyr like fragment is colored orange, the Trp like fragment is colored light magenta, the Ala like liphophilic fragment is colored dark magenta and the Leu like liphophilic group is colored green. The APWLY peptide is colored cyan. The conformation of the peptide is after energy optimization of the peptide in the B3 combining site.

Figure 4. Stereo view of the overlap of the putative peptide with the LeY tetrasaccharide core. The peptide and the LeY structure are those of the binding mode conformation within the B3 combining site. In this orientation of the peptide within the site the Ala and Pro residues of the putative peptide sequence are observed to be spatially similar to the GlcNAc residue of the LeY structure.

Figure 5. The putative peptide in the B3 combining site. This rendering highlights the interaction of the Ala at position H97 in B3, colored yellow, with the Ala of the putative peptide, also colored yellow. Substitution of the Ala at H97 with Asp results in destabilizing the peptide interaction with B3. Asp is the native residue in the anti-LeY antibody BR55-2. The LeY mimicking peptide does not bind to BR55-2 as assessed in competitive binding assays with LeY antigen (data not shown).

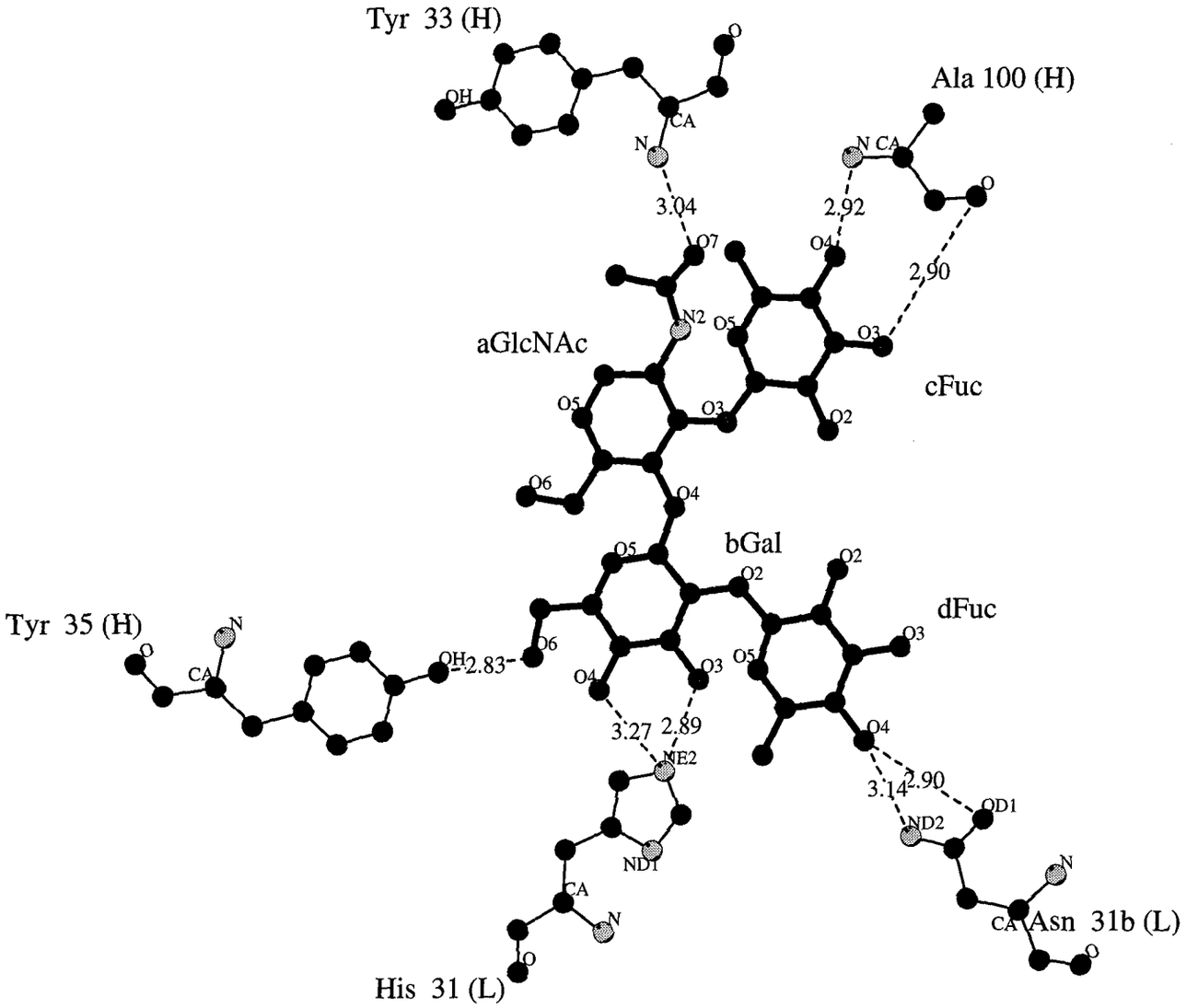
Tyr 33 (H)
Ala 100 (H)
aGlcNAc
cFuc
bGal
dFuc
Tyr 35 (H)
His 31 (L)
Asn 31b (L)
3.04
2.92
2.90
2.83
3.27
2.89
3.14
2.90

Figure 1

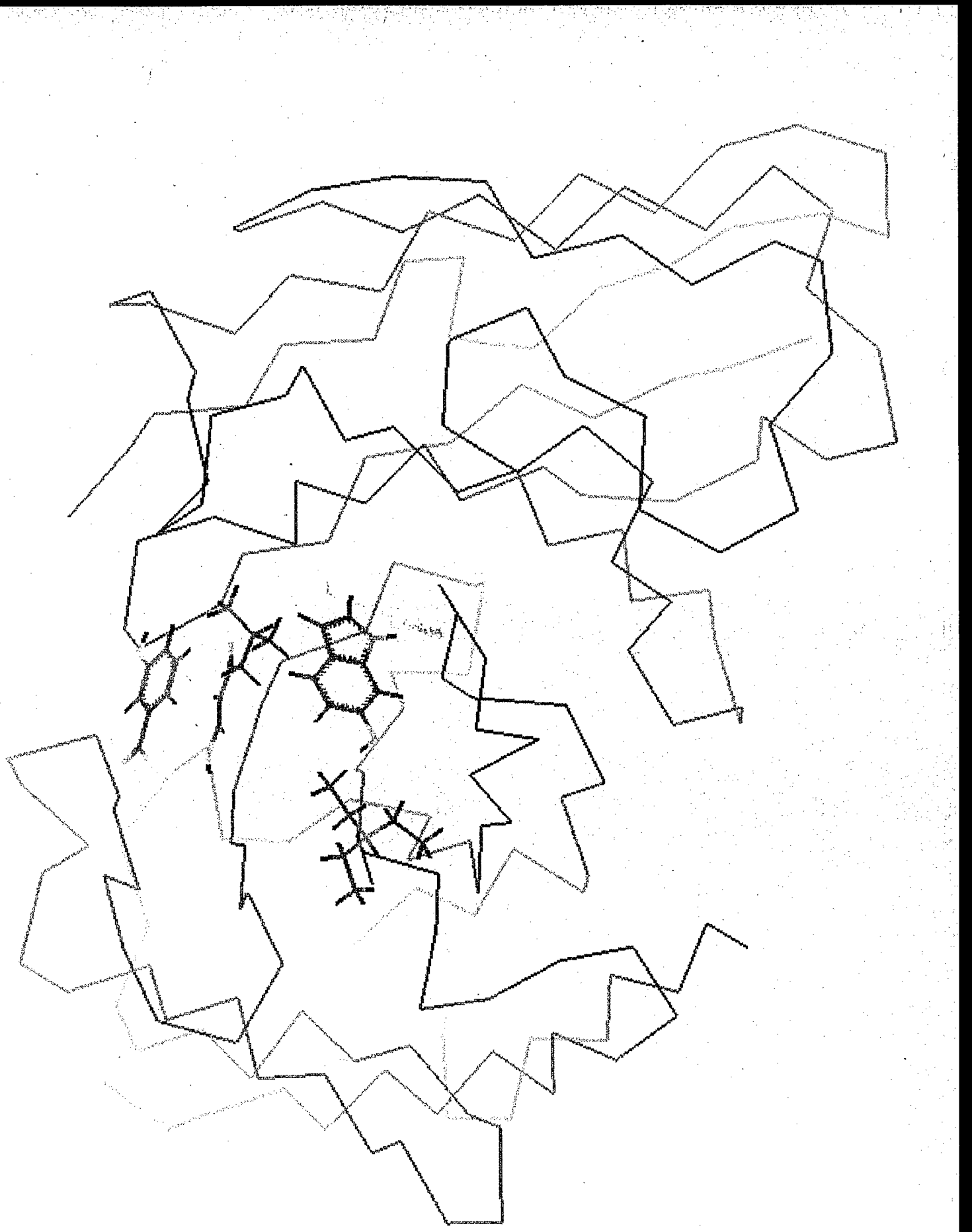

Figure 2

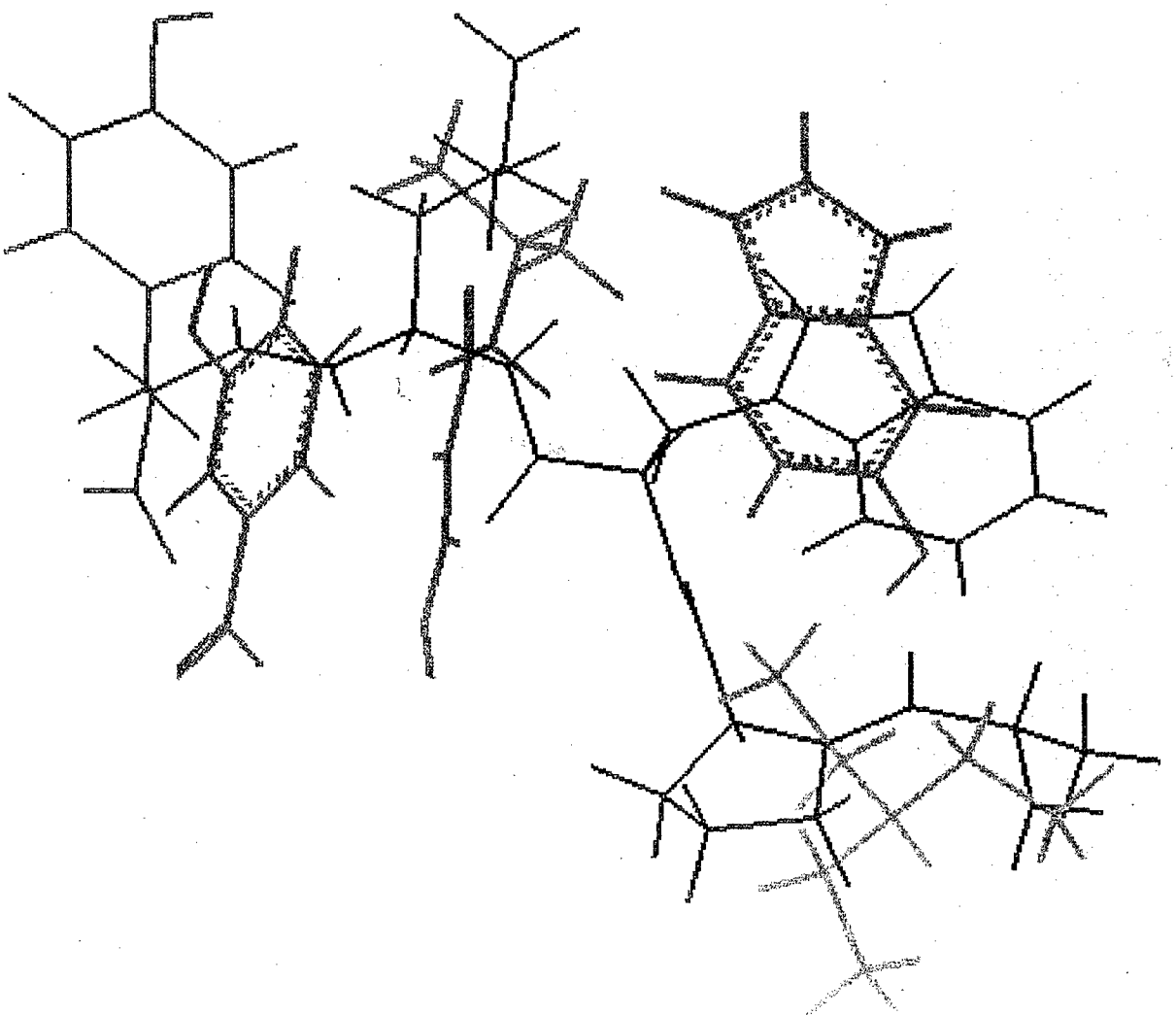

Figure 3

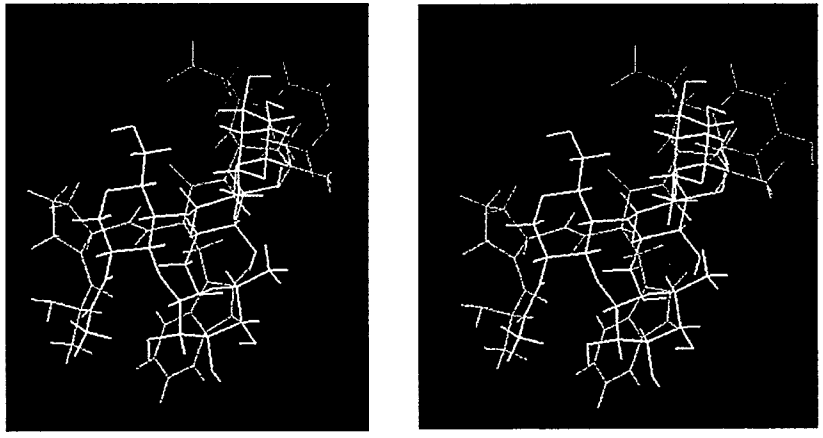

Figure 4

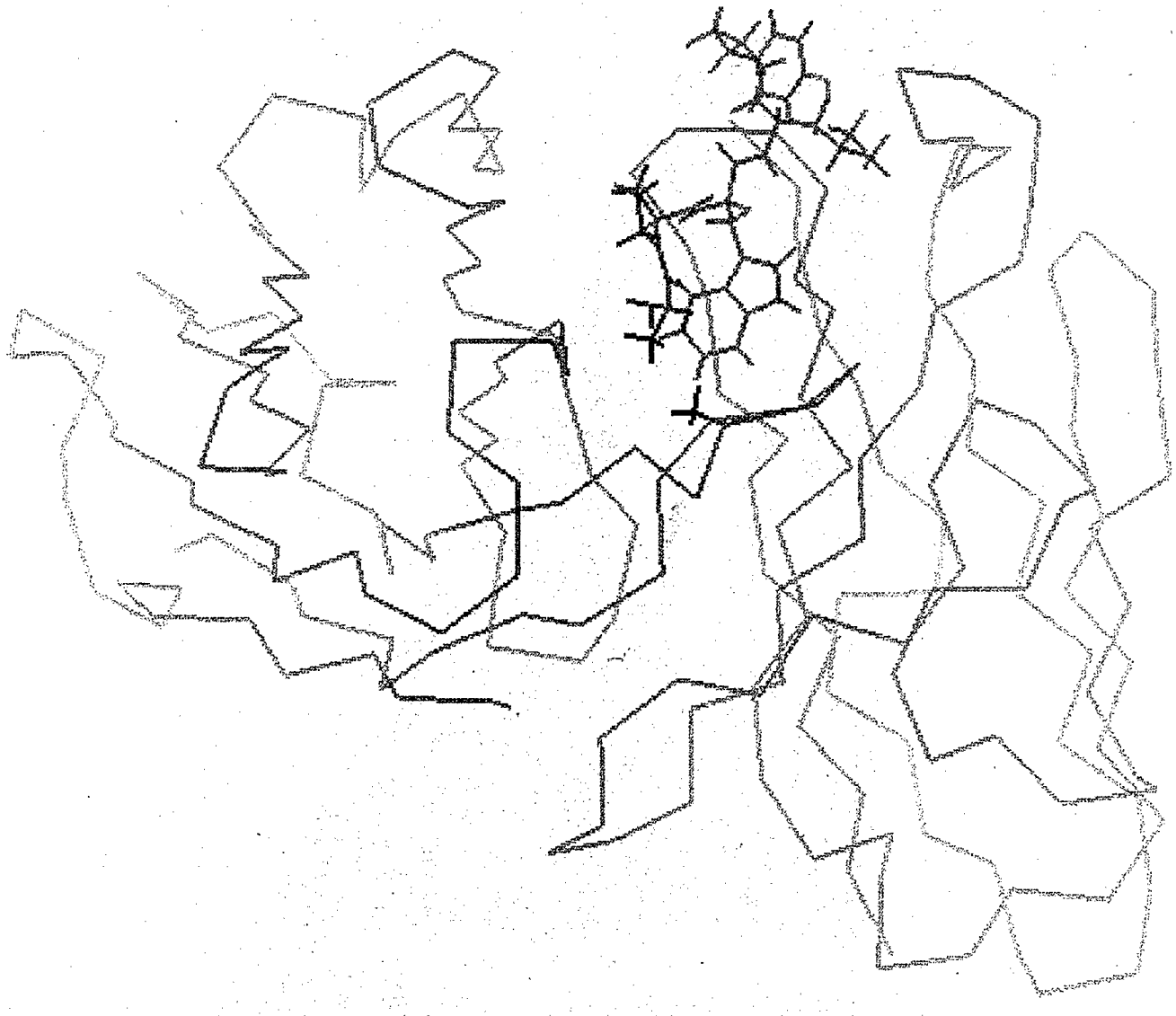

Figure 5

Recd 7/19/2000

DEPARTMENT OF THE ARMY
US ARMY MEDICAL RESEARCH AND MATERIEL COMMAND
504 SCOTT STREET
FORT DETRICK, MARYLAND 21702-5012

REPLY TO
ATTENTION OF:

MCMR-RMI-S (70-1y) 6 Jul 00

MEMORANDUM FOR Administrator, Defense Technical Information Center, ATTN: DTIC-OCA, 8725 John J. Kingman Road, Fort Belvoir, VA 22060-6218

SUBJECT: Request Change in Distribution Statements

1. The U.S. Army Medical Research and Materiel Command has reexamined the need for the limitation assigned to technical reports written for the following awards:

DAMD17-94-C-4068	ADB218322
DAMD17-94-V-4036	ADB232944
DAMD17-94-J-4481	ADB222571
DAMD17-95-C-5054	ADB227112
DAMD17-96-1-6016	ADB228823
DAMD17-96-1-6073	ADB248567
DAMD17-94-J-4057	ADB221437, ADB247857
DAMD17-96-1-6069	ADB230256, ADB239319
DAMD17-95-1-5067	ADB236775, ADB249592
DAMD17-94-J-4308	ADB225776, ADB234457, ADB249935
DAMD17-96-1-6087	ADB232086, ADB238945, ADB250354
DAMD17-96-1-6075	ADB228777, ADB238338, ADB249653
DAMD17-95-1-5008	ADB225250, ADB236089, ADB243691
DAMD17-94-J-4310	ADB222453, ADB235860, ADB247801

Request the limited distribution statement for Accession Document Numbers be changed to "Approved for public release; distribution unlimited." These reports should be released to the National Technical Information Service.

2. Point of contact for this request is Ms. Virginia Miller at DSN 343-7327 or by email at Virginia.Miller@det.amedd.army.mil.

FOR THE COMMANDER:

Phyllis Rinehart

PHYLLIS M. RINEHART
Deputy Chief of Staff for
Information Management